NOCTILUCENT CLOUDS

A

DISSERTATION

Presented to the Faculty of the

University of Alaska in Partial Fulfillment

of the Requirements

for the Degree of

Doctor of Philosophy

by

Benson Tarrant Fogle, B.S., M.S.

College, Alaska

May, 1966

NOCTILUCENT CLOUDS

APPROVED:

Dr. Dharmbir Rai

Dr. Gerald Romick

Dr. Bernhard Haurwitz

Chairman: Dr. Sydney Chapman

Department Head: Dr. Manfred Rees

APPROVED:

Dean of the College of Mathematics, Physical Science, and Engineering

Vice President for Research and Advanced Study

FOREWORD

During a course of lectures on the kinetics of the upper atmosphere in the spring of 1962, Prof. S. Chapman brought the subject of noctilucent clouds to my attention and aroused my interest in them. At that time there was only one well-documented observation of NLC over North America and there were no well-documented reports of these clouds from the southern hemisphere. During the summer of 1962 I began a watch for NLC in Alaska which resulted in the observation of five displays; and I prepared a proposal for organized study of NLC, which was sent to the National Science Foundation in the fall of 1962 and funded by them in the summer of 1963. In the fall of 1962, a major effort to establish a large network of noctilucent cloud observing stations in the northern and southern hemisphere was begun. Several hundred meteorological stations in Alaska, Canada, Greenland, Iceland, Chile, Argentina, the Antarctic, and the islands in the region 45°-70°S are now participating in this network. NLC observation manuals for both the northern and southern hemispheres have been prepared and sent to all participating stations. From the data obtained by these many stations around the world, new information on the dependence of the frequency of occurrence upon season and latitude, and as to the lifetime, spatial extent, and velocity of NLC has been obtained.

Deliberations with representatives of WMO, IAMAP, the USSR, and Great Britain at the IQSY meeting in Madrid (1965) on the subject of NLC resulted in preparations to have all meteorological stations in the northern and southern hemispheres (between 45 and 90 degrees latitude)

make routine NLC observations using uniform procedures, and to report their observations to one of three collection centers--College, Alaska, Tartu, Estonia, and Edinburgh, Scotland. In the fall of 1965 I prepared a new, more comprehensive observation manual which was sent to WMO for consideration as the official NLC observation manual.

In addition to the organization and operation of the network of observing stations, a number of special measurements and experiments were planned and carried out over the past four years. Among these were: time-lapse motion-picture studies of the transformations occurring in NLC; measurements of the spectrum, polarization, and lifetime; determinations of the velocity, frequency of occurrence, latitudinal distribution, spatial extent, possible latitudinal shift of NLC with season; and a set of rocket experiments to attempt to create artificial NLC.

Also a detailed analysis of the observational morphology of NLC was made and the observations and results of other workers over the past 80 years were collected and combined with ours into more meaningful statistics on the characteristics of NLC.

The following parts of this dissertation contain new material and results obtained by the author: Chapters 2, 3, 4, 7, and Section 6.3.

ABSTRACT

This dissertation contains a detailed account of 4 years of experiments and observations on noctilucent clouds (abbreviation: NLC) organized by the author in North America and in the southern hemisphere as well as a comprehensive summary and discussion of the material published by other researchers.

The collection and analysis of all available data on NLC provides the following picture of their characteristics:

Characteristics of Northern Hemisphere NLC

color	:	bluish-white
height (average)	:	82.67 km
latitude of observations	:	45°N to 80°N, best at about 60°N
season for observations	:	March through October, best in June through August
times for observations	:	nautical and part of astronomical twilight
spatial extent	:	10,000 km^2 to more than 4,000,000 km^2
duration	:	several minutes to more than 5 hours
velocity (average)	:	40 m/sec towards SW
thickness	:	0.5 to 2 km
vertical wave amplitude	:	1.5 to 3 km
particle diameter (average)	:	0.3 microns
number density of particles	:	10^{-2} to 1 per cm^3
composition of particles	:	ice-coated extraterrestrial dust
temperature in presence of NLC:		about 130°K

The results of the study of NLC over North America show that:

(1) NLC occur over North America as frequently as over Europe and the USSR.

(2) They are observed during nautical and part of astronomical twilight when the sun is between 6° and 16° below the observer's horizon.

(3) Sunlight passing closer than about 20 km to the earth's surface is greatly attenuated in the 4000A-7000A range and cannot adequately illuminate the clouds.

(4) Spectra of NLC obtained during the summer of 1965 show that the light from NLC is scattered sunlight and that the cloud particles scatter light best at shorter wavelengths (around 4500A) than at longer ones (6500A).

(5) The earliest and latest dates of NLC displays over North America were April 1 and September 28 respectively.

(6) The peak of NLC activity falls around July 20, one month after the summer solstice.

(7) Ninety-two percent of the displays were observed during the months of June - August.

(8) Eighty-two percent of the displays were observed after the summer solstice.

(9) No NLC were seen in winter, although a careful watch for them was kept by experienced observers.

(10) Displays occurring before the summer solstice were faint and covered small areas, whereas after the solstice they were bright and extensive.

(11) NLC have been observed over North America from geographic latitudes as low as 45°N and as high as 71°N, but the optimum latitude for NLC observations is around 60°N.

(12) NLC displays are generally first seen before midnight but are brightest and most extensive after midnight.

(13) Occasionally NLC displays extend over an area of millions of square kilometers and are observed on the same night by many observers over North America, Europe, and Russia.

(14) NLC occur more often than previously supposed. During the month of July they are seen nearly every night in some part of the northern hemisphere. An observer at 60°N might expect to see NLC on about 75% of the clear nights during the month of July.

(15) The wavelengths of the well-defined wave structure often observed in the clouds range from several to more than 100 km with the billow structure having wavelengths of around 10 km.

(16) NLC displays are generally quite persistent and last for periods up to and greater than 5 hours, but individual parts (particularly the billow structure) often form and decay within a few minutes or tens of minutes.

During our expedition to western Canada in the summer of 1965, simultaneous NLC and aurora were observed on 13 occasions. On six of the seven occasions when the aurora occurred in the same part of the sky as the NLC, interesting changes were observed in the NLC within 30 minutes to an hour after onset of aurora. The general effects observed were a reduction of NLC intensity and extent and a transformation of their well-ordered structure into swirls and formless veils. The changes observed in the NLC suggest heating at or below the mesopause.

Our work on NLC in the southern hemisphere has resulted in the proof of the existence of NLC there and the determination of some of their characteristics. Our first well-documented sighting of NLC in the southern hemisphere was made on the night of 9 January 1965, from Punta Arenas, Chile (53.1°S). On our expedition to Punta Arenas during the austral summer of 1965-66 NLC were observed on 9 nights, the first and last displays being seen on December 25, 1965 and January 22, 1966, respectively. These displays were found to have a general drift motion towards the west-northwest. The brightest and most extensive display observed on this expedition took place on the night of January 3, 1966. The peak of NLC activity at 53.1°S falls around January 10, twenty days after the austral summer solstice.

A comparison of NLC activity with volcanic eruptions, meteor showers, and the sunspot cycle shows no correlation between these events.

An examination of the various theories of NLC formation points to the need for more and better data on NLC and the region in which they are formed before a satisfactory explanation of them is obtained.

ACKNOWLEDGEMENTS

This investigation has been supported by State of Alaska Funds and through the Atmospheric Sciences Section of the National Science Foundation under grants numbered GP-1759 and GP-5197.

The author is indebted to many people at the Geophysical Institute and elsewhere for their interest and assistance in this program. Foremost among them is Professor Sydney Chapman, my graduate advisor and committee chairman, who brought the subject of noctilucent clouds to my attention during a course of lectures on the kinetics of the upper atmosphere in the spring of 1962, and who has been a constant source of inspiration and guidance throughout the course of this investigation. To the other members of my graduate committee--Dr. Bernhard Haurwitz, Dr. Dharmbir Rai, and Dr. Gerald Romick--I am grateful for many helpful suggestions and advice. I would particularly like to thank Professor Keith B. Mather, Director of the Geophysical Institute, for his encouragement and many helpful discussions. I am indebted to Mr. Yngvar Gotaas, formerly with the Geophysical Institute, for his participation in setting up the program during the initial stages. Without the assistance of Mrs. Carol Echols who prepared all the necessary electronic computer programs and participated in much of the data reduction and observations, the whole project would have suffered. I would like to thank Mr. A. P. McNeil, Mr. Neal Brown, Mr. Jerry Chao, Mr. James Ellfeldt, and Mr. William Stringer for their assistance in the noctilucent cloud field work. I am grateful to Mr. Al Belon, Mr. Charles Deehr, Dr. C. T. Elvey, and Dr. Charles Wilson for their helpful discussions.

The Office of Naval Research kindly provided us with the use of their facilities (including aircraft) at the Arctic Research Laboratory, near Point Barrow, Alaska on two occasions during 1965. I would like to thank Dr. Max E. Britton of the Office of Naval Research and Dr. Max C. Brewer, director of the Arctic Research Laboratory, for their assistance in arranging for the use of these facilities.

The following persons and agencies are to be thanked for their assistance in organizing the extensive network of noctilucent cloud observers in the northern and southern hemisphere:

Oliver Ashford, World Meteorological Organization, Geneva, Switzerland

Karl Andersen, Director of Der Danske Meteorlogiske Institut, Denmark

J. Bessemoulin, Permanent representative of France to the World Meteorological Organization, Paris, France

Mac Emerson, Regional Director of the U. S. Weather Bureau, Anchorage, Alaska

Institut Royal Meteorologique de Belgique, Brussels, Belgium

G. E. McDowell, Regional Director of Air Services, Department of Transport, Edmonton, Alberta

G. A. McMurray, Chief of Flight Service Branch, U. S. Federal Aviation Agency, Anchorage, Alaska

New Zealand Meteorological Service, Wellington, New Zealand

J. R. H. Noble, Director of the Meteorological Branch, Canadian Department of Transport, Toronto, Ontario

B. G. Pedersen, Danish Meteorological Office, Sondrestromfjord, Greenland

Charles Roberts, Polar Operations Project, U.S. Weather Bureau, Washington, D.C.

R. W. Savory, Chief Pilot, Pan American World Airways, Seattle, Washington

H. Sistryggsson, Director, Icelandic Meteorological Service, Reykjavik, Iceland

In closing, I would like to thank the several thousand observers at the meteorological stations participating in the noctilucent cloud observational program in Alaska, Canada, Greenland, Iceland, and in the southern hemisphere.

TABLE OF CONTENTS

TABLE OF CONTENTS (CONT'D)

LIST OF ILLUSTRATIONS

LIST OF TABLES

CHAPTER 1

INTRODUCTION

Noctilucent or night-luminous clouds (abbreviation: NLC) are truly remarkable and of great interest because of their surprising height (about 82 km) above the earth. The nature and origin of these clouds are still not well understood, although they have been under investigation for 80 years.

These clouds, as their name implies, are seen against the background of a dark sky while they are still illuminated by sunlight, when the sun is well below the horizon (Figs. 1.1 - 1.3). They generally resemble cirrus or cirrostratus, often having a delicate filigree pattern, with marked wave structure. They are generally tenuous so that stars shine through them almost undimmed. In brightness and extent they have a considerable range. They are observed most often during the summer months in high latitudes.

NLC are formed in the altitude region known as the mesopause where the lowest temperature in the earth's atmosphere occurs (Fig. 1.4). This region manifests a number of other important features--the ionospheric D-region, the sodium layer, the peak of the OH emissions, and sometimes perhaps the lower border of the aurora. The dynamics and photochemistry of the mesopause are poorly understood at present because of its inaccessibility to both balloons and satellites. This region is accessible to rockets, but the large expense involved with this type of measurement coupled with the short sampling time available makes it impractical to obtain sufficient data by this means alone.

15/16 JULY 1965 DISPLAY
Grande Prairie, Alberta

27/28 JULY 1965 DISPLAY (WITH AURORA)
Watson Lake, Yukon Territory

COMMERCIAL PRINTING [redacted] 273 COMPANY, INC
FAIRBANKS, ALASKA

26/27 JULY 1965 DISPLAY
Watson Lake, Yukon Territory

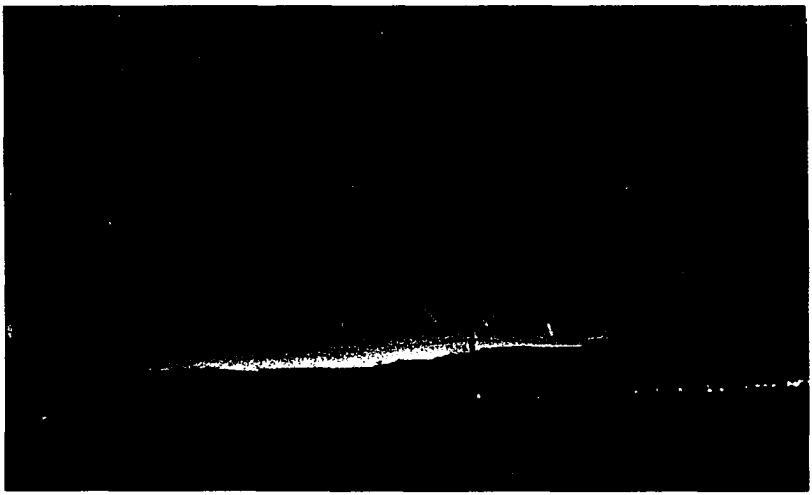

3/4 JANUARY 1966 DISPLAY
Punta Arenas, Chile

Unusual noctilucent cloud displays

J. Zoller

27/28 JULY 1957 DISPLAY
Anchorage, Alaska

A. McNeil

26/27 JULY 1963 DISPLAY
Watson Lake, Yukon Territory

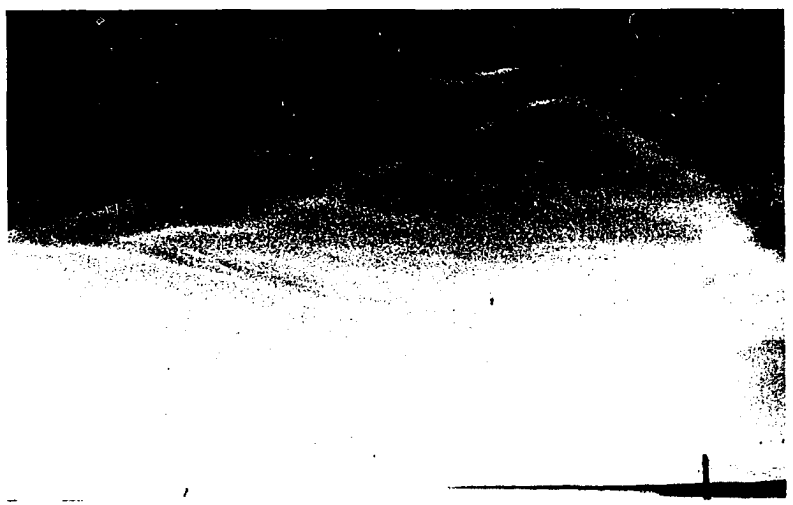

J. Veilleux

5/6 JULY 1964 DISPLAY
Fort Chimo, Quebec

J. Gardey

28/29 JULY 1964 DISPLAY
Anchorage, Alaska

Figure 1.2. Nostilucent clouds over North America, 1957-1964.

29/30 JUNE 1965 DISPLAY
Grande Prairie, Alberta

26/27 JULY 1965 DISPLAY
Watson Lake, Yukon Territory

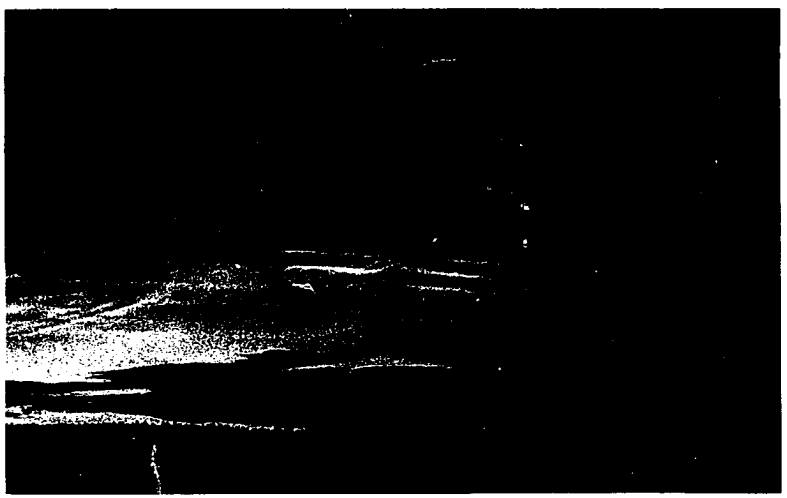

27/28 JULY 1965 DISPLAY
Watson Lake, Yukon Territory

1/2 AUGUST 1965 DISPLAY
Watson Lake, Yukon Territory

Figure 1.3 Noctilucent Clouds over North America during 1965

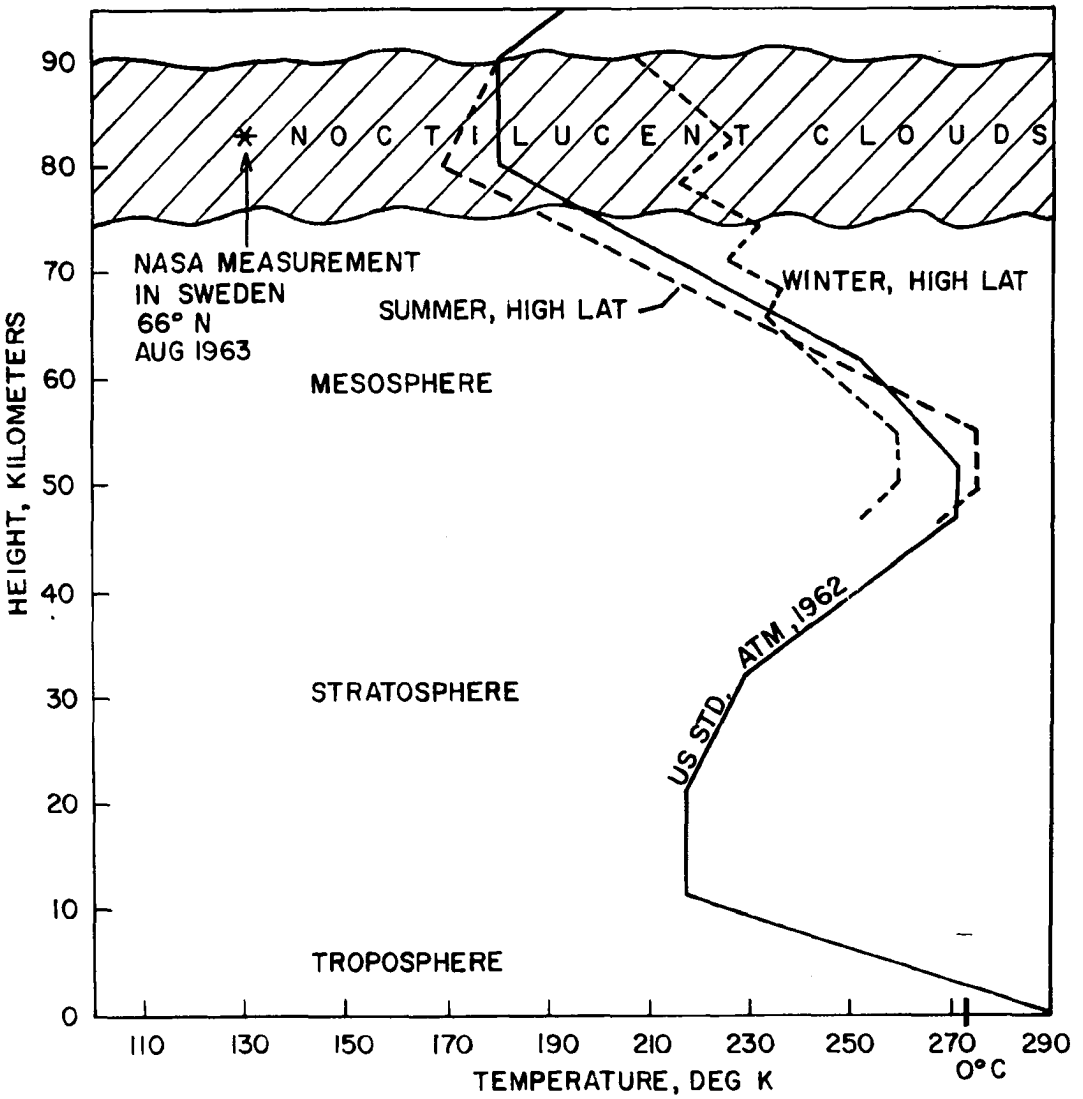

Fig. 1.4. Temperature distribution in the upper atmosphere.

As a result of these difficulties there is a scarcity of information on the parameters of this region. In view of these considerations the importance of ground-based measurements of processes occurring in the mesopause is enhanced. NLC lend themselves nicely to ground-based measurements, and a thorough understanding of how these clouds are formed and their characteristics should provide us with more knowledge of the dynamics, physics and perhaps also of the photochemistry of the mesopause. Thus considerable interest has developed in NLC in recent years.

The earliest recorded observations (1885) came when dust from the great volcanic eruption at Krakatoa (1883) has spread over the globe, producing sunsets of unusual brightness and splendor; this led to the sky being more widely observed at that time, but statistics do not support the view that volcanic eruptions can be the main cause of NLC. The first recorded recognition of observed clouds as being an unusual phenomenon with respect to height, was made by T. W. Backhouse (1885) at Kissingen, Germany on June 8 of that year. Doubtless such clouds had been noticed earlier, but the published accounts are not sufficiently definite for them to be identified uniquely as NLC (see Arago, 1854 and Scultetus, 1949). These clouds were first studied systematically by Jesse in Germany and by Tseraskii in Russia in 1885 and later years.

To Jesse we owe the name Leuchtenden Nachtwolken, or noctilucent clouds, and the first accurate height and velocity measurements. Interest in these clouds waned during the period 1909-1924 but picked up again in 1925 when Astapovich in the USSR began to study them. A few years later (1932) Störmer observed and measured the height of these clouds in Norway, using the observing facilities he had organized

there for the observation and position determination of auroras. In 1933, Vestine made the first reported observation of NLC over North America, and a year later he published the first comprehensive discussion of these clouds (Vestine, 1934). Interest in NLC again waned during the period 1936-1947, but around 1948, Paton in Scotland and Khvostikov and Grishin in the USSR began their work on NLC. Grishin (1955) published the first detailed classification of NLC structure and a year later published the first spectrum of these clouds (Grishin, 1956). The interest in NLC was intensified during the IGY when a large network of observing stations was set up in the USSR to make systematic observations of them. Also at this time F. H. Ludlam initiated a study of these clouds in Sweden which has since been continued with great vigor by Georg Witt at the University of Stockholm. Since the IGY, interest in NLC has continued to grow and the number of scientists actively working in this field has increased considerably. Systematic observations for NLC are now being made at meteorological stations over the northern and southern hemisphere between the latitudes 45-90 degrees (Figs. 1.5, 1.6), and these data are processed and published by collection centers located at College, Alaska, Edinburgh, Scotland and Tartu, Estonia.

Prior to the summer of 1962 only a few sightings of these clouds had been reported from North America while hundreds of observations had been reported from Europe and the USSR. This scarcity of observations over North America led people to wonder whether for some unknown meteorological reason, NLC did not occur here as often as elsewhere. To check this speculation, and to improve our general knowledge of NLC

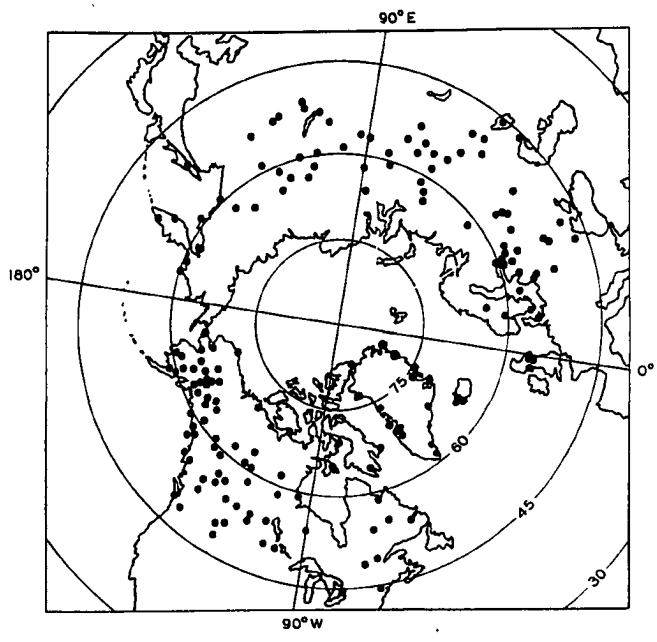

Fig. 1.5. Network of NLC observing stations in the northern hemisphere.

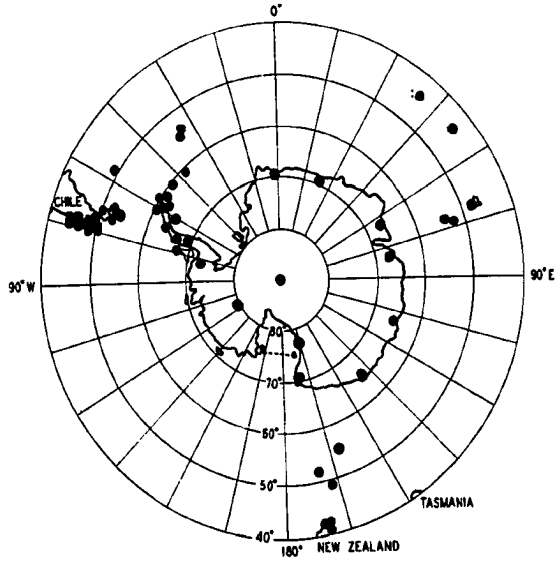

Fig. 1.6. Network of NLC observing stations in the southern hemisphere.

B. Fogle of the Geophysical Institute at College, Alaska in 1962 initiated a study of NLC over North America. Arrangements were made with the Canadian Department of Transport, the U. S. Weather Bureau, and the U.S. Federal Aviation Agency to have the meteorological stations in Alaska and Canada make systematic observations of NLC (see Fig. 1.5). A "Noctilucent Cloud Observation Manual" (Fogle and Gotaas, 1963) was prepared and sent to all participating stations. The data obtained by this network of observing stations shows that NLC occur as frequently over North America as over Europe and the USSR and that the previous scarcity of observations was probably due to the lack of interested and informed observers here.

Since 1885, the number of NLC displays reported per year has fluctuated, partly depending on the attention given to them by interested observers. Over a thousand occurrences are on record so far (Fogle and Echols, 1965) and many of their characteristics have been studied.

NLC are to be distinguished from nacreous, or mother-of-pearl, clouds which are formed at an altitude of 17 to 35 km in high latitudes during the winter months. Hoffmeister (1951) has reported another high altitude cloud-like formation which he has named "Leuchtstreifen" or light strips. These light strips have been observed at a mean height of 120 km.

CHAPTER 2

OBSERVATIONAL MORPHOLOGY

It is now well established that the light from noctilucent clouds is scattered sunlight. This is proved by the spectrum of these clouds, which shows a continuum, and also by their disappearance from view when the 82 kilometer region is no longer sunlit. In order that the NLC may be visible from the ground: (1) the sky must be relatively free of tropospheric clouds, (2) the 82 km region must be sunlit--this condition is fulfilled when the sun is not more than 16° below the observer's horizon, and (3) the sky background must be dark enough for the clouds to stand out--this requires that the sun is at least 6° below the horizon.

NLC are so tenuous that they cannot be observed during daylight. Occasionally, very bright NLC may be visible during civil twilight when the sun is between 0° and 6° below the horizon, but at such times it is difficult to distinguish them from high cirrus.

The geometry of NLC scattering is shown in Fig. 2.1. An observer at O can see NLC at the 82 km level over an arc extending in the vertical through the sun between angular elevations κ, κ' when the true solar depression angle is α. At elevation angles less than κ, the sky background is too bright for the NLC to be visible, and at elevation angles greater than κ', the NLC are no longer illuminated. The angles, κ, κ' are functions of the solar depression angle, the NLC height, and the screening height (H_{SC}) of the earth's atmosphere.

Sunlight passing closer to the earth than a height H_{SC} is so greatly attenuated by scattering and absorption that only those rays

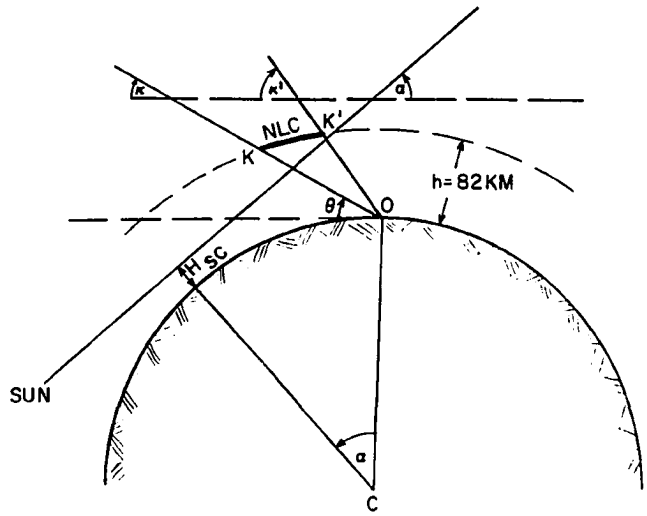

Fig. 2.1. Geometrical conditions under which NLC may be seen.

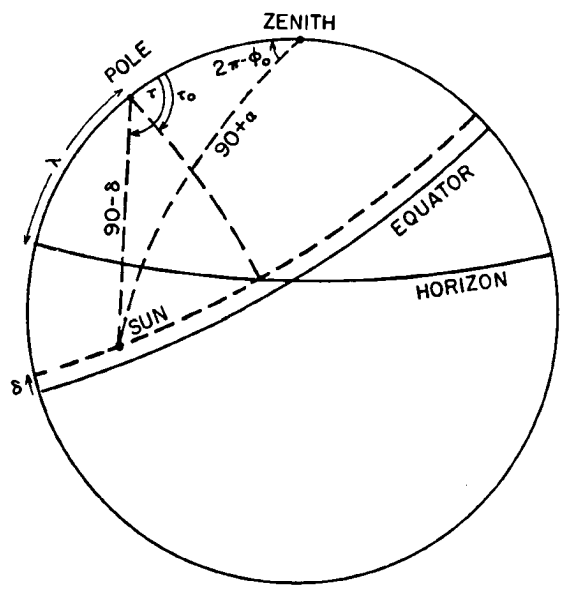

Fig. 2.2. The celestial sphere illustrating the relationships of of α to δ, λ, and τ.

passing above this height have sufficient intensity to make NLC visible.

2.1 Variation of Viewing Conditions with Latitude, Season and Time of Day

The NLC observation period (solar depression angle = 6° to 16°) varies markedly with latitude and season. The relationship between the true solar depression angle (α), the solar declination (δ), and time (τ, the hour angle of the sun) is illustrated in Fig. 2.2 for an observer in the northern hemisphere (the geometry is the same for the southern hemisphere if δ and λ are measured positive toward the south instead of the north pole). One of the cosine formulae for the spherical triangle (Fig. 2.2) formed by the sun-pole-zenith is

$$\sin \alpha = - \sin \delta \sin \lambda - \cos \delta \cos \lambda \cos \tau \qquad (2.1)$$

where

α = true solar depression angle

δ = solar declination

λ = latitude of observer

τ = hour angle of the true sun = $(t - 12^h + \Delta\ell + E)$, t is the standard time at a station, $\Delta\ell$ is the difference in longitude of the station and the standard meridian and is positive when the station is east of the meridian and negative when it is west of the meridian. E, the equation of time, is defined as the hour angle of the true sun minus the hour angle of the mean sun.

The values of δ and E are obtained from the Astronomical Ephemeris.

Using the same triangle and the law of cosines, one obtains the following expression for the azimuth of the sun, ϕ_o, (measured positive towards the east from north):

$$\cos \phi_o = \frac{(\sin \alpha \sin \lambda + \sin \delta)}{(\cos \alpha \cos \lambda)} \qquad (2.2)$$

Given the date and time of observation and the latitude and longitude of the observing station, equation 2.1 can be solved to obtain the solar depression angle (S.D.A.) corresponding to the observation. One can also determine the time at which a given solar depression angle occurs on a particular day at a particular latitude and longitude, by solving this equation for t. Using this procedure, NLC observation time curves can be constructed as shown in Figs. 2.3 - 2.8 for latitudes 45° - 70° north. Figure 2.9, derived from these curves, shows the variation in NLC observation times with latitude and season.

These curves show that below about 60° latitude, NLC if present, could be observable over the whole year. North of 60° there are weeks or months, centered about the solstice, when NLC cannot be observed because the sun does not sink more than 6° below the horizon during these times. Below 50° latitude the daily duration of the observing period changes little throughout the year, and totals about an hour. Below 50° the observing period is not continuous through midnight, but above that latitude there are times during the year when the observing period is continuous through midnight. At the poles, NLC can be seen, if present, for 24 hours a day during several weeks of the year.

2.2 The Shadow Height (H_{SH}) of the Earth and the Atmospheric Screening Layer

A useful method used for estimating the approximate height of NLC is that based on considerations of the height (H_{SH}) of the shadow of the solid earth plus atmospheric screening layer at the time the upper border of the NLC fades from view. The geometry of this problem is shown in Fig. 2.10. The equation for H_{SH} as derived by Chamberlain

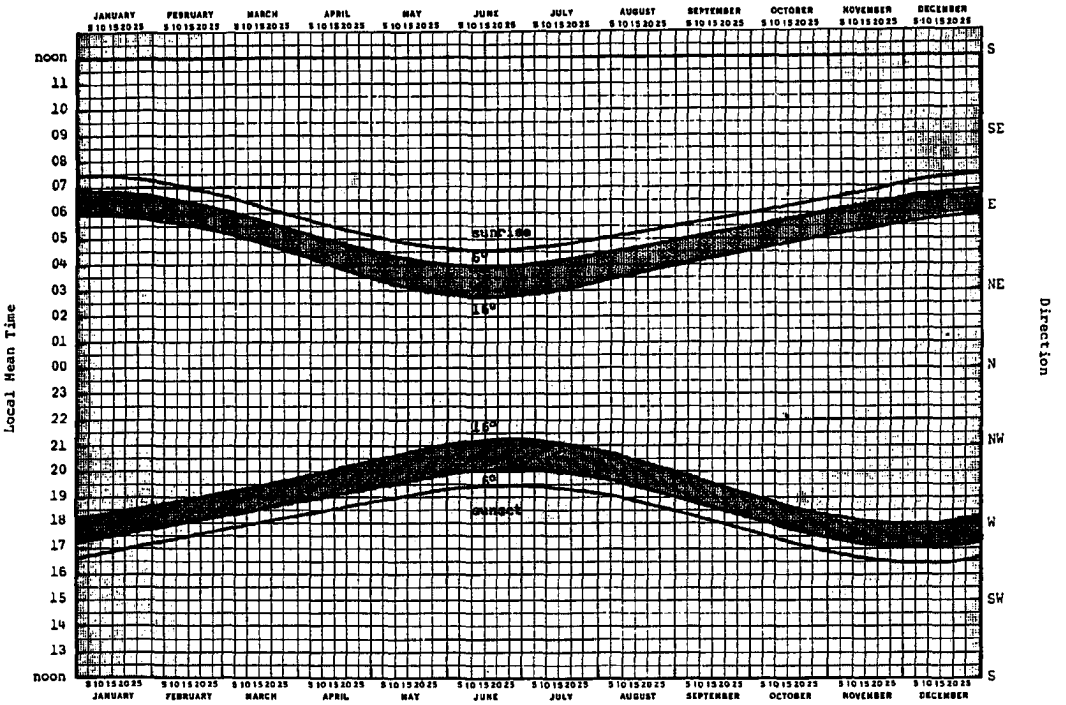

NOCTILUCENT CLOUD OBSERVATION PERIODS (SHADED AREA) FOR 40°N.

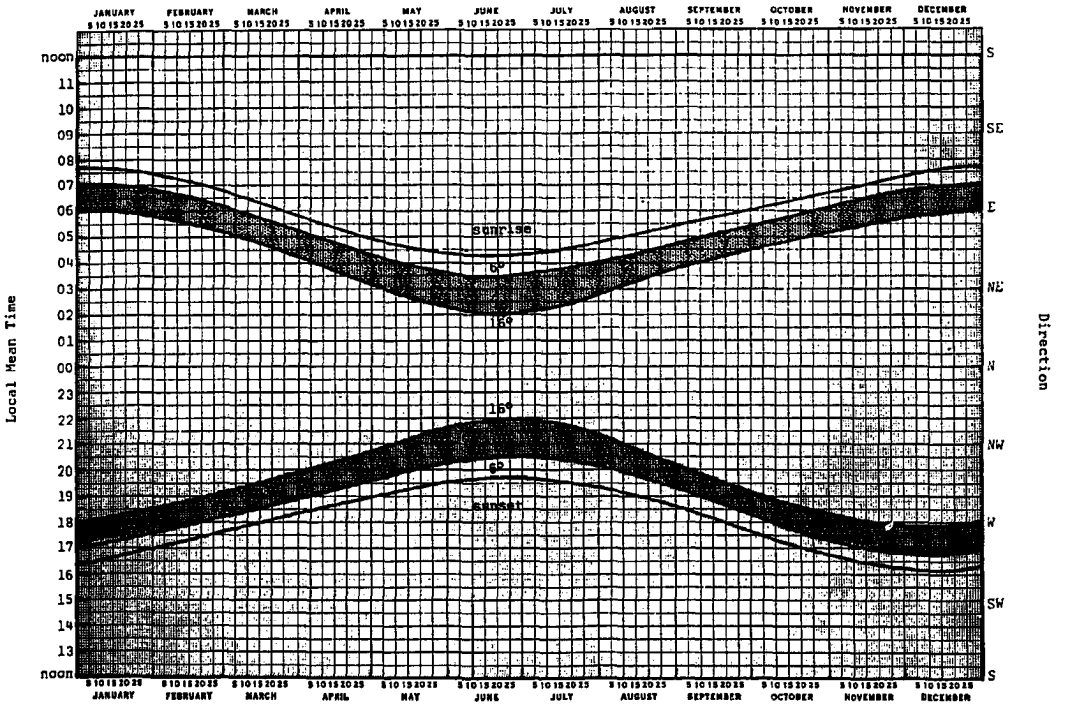

NOCTILUCENT CLOUD OBSERVATION PERIODS (SHADED AREA) FOR 45°N.

Fig. 2.3. NLC observation periods for 40°N and 45°N.

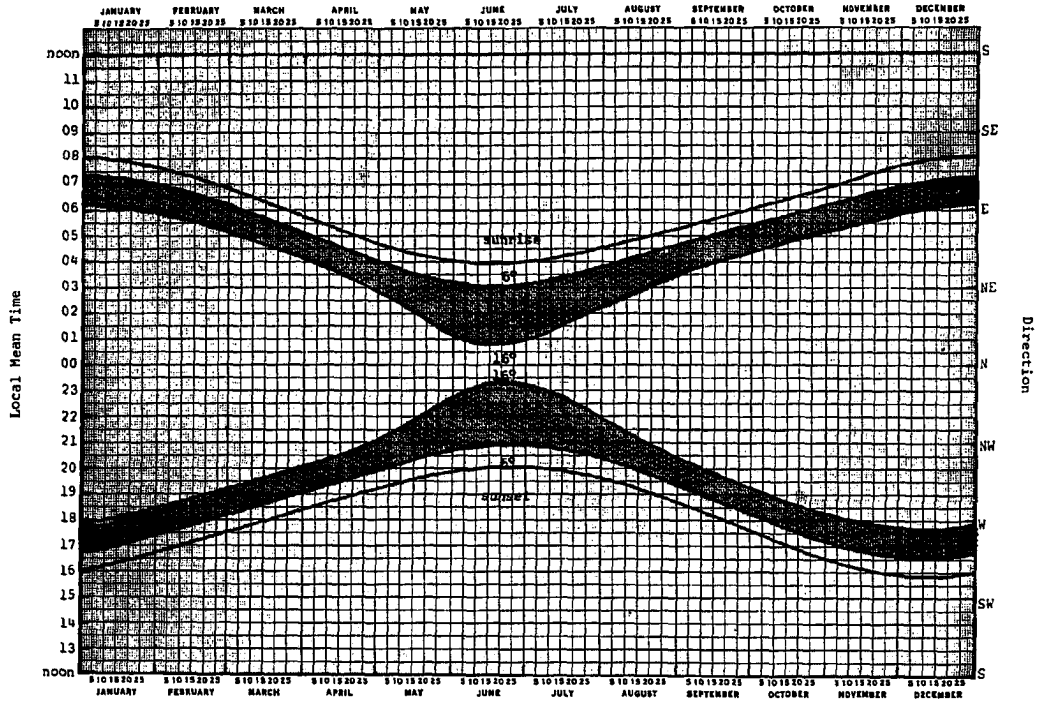

NOCTILUCENT CLOUD OBSERVATION PERIODS (SHADED AREA) FOR 50°N.

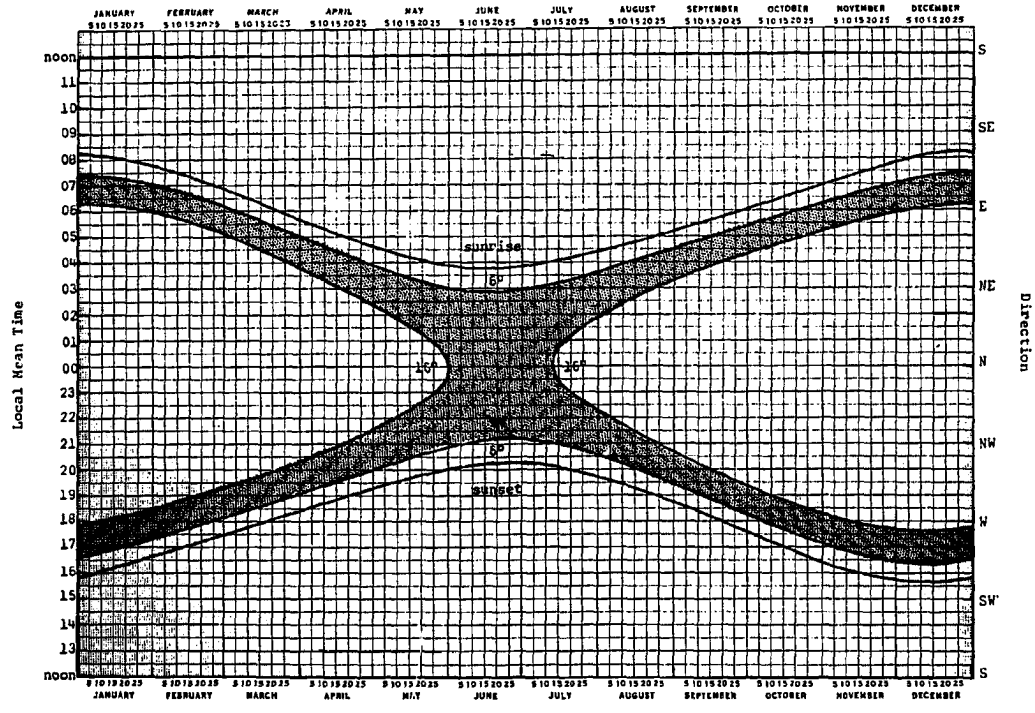

NOCTILUCENT CLOUD OBSERVATION PERIODS (SHADED AREA) FOR 52°N.

Fig. 2.4. NLC observation periods for 50°N and 52°N.

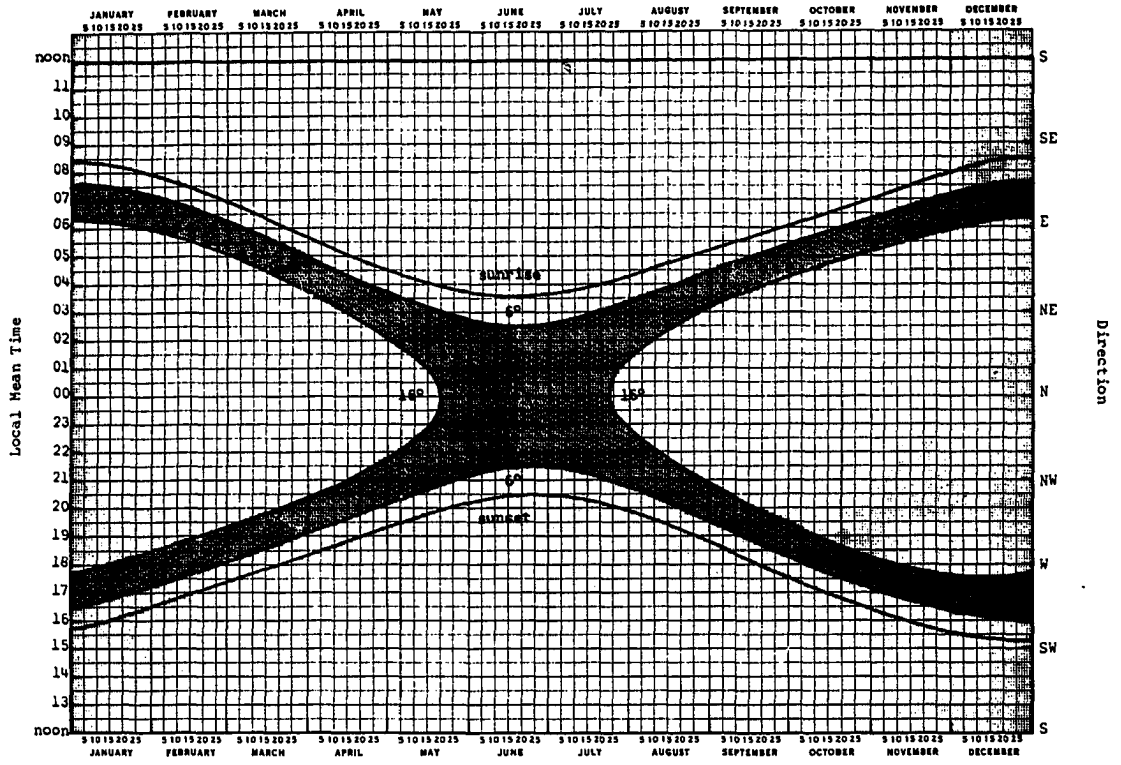

NOCTILUCENT CLOUD OBSERVATION PERIODS (SHADED AREA) FOR 54°N.

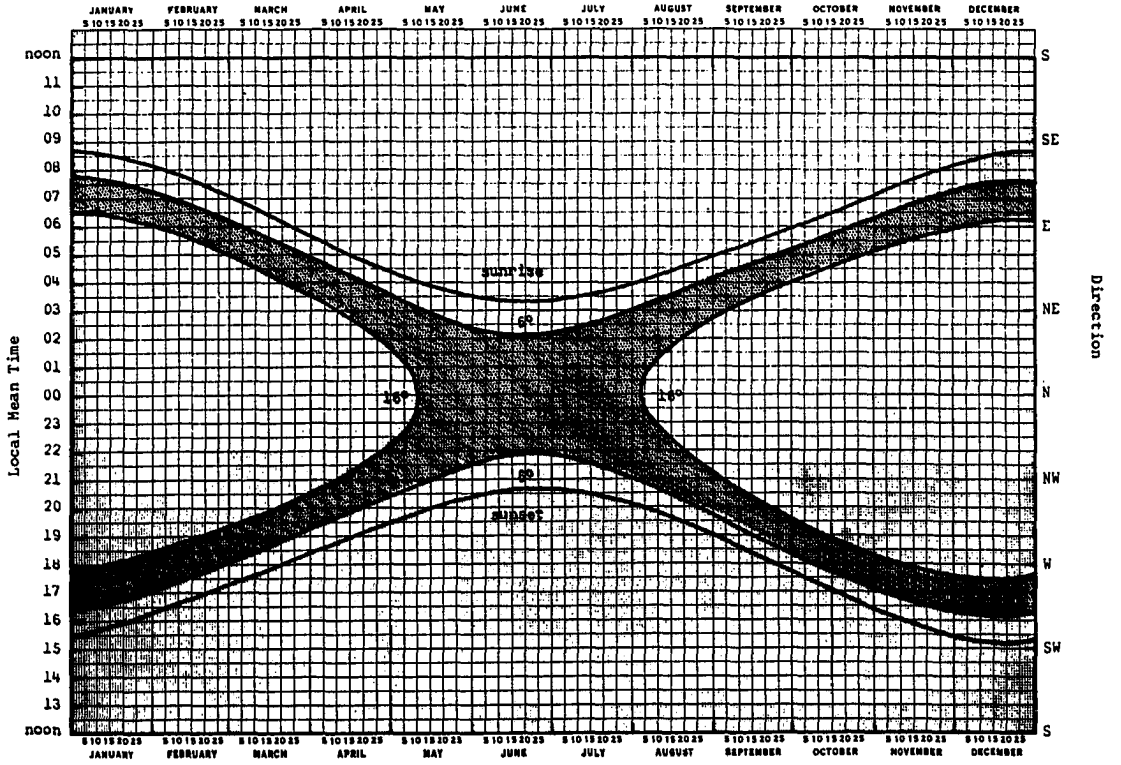

NOCTILUCENT CLOUD OBSERVATION PERIODS (SHADED AREA) FOR 56°N.

Fig. 2.5. NLC observation periods for 54°N and 56°N.

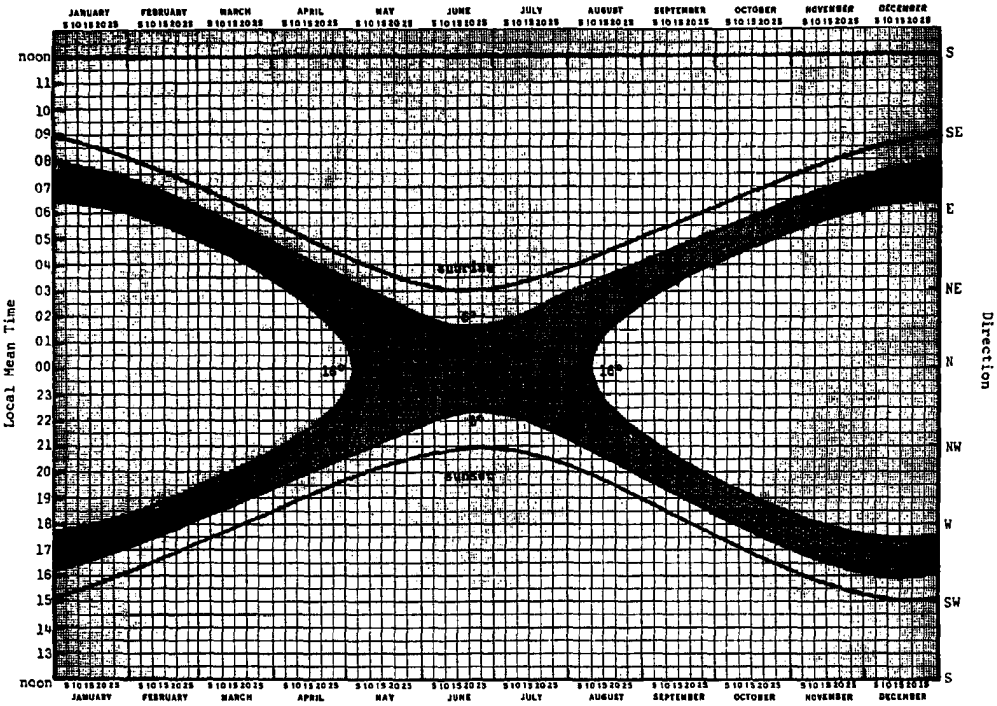

NOCTILUCENT CLOUD OBSERVATION PERIODS (SHADED AREA) FOR 58°N.

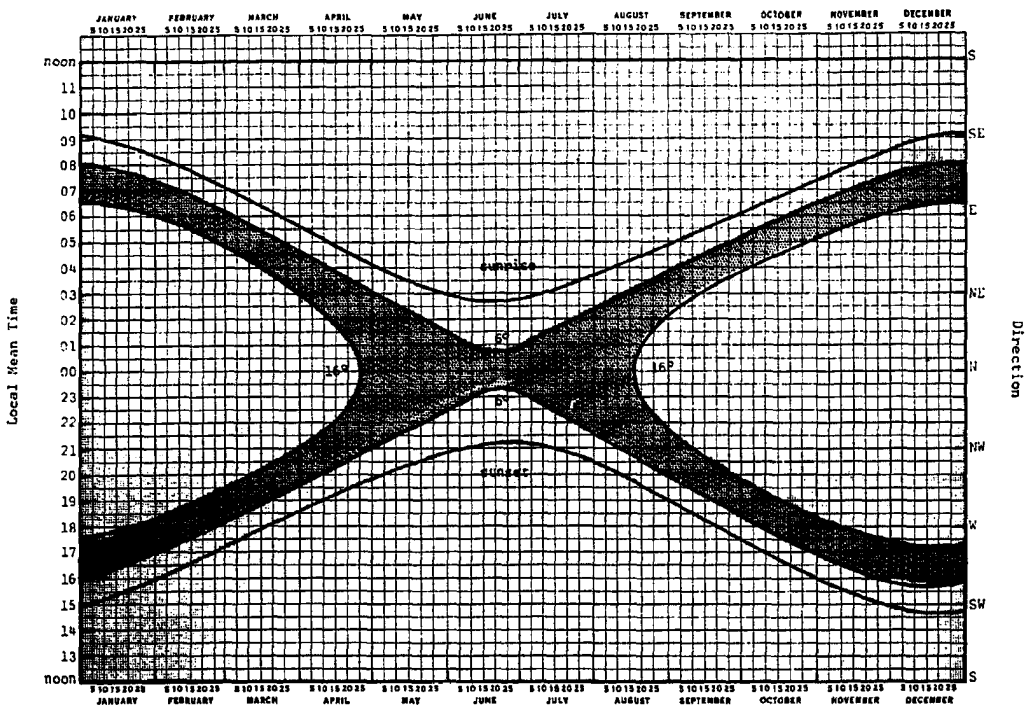

NOCTILUCENT CLOUD OBSERVATION PERIODS (SHADED AREA) FOR 60°N.

Fig. 2.6. NLC observation periods for 58°N and 60°N.

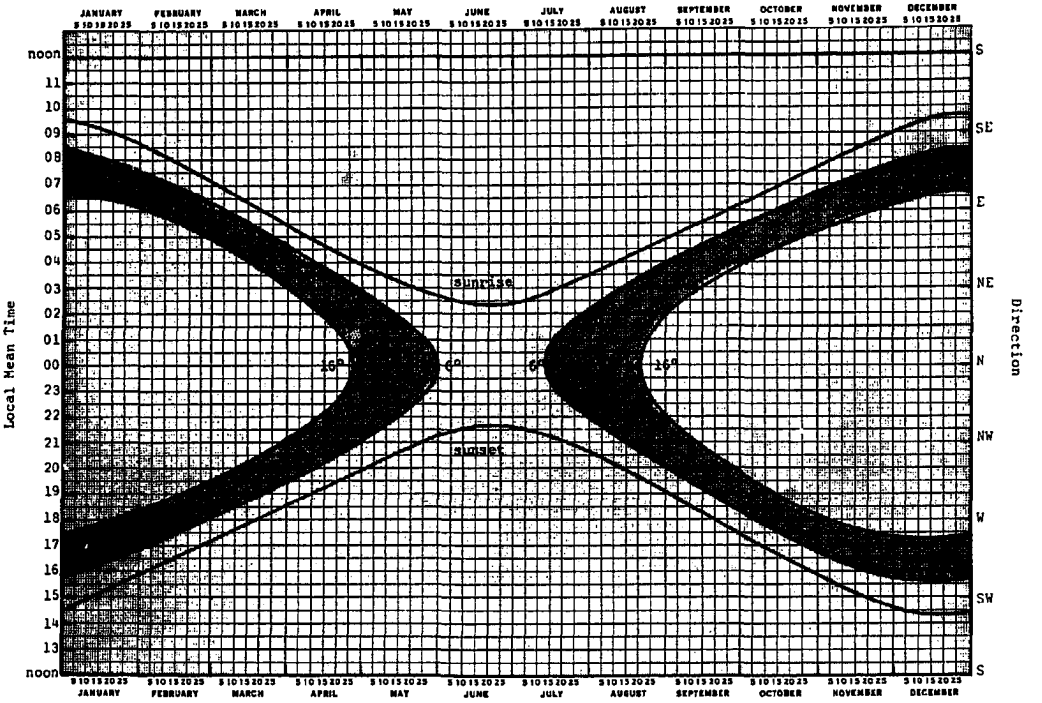

NOCTILUCENT CLOUD OBSERVATION PERIODS (SHADED AREA) FOR 62°N.

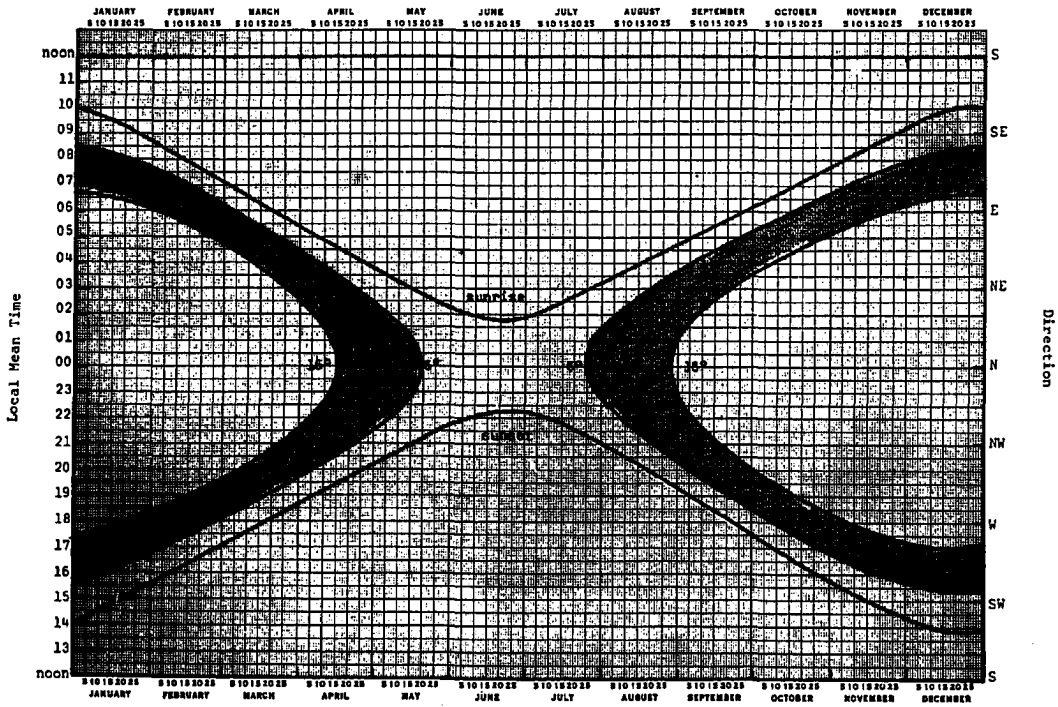

NOCTILUCENT CLOUD OBSERVATION PERIODS (SHADED AREA) FOR 64°N.

Fig. 2.7. NLC observation periods for 62°N and 64°N.

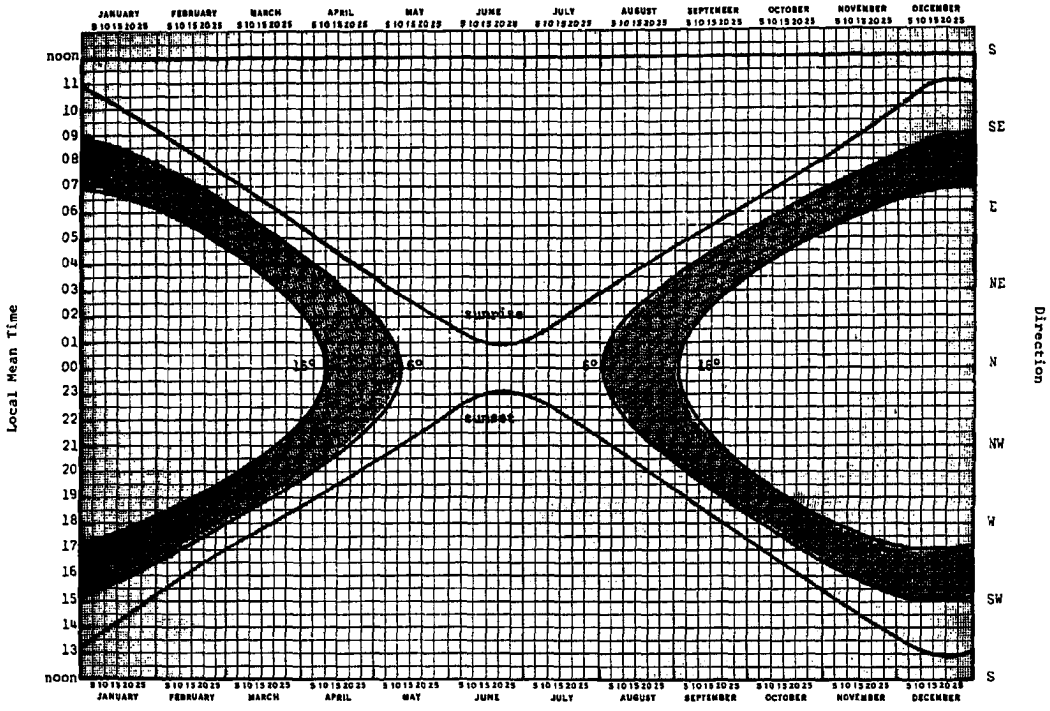

NOCTILUCENT CLOUD OBSERVATION PERIODS (SHADED AREA) FOR 66°N.

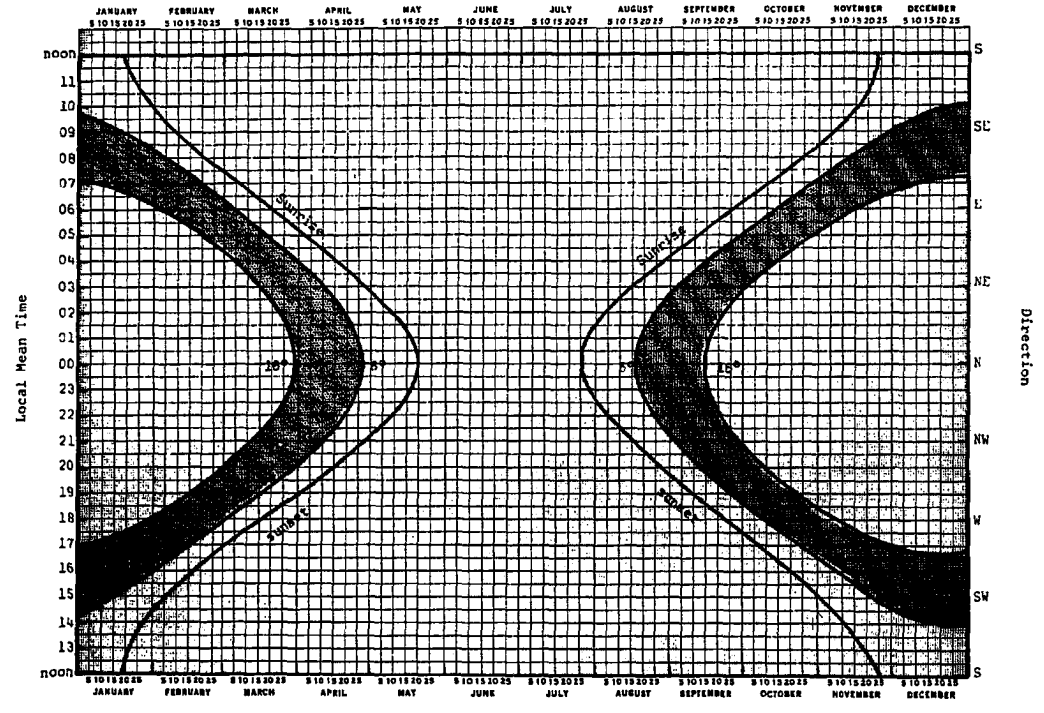

NOCTILUCENT CLOUD OBSERVATION PERIODS (SHADED AREA) FOR 70°N.

Fig. 2.8. NLC observation periods for 66°N and 70°N.

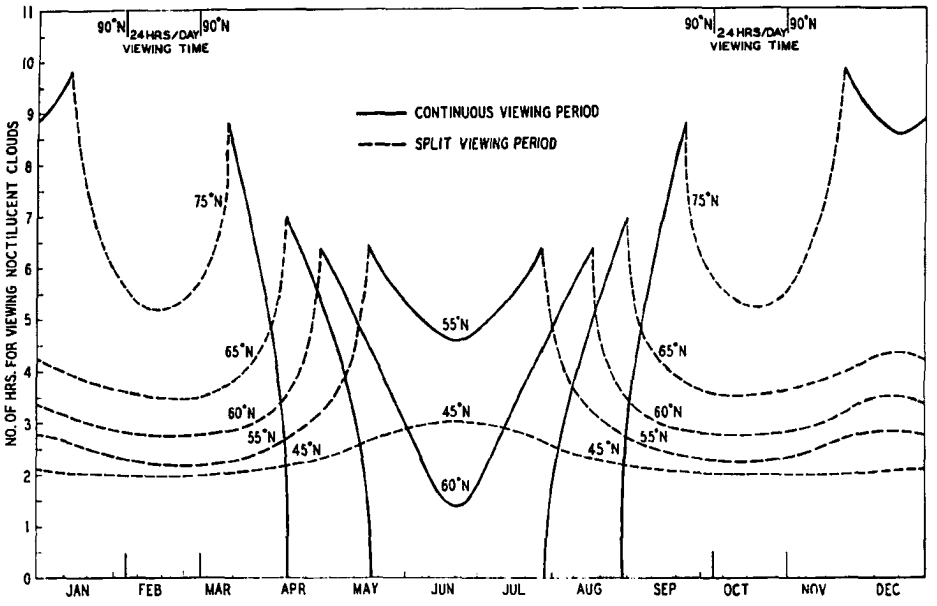

Fig. 2.9. Variation with latitude and season of the total number of hours per night for viewing NLC.

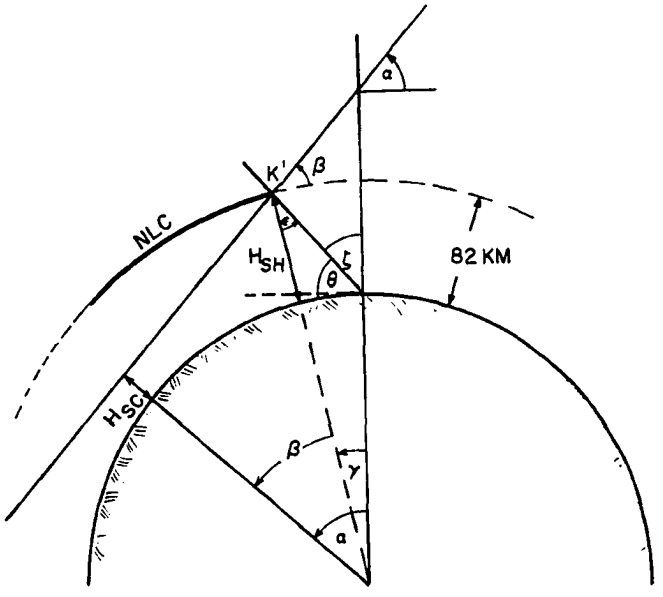

Fig. 2.10. Geometry of NLC observations illustrating the calculation of H_{SH}.

(1961) is:

$$H_{SH} = \frac{a}{2}\frac{[\sin(\zeta \mp \alpha) - \sin\zeta]^2}{\cos^2(\zeta \mp \alpha)} + H_{SC}\frac{\sec\beta}{1 + \tan\varepsilon \tan\beta \cos(\Delta\phi)} \qquad (2.3)$$

This equation is valid for $H_{SH} << a$ and is only applicable to observations in the plane of the sun ($\Delta\phi=0$). Refraction effects and the finite size of the sun are not taken into account. In this equation,

H_{SC} = atmospheric screening height

a = radius of the earth = 6361 km at 65°N

α = true solar depression angle

ζ = zenith angle of observation = $90^\circ - \theta$

θ = elevation angle of observation

$\varepsilon = \zeta - \gamma = (\zeta \mp \alpha) \pm \beta$

$\beta = \alpha \mp \gamma$ = solar depression angle at the cloud point measured

$\Delta\phi$ = angle between sun's azimuth and azimuth of observation

Wherever double signs appear in the above relations, the upper sign refers to the half plane between the observer and the sun ($\Delta\phi = 0°$) and the lower sign refers to $\Delta\phi = 180°$.

Using this equation, one can construct nomograms of H_{SH} versus θ and α for a given value of H_{SC}: Nomograms of this sort for H_{SC} = 0, 10, 15, 20, 25, 30 and 40 km are shown in Figs. 2.11 - 2.14. An examination of these curves show that in order for NLC (at 82 km) to disappear from view at SDA = 16° (as the observational results indicate) the appropriate value of H_{SC} must be around 20 km. If H_{SC} were much larger than this value, say 30 km, the NLC could not be illuminated at SDA = 16° even at the horizon.

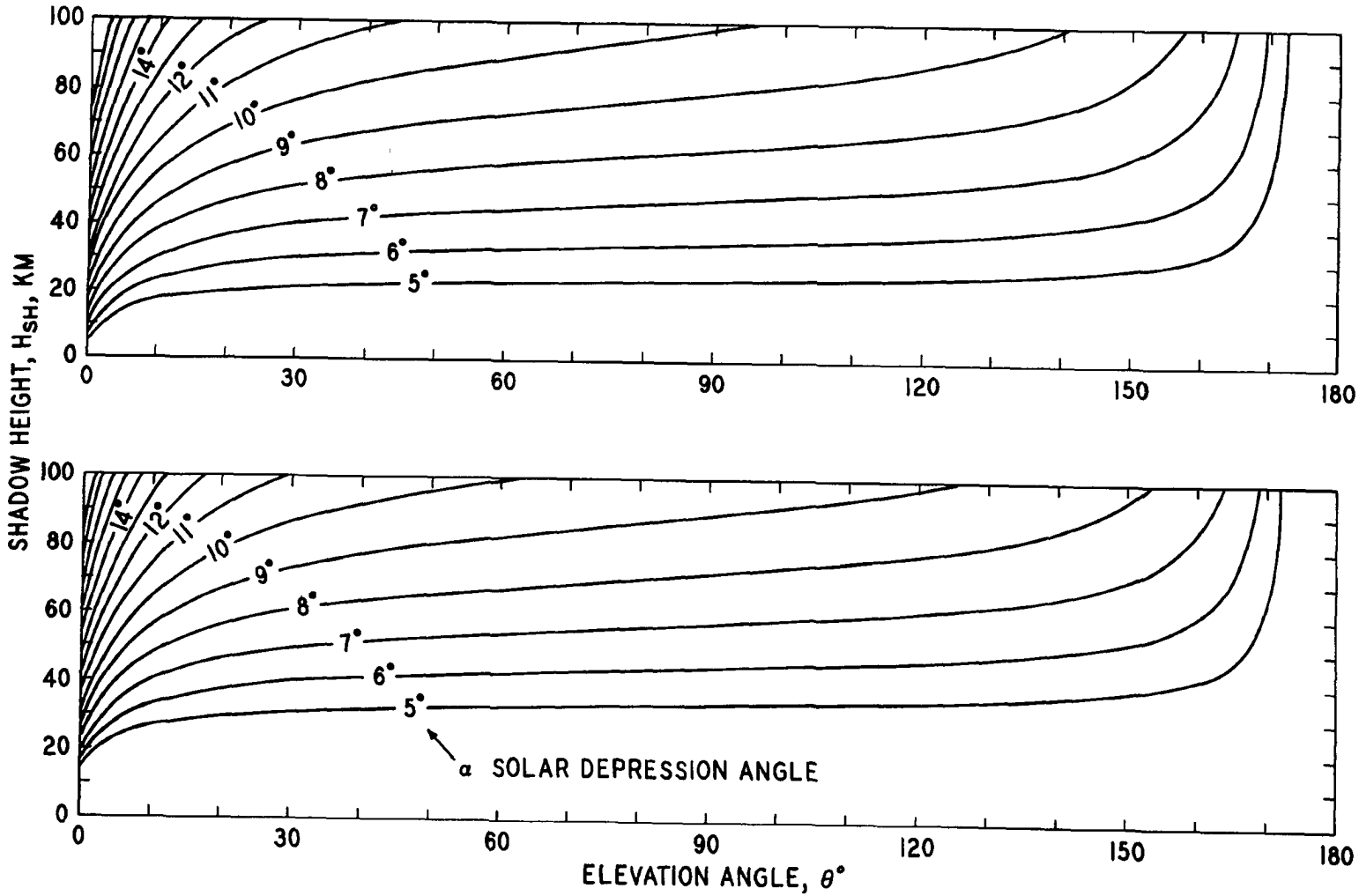

Fig. 2.11. Dependence of the shadow height in the sun-cloud-observer plane on elevation angle and solar depression angle for H_{SC} = 0 km and 10 km.

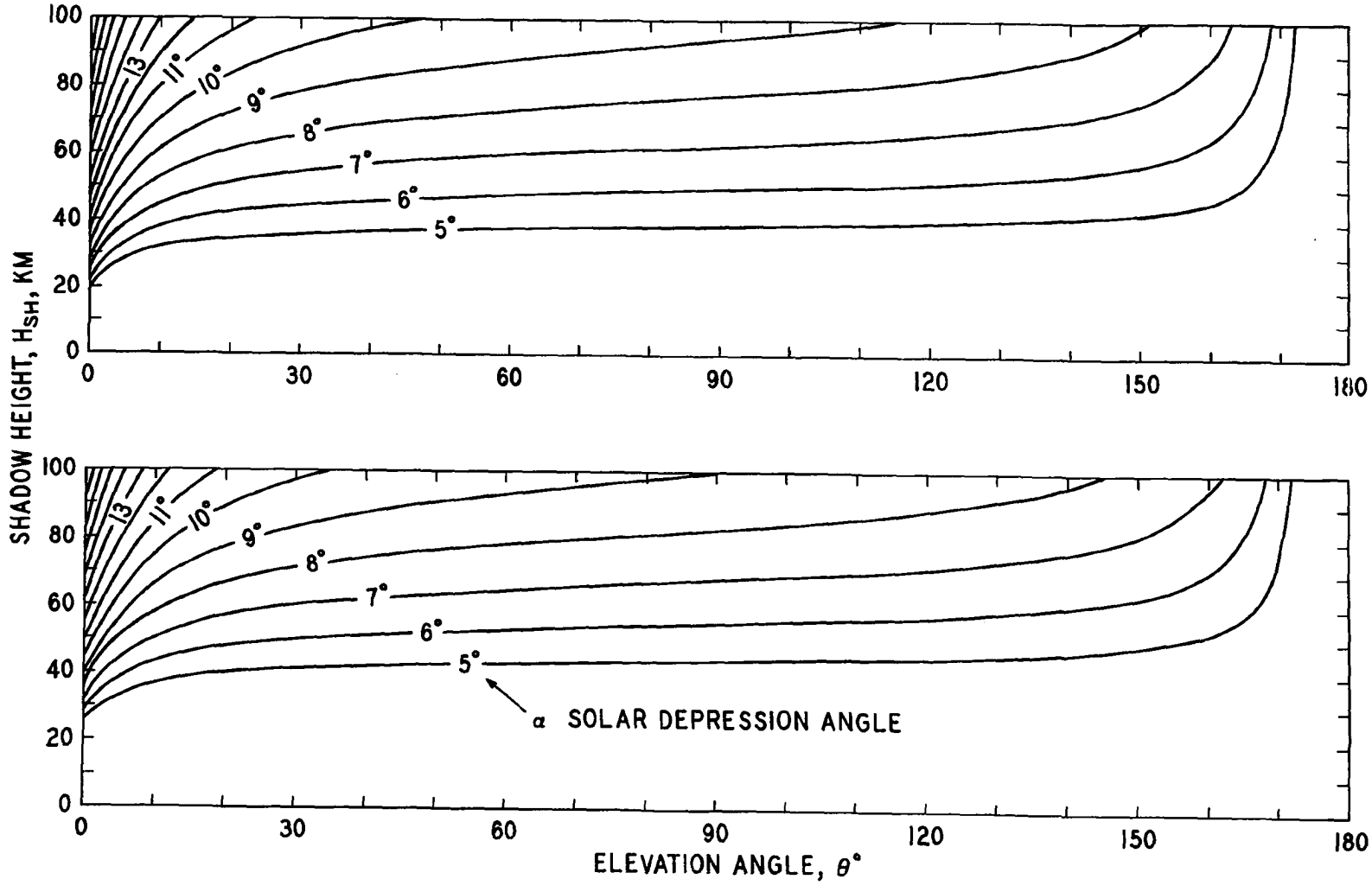

Fig. 2.12. Dependence of the shadow height in the sun-cloud-observer plane on elevation angle and solar depression angle for H_{SC} = 15 km and 20 km.

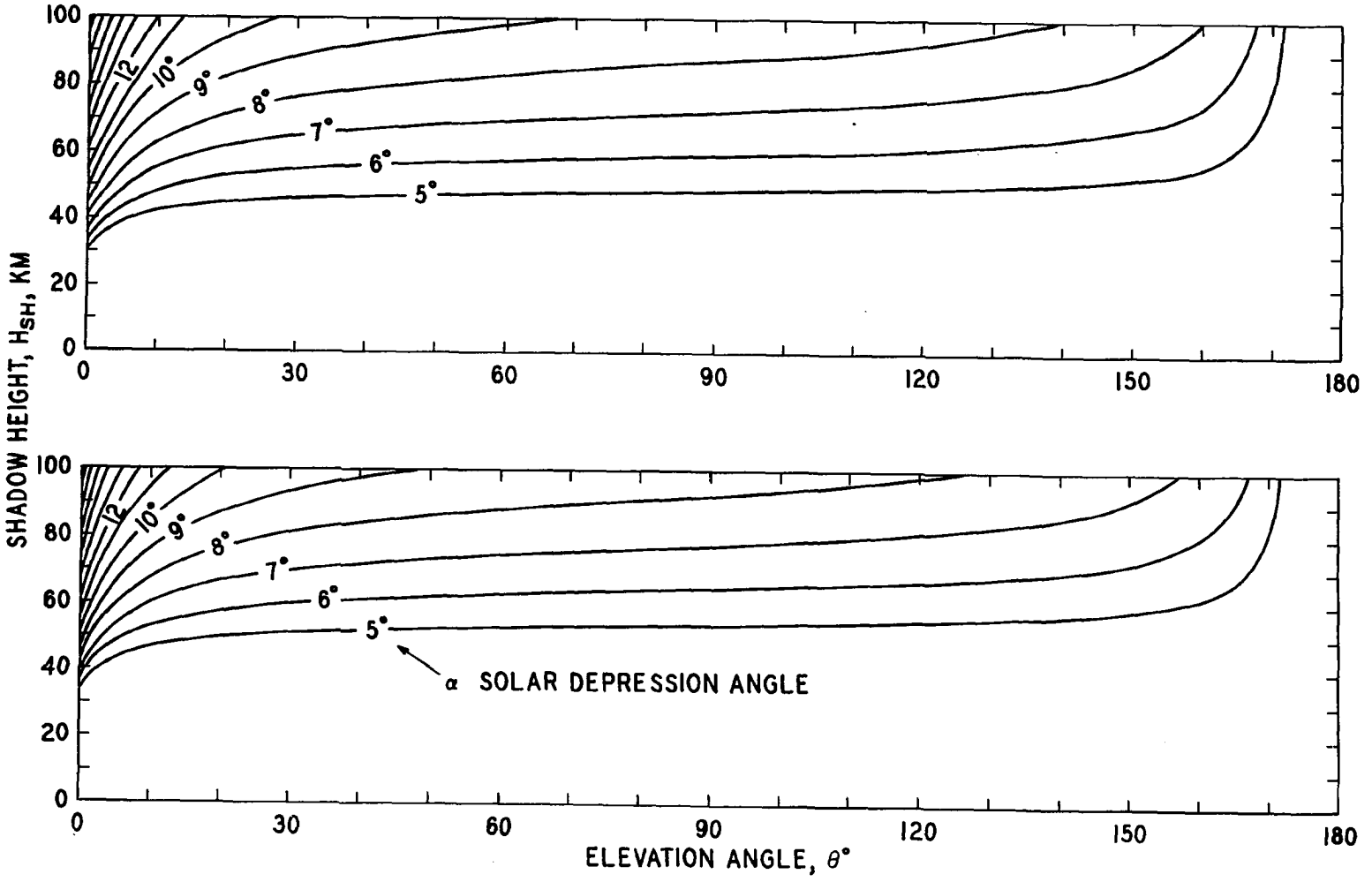

Fig. 2.13. Dependence of the shadow height in the sun-cloud-observer plane on elevation angle and solar depression angle for H_{SC} = 25 km and 30 km.

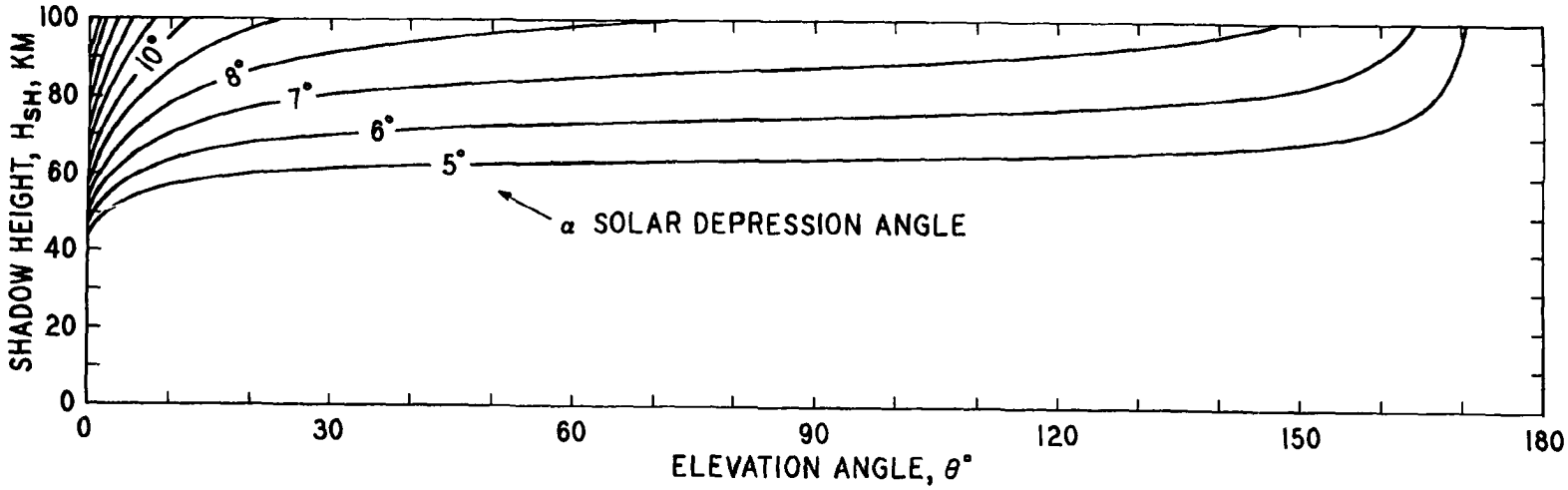

Fig. 2.14. Dependence of the shadow height in the sun-cloud-observer plane on elevation angle and solar depression angle for $H_{SC} = 40$ km.

A simple method for estimating the approximate shadow height of the solid earth at the observer's zenith is to square the solar depression angle (α) expressed in degrees, i.e. $H_{SH}(km)=\alpha^2$. This method gives fairly accurate results for small values (0 to 12°) of α.

2.3 Atmospheric Screening Height (H_{SC})

Sunlight passing closer to the earth than a distance H_{SC} (the atmospheric screening height) is severely attenuated by scattering and absorption in the atmosphere and does not have sufficient intensity to render NLC visible. The degree of extinction or screening of the incident beam by the atmosphere depends on the wavelength. For the far ultraviolet (1000 - 2000 Å), the effective screening height exceeds 100 km (Chamberlain, 1961), whereas for 5893 Å, H_{SC} 10 km (Hunten, 1956). As the intensity of NLC is strongest in the blue, one may expect H_{SC} to be between 10 and 100 km. In section 2.2 a value of 20 km was determined for H_{SC} from geometrical considerations. One can also determine the values of H_{SC} appropriate for NLC from measurements of its upper border (point K' in Fig. 2.1). Several such determinations made by Ludlam (1957) and Paton (1964) are given in Table 2.1 below.

TABLE 2.1

OBSERVED VALUES OF H_{SC}

Reference	Values of H_{SC} (km)
Ludlam (1957)	10,12,29,30,32,34,34,37,43,45,45,54
Paton (1964)	14,23,24,25,28

Ludlam's values range from 10 to 54 km and Paton's from 14 to 28 km. Since NLC do not always extend to elevation κ' only the minimum values are likely to be significant. A difficulty with measurements of this sort is that the upper border is not sharply defined. This leads to error in determining the correct elevation angle of the upper border and consequently error in the value of H_{SC}.

To facilitate determinations of H_{SC} by this method, a curve relating H_{SC} to the elevation angle of the upper border and to the solar depression angle is given in Fig. 2.15. It was derived from the H_{SH} curves for different values of H_{SC} (Figs. 2.11 - 2.14).

Assuming that H_{SC} = 20 km for NLC and that these clouds cannot be seen when H_{SH} <40 km because of the bright sky background, one can construct a diagram (Fig. 2.16) showing the angular elevation of the upper and lower borders of the NLC as a function of the solar depression angle. This diagram shows that NLC are likely to be visible only when the solar depression angle is between about 6° and 16°.

2.4 Range and Wavelength

Assuming the height of NLC to be constant at 82 km (see section 3.1), one can determine the distance (D) from the observer to the cloud, the distance (R) from the observer to the plan position of the cloud on the earth's surface, and the wavelength (S) present in NLC. Figure 2.17 illustrates the calculation of D, R, and S. Using triangle COP_1 in Fig. 2.17, one obtains for the distance D to the cloud:

$$(a + h)^2 = a^2 + D^2 - 2\,a\,D.\ \cos(90° + \theta) \qquad (2.4)$$

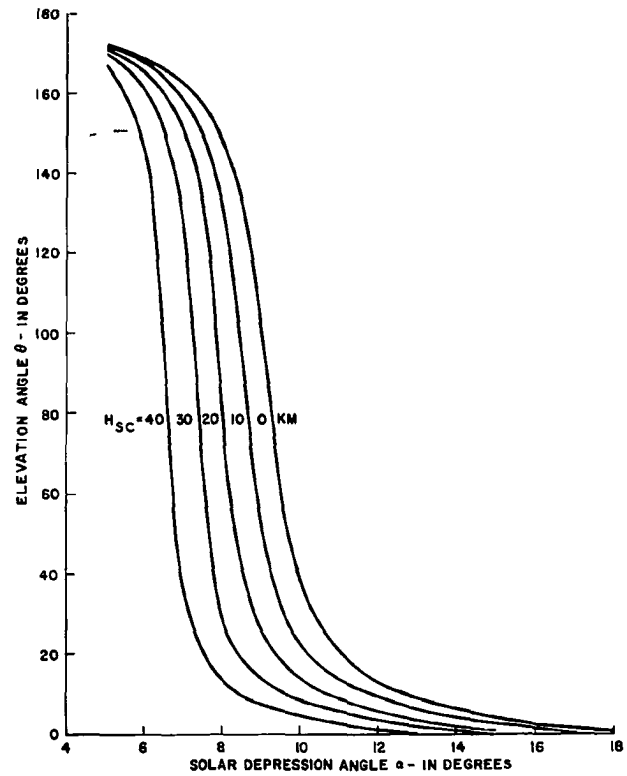

Fig. 2.15. Dependence of H_{SC} on solar depression angle and elevation angle of upper border of NLC.

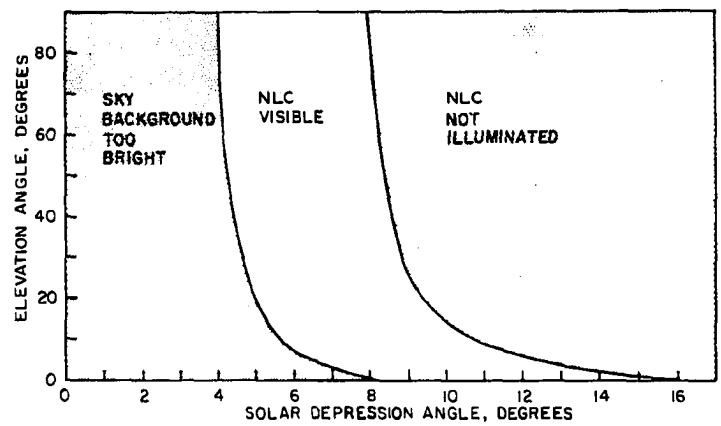

Fig. 2.16. Angular elevation of the upper and lower borders of the region (in the azimuth of the sun) in which NLC at 82 km may be seen as a function of the true solar depression angle.

Hence

$$D = \sqrt{h^2 + 2ah + a^2 \sin^2 \theta} - a \sin \theta \qquad (2.5)$$

where h = 82 km, a = 6361 km and θ = elevation angle

The expression for R is obtained by first applying the law of sines to triangle COP_1 to get γ:

$$\frac{D}{\sin \gamma} = \frac{a + h}{\sin(\theta + 90^\circ)}$$

$$\gamma = \arcsin \left[\frac{D \cos \theta}{a + h} \right] \qquad (2.6)$$

R is then

$$R \text{ (km)} = a \text{ (km)} \times \gamma \text{ (radians)} \qquad (2.7)$$

The expression for the wavelength, S is

$$S = (a + h)(\gamma_1 - \gamma_2) \qquad (2.8)$$

where γ is obtained from equation 2.6.

Solving equations 2.5, 2.7, and 2.8 with the aid of an electronic computer, curves of R vs θ, D vs θ, and S vs θ and $\Delta\theta$ were prepared and these are given in Figs. 2.18 and 2.19. These curves are of great practical use in mapping the projection of the cloud masses on the earth's surface and in determining the wavelengths in the clouds from measurements of the elevation angle and angular separation between the bands.

2.5 Visible area of NLC

The area of sunlit sky at 82 km visible to an observer varies markedly with solar depression angle as shown in Fig. 2.20. This

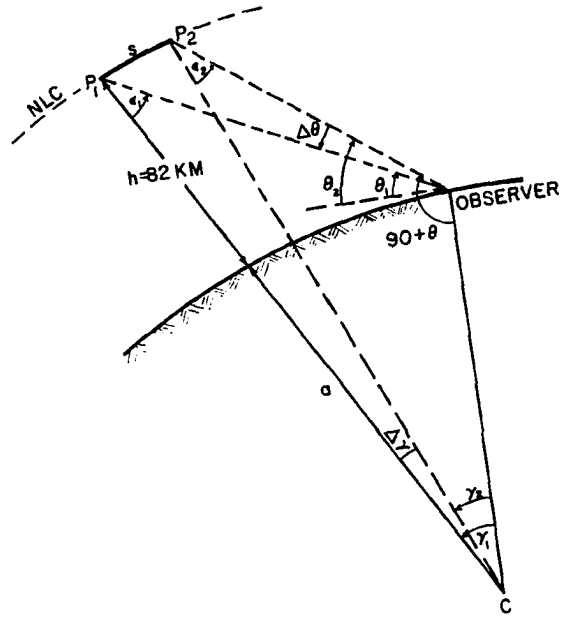

Fig. 2.17. Geometry of NLC observation illustrating the calculation of D, R, and S.

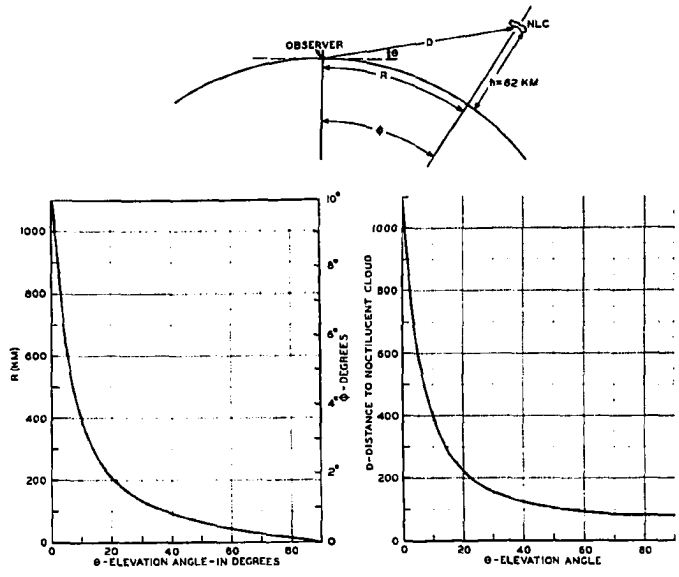

Fig. 2.18. Variation with elevation angle of the distance (D) from the observer to the cloud and the range (R) to the plan position of the cloud.

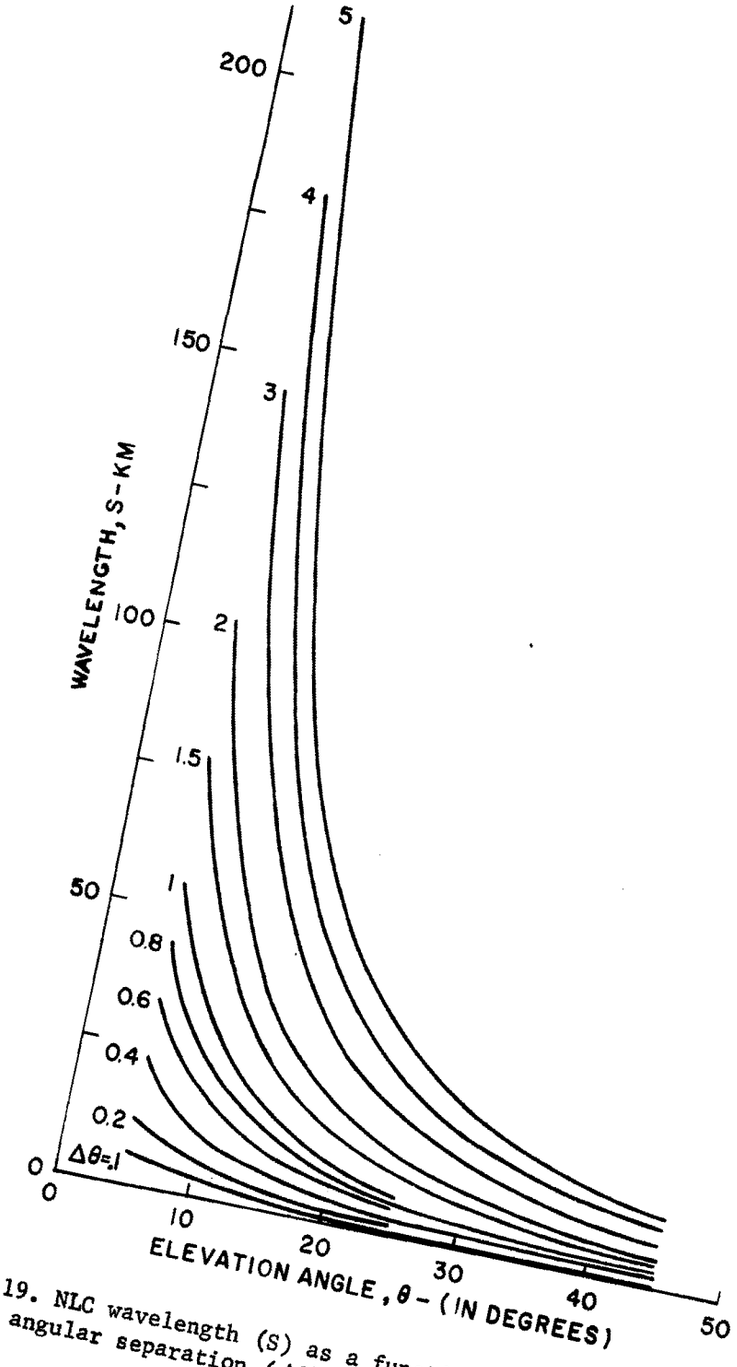

Fig. 2.19. NLC wavelength (S) as a function of elevation angle (θ) and the angular separation ($\Delta\theta$) between the bands.

diagram was derived from curves of H_{SH} vs θ and α with H_{SC} = 20 km. It shows the variation with solar depression angle (α) of the azimuth and elevation angles of the boundary of the sunlit 82 km region.

In analysing the NLC observational data from a number of stations, it is of interest to know over what range of latitudes and longitudes can NLC at 82 km be simultaneously observed on any night during the year. This can be determined from the curves of NLC observation times for different latitudes, examples of which are shown in Figs. 2.3 - 2.8. A diagram of this nature (Fig. 2.21) shows that NLC could be observed simultaneously from stations over a latitude range of around 10° and a longitude range of around 100° on the night of July 10 in the northern hemisphere. Later in the summer, on August 10, stations over a longitude range of about 130° can see NLC simultaneously. The variation with date of the range of latitudes and longitudes over which NLC may be simultaneously observed is given in Table 2.2.

TABLE 2.2

VARIATION WITH DATE OF THE RANGE OF LATITUDES AND LONGITUDES OVER WHICH NLC MAY BE SIMULTANEOUSLY OBSERVED IN THE NORTHERN HEMISPHERE

Date	Maximum latitude range	Maximum longitude range
20 June	10°	100°
10 July	10°	100°
20 July	10°	110°
30 July	10°	120°
10 August	10°	130°

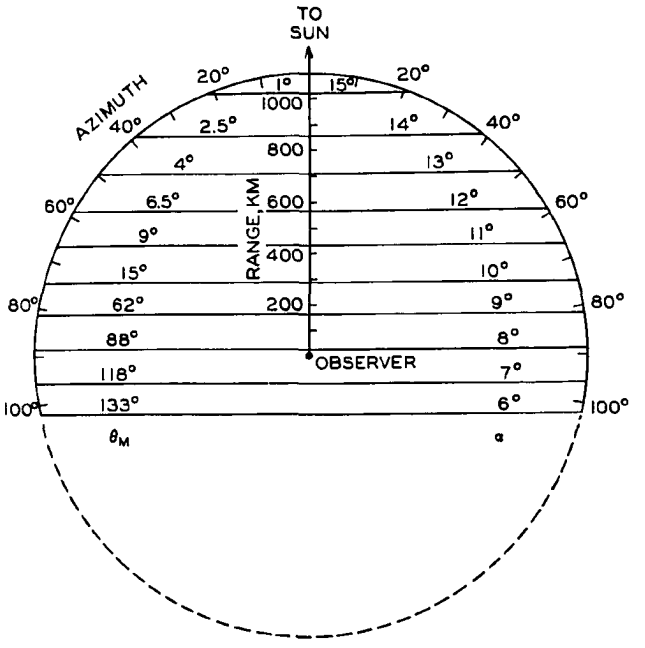

Fig. 2.20. The area of sky, visible from one station, over which the 82 km level can be illuminated for different values of the solar depression angle, α. θ_m is the maximum elevation angle of the upper border of the illuminated 82 km region. A screening height of 20 km is assumed.

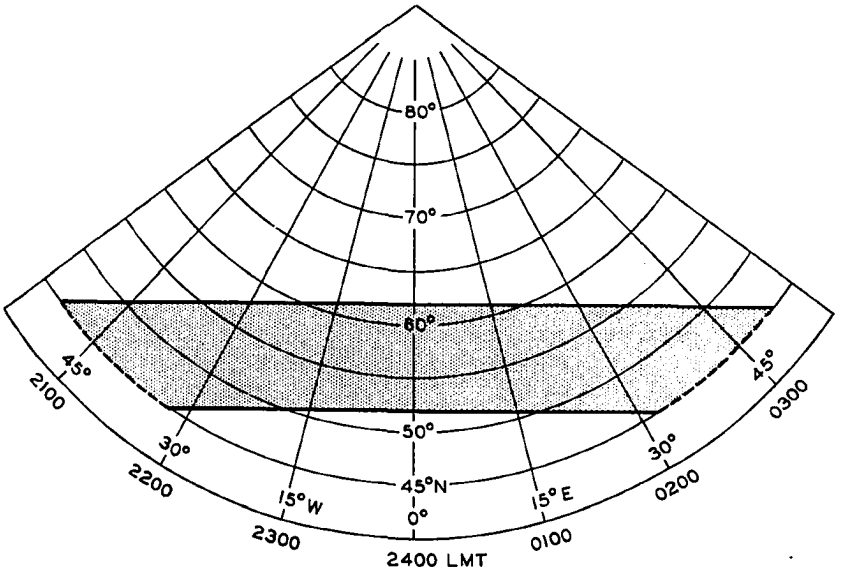

Fig. 2.21. Approximate area on earth's surface from which NLC at 82 km may be simultaneously observed on the night of July 10 in the northern hemisphere.

CHAPTER 3

CHARACTERISTICS OF NOCTILUCENT CLOUDS

Over the past 80 years many of the characteristics of NLC have been studied. Among these are the height, thickness, velocity, spatial extent, lifetime, dependence of frequency occurrence upon season and latitude, geographical distribution, number density and size distribution of particles in the clouds. There is much uncertainty associated with some of these characteristics, whose measurement is difficult. In their case additional and more accurate measurements are needed. In this chapter the present state of our knowledge of NLC is reviewed in detail.

3.1 The Height, Thickness, and Vertical Wave Amplitude

The most striking feature of NLC is their great height above the earth. Since 1885 more than 500 height determinations have been made (Jesse 1890, Jesse 1896, Størmer 1933, Størmer 1935, Paton 1949, Burov 1959, Witt 1962, also see Khvostikov 1952 for measurements by Tseraskii and by Pokrovskii). The values obtained (Table 3.1 and Fig. 3.1) range from 74 to 92 km, the average being 82.67 km. The lowest and highest values were obtained by Størmer in 1932. Part of this range of values is probably due to observational errors. Størmer (1933) found evidence of two layers of NLC in the display occurring on the night of 10 July 1932. He states "A stereoscopic view of two pictures from Oslo and Kongsberg gives the impression that the clouds were arranged in two layers of different altitude. This is in accordance with the measured heights, 83 and 84 km for the points

Table 3.1

Distribution of measured NLC heights

Height Interval	References: Jesse (1890)	Jesse (1896)	Størmer (1933)	Størmer (1935)	Burov (1959)	Total
73.5-74.5			2			2
74.5-75.5			3			3
75.5-76.5			1			1
76.5-77.5			1			1
77.5+78.5			3	1		4
78.5-79.5	16		3			19
79.5-80.5	32		2			34
80.5-81.5		44	4	7	8	63
81.5-82.5	15	68	4	15	8	110
82.5-83.5	32	118	3	11	4	168
83.5-84.5		19	3	6	4	32
84.5-85.5		3	2	1	6	12
85.5-86.5		10	1			11
86.5-87.5		10	0			10
87.5-88.5		15	2			17
88.5-89.5			1			1
89.5-90.5	13		1			14
90.5-91.5						0
91.5-92.5			1			1
92.5-93.5						0
93.5-94.5						0
Total Obs.	108	287	37	41	30	503
No. of Displays	3	8	2	1	1	15
Range (km) of Values	79.2-90.0	80.27-88.53	74-92	78-85	80.5-85.1	74-92
Mean (km)	82.17	83.04	81.4	82.2	82.6	82.67

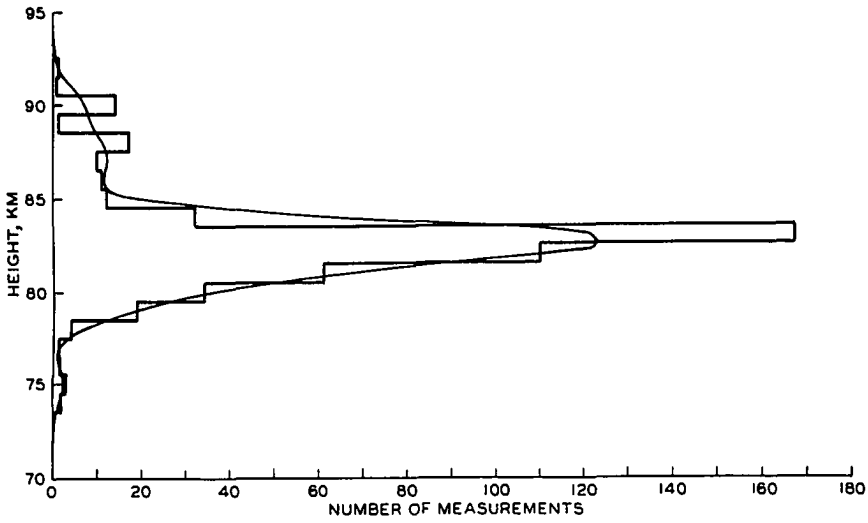

Fig. 3.1. Distribution of 503 NLC height measurements on 15 displays, values range from 74 to 92 km with the mean value being 82.67 km.

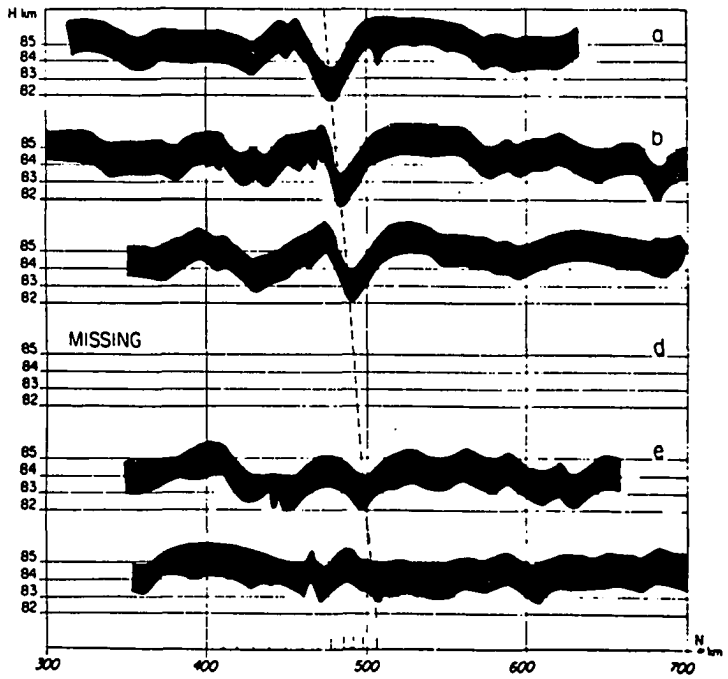

Fig. 3.2. Thickness and vertical wave amplitude of NLC (Witt, 1962).

2 and 3, and 88, 90, 92 km for the points 4, 5, and 6."

The height is determined from simultaneous photographs taken at two or more stations adequately separated. The procedure is the same as that developed by Størmer (1933) and Harang (1951) for auroral height determinations; also see Witt (1962), Brandy and Hill (1964), and Koenig and Brandy (1965). For good height determinations of NLC, base line distances and angle have to be measured very accurately. Optimum base line distances between the two stations are 20-50 km, and the best orientation of the base line is approximately east-west.

An optical radar device that Fiocco and Smullin (1963) have recently developed promises to be a valuable tool for height and thickness measurements of NLC. In the summer of 1964 Dr. Giorgio Fiocco of M.I.T. set up an optical radar unit to measure NLC heights at the Geophysical Institute's Ester Dome field site, near Fairbanks, Alaska. Unusually persistent overcast conditions prevailed over this station during that summer, and no useful NLC data were obtained.

NLC are so tenuous that it is difficult to measure the thickness, or even the vertical wave amplitude, which may be greater. The lower edge of NLC appears to be sharply defined whereas the upper one is diffuse. Witt's (1962) measurements suggest thicknesses of 2 km or less, perhaps only 1 km, and vertical wave amplitudes around 2 km, perhaps ranging up to 3 km. (Fig. 3.2). Measurements by Vassilyev (1961) indicate a thickness of 0.5 to 1 km and a vertical wave amplitude of 1 to 5 km.

3.2 Brightness, Color and Form

In brightness, NLC have a considerable range. Occasionally the

clouds are so bright as to cast shadows and allow the reading of ordinary printed matter outdoors. Usually however their brightness is low and they are so tenuous that stars shine through them almost undimmed. According to Khvostikov (1952) the upper limit of NLC brightness is 0.4 candles/cm^2. Sharanov (1960) gives the apparent albedo of NLC as 2.3×10^{-5} to 4.7×10^{-5}. Exposure times for photographing the NLC are mainly governed by the brightness of the sky background and the speed of the film and lens used. During weak to moderate displays in North America the clouds were photographed on high speed ektachrome (ASA 160) with exposures varying from 1/30 sec at a solar depression angle of 6° to as much as 30 seconds at a solar depression angle of 12° at an aperture of f/2.0.

The color of NLC is generally silvery white with a bluish tinge at high elevations and a yellowish or orange tinge near the horizon (see color photos in Fig. 1.1). Spectra of NLC show that these clouds scatter sunlight better at short wavelengths. This accounts for the silvery color of the clouds. Paton (1954) once observed a slow change of color in a NLC display from a vivid blue to white. This color change may have been due to the change in the color of the sky background, rather than a change in the color of the NLC. Measurements show that the light from NLC is strongly polarized in the same sense as, but less strongly than, the twilight sky, and this property is sometimes useful in distinguishing faint NLC from cirrus feebly illuminated by scattering from the twilight sky. NLC, particularly well developed displays, exhibit a variety of structural forms. At first appearance, these clouds are usually in the form of thin cirrus-like streaks seen against a diffuse bluish white structureless

background. Sometimes only one or two isolated bands are visible, while at other times the cloud elements are closely compacted in an almost continuous mass, resembling cirrocumulus or altocumulus undulatus. With the aid of binoculars the clouds may be detected as much as half an hour before they are visible to the naked eye. The forms observed in NLC have been described by various authors (Störmer 1933 and 1935, Vestine 1934, Grishin 1955, Ludlam 1957, Paton 1964, Fogle and Gotaas 1963, and Fogle 1965c). The classification is as follows:

I. Veil
II. Bands
III. Billows
IV. Whirls

Photographs of NLC with these forms are shown in Figs. 1.1 - 1.3.

Type I: Veils are very tenuous, lacking well-defined structure; they are often present as a background for other forms. They resemble cirrus clouds of uncertain shape, and occasionally show a faintly visible fibrous structure. The veils often flicker. They are the simplest form of NLC and often precede (by half an hour) the appearance of NLC with well-defined structure.

Type II: Bands are long streaks (sometimes hundreds of kilometers long) with diffuse edges (Type II.a) or sharply defined edges (Type II.b.). They often occur in groups arranged roughly parallel to each other or interwoven at small angles. Occasionally an isolated band is observed by itself. Little if any change with time is observed in bands. Blurred bands of little mobilitary are often the predominant structure in the noctilucent cloud field, particularly when the brightness is low. These bands are often

observed throughout the display (for several hours). They often move in a direction and with a speed that is different from that of the display as a whole. This form is perhaps the most striking feature of an NLC display. Sometimes smaller streaks with twists or bends may lie across the bands or branch out from them, giving the appearance of a feather. The distance separating pairs of bands ranges from tens of kilometers to over a hundred kilometers.

Occasionally very closely spaced and roughly parallel thin streaks (called serrations) are in the veil background. To the unaided eye they appear as an almost continuous cloud mass. The distance separating serrations is of the order of a few kilometers.

Type III: Billows are groups of closely spaced short bands. Billows may consist of straight and narrow, sharply outlined parallel short bands (Type III.a), or they may exhibit a wave-like structure in the short bands (Type III.b). The distance separating pairs of billows is of the order of 10 km. Billows often lie across the direction of the long bands and their alignment usually differs noticeably in neighboring parts of the sky. At other times they appear alone against the veil background. Unlike the long bands, billows may change their form and arrangement or appear and disappear within several minutes or tens of minutes.

Type IV: Whirls of varying degree of curvature are sometimes observed in the veil, band, and billow forms; on rare occasions complete rings with dark centers are formed. Whirls of small curvature (radius of 0.1° to 0.5°) are classified as Type IV.a. Whirls having the form of a simple bend of one or several bands with a radius of 3°-5° are

classified as Type IV.b. Large scale whirls are classified as Type IV.c.

Sometimes intersecting groups of long bands are observed. At the points of intersection, bright knots appear; they move at greater speeds and in different directions from the band systems. Determinations of the drift motion of NLC should not be made using these knots, as they do not represent the true motion of the air at NLC heights. The occurrence of these groups of intersecting bands has led to the speculation that they may be a double mesopause and two closely spaced layers of NLC. A few additional bits of evidence pointing to the possibility of a double mesopause have been obtained by Störmer (1933) and by Schilling (1964). Precision height measurements of the individual bands of the two intersecting groups should settle the question of whether or not there are sometimes two layers of NLC.

In complex displays, two or more (sometimes all) of the above forms are observed simultaneously. A powerful method for examining the structural changes and the growth and decay of NLC is to use time-lapse photography. The NLC features change so slowly and at such a distance from the observer that they are almost imperceptable to the naked eye, and it is only with the help of time-lapse motion pictures that one can obtain information on the evolution of the structural details. During the course of our work on NLC over North America and in the southern hemisphere, we have obtained time-lapse films of 29 NLC displays. These films show the complicated wave motions and the evolution of the various forms in NLC. Measurement of the velocity, wavelength, and lifetimes of the various forms have been made from these films. They have also proved to be an invaluable

aid in training NLC observers. To make these time-lapse films, we used a 16 mm Bolex fitted with a solenoid operated pulsing unit. Exposure time ranged from 4 to 6 seconds/frame depending on the display. High speed ektachrome film (ASA 160) and a fast lens (25 mm Angenieux f0.95) were used.

3.3 Variation of NLC Occurrence with Season, Latitude, Longitude, and Year

Since the first recorded observation of NLC in the summer of 1885 over a thousand occurrences have been reported. Prior to 1957, the observational material consisted of either irregular series or random individual observations. Beginning in 1957 with the IQSY, a successful effort to put NLC observations on a systematic basis was initiated so that now routine observations of these clouds are being made at most of the meteorological stations in the northern and southern hemispheres between 45 and 90° latitude. Systematic NLC observations have been made in Scotland, Sweden, and the USSR since 1957, in North America since 1962, and in the southern hemisphere since 1964. The observational data is being collected and analysed at three centers: College, Alaska (for the data from North America, Greenland and Iceland, and all the southern hemisphere); Edinburgh, Scotland (for the data from the North Atlantic and Europe), and Tartu, Estonia (for the data from the USSR). An effort is now being made by the three centers, with the assistance of WMO, to standardize the procedures for observing and reporting NLC, and to put NLC observations by all meteorological stations in high latitudes on a permanent basis. The systematic NLC observations made to date allow one to determine the variation of NLC occurrence with season, latitude, longitude, and

year. These features are discussed below.

3.3.1: Variation of NLC Occurrence with Season

The total number of reports of NLC displays over North America since the first observation in 1933 by Vestine (1934) is 148. A number of additional reports had to be discarded because of insufficient documentation or because they were definitely not NLC. Twelve of the 148 displays were observed prior to 1962 when our work on NLC began. Five displays were observed in 1962, 25 in 1963, 57 in 1964, and 49 in 1965. The increase in the reported number of displays observed per year from 1962 to 1964 is probably due to the increase in the number of observing stations and the increased latitudinal and longitudinal extent of the network of these observing stations, rather than a real increase in the frequency of occurrence of NLC. The number of stations making NLC observations over North America during the years 1962-1965 is given below:

1962: 2 stations in Alaska
1963: 51 stations in Alaska and Western Canada
1964: 90 stations in Alaska and Canada
1965: 105 stations in Alaska, Canada, Greenland and Iceland

The network of stations now operating over North America, Greenland, and Iceland is shown in Fig. 1.5.

To determine the apparent frequency of observed occurrence of NLC with season over North America, all the observations (see Table 3.2), independent of latitude and longitude were grouped into ten day intervals, and the number of displays per ten day interval was determined. The results obtained are shown in Fig. 3.3 in the form of a histogram and a smoothed curve. The smoothed curve was derived from the

Table 3.2

Noctilucent Cloud Sightings from North America, 1933-1965

Year	Night of	Observing Station	Geographic Coordinates Lat.	Long.
1933	20 July	Meanook	54.6° N	113.3° W
1956	26 June	Edmonton	53.6	113.5
	27 June	"	"	"
	28 June	"	"	"
1957	27 July	Anchorage	61.2	150
		Gulkana	62.2	145.5
	7 Aug	Anchorage	61.2	150
1958	1 June	Gimli	51	97
	12 Aug	Yellowknife	62.5	114.6
1959	3 July	S.S. Lismorice	50	63
1960	8 Aug	Anchorage	61.2°	150.0
1961	23 July	Saskatoon	52.2	106.6
	13 Sept	Arlis II Ice Island	76.3	170.6
1962	6 May	Anchorage	61.2	150
	11 Aug	"	"	"
	13 Aug	College	64.9	148
	14 Aug	"	"	"
	16 Aug	"	"	"
1963	1 May	Juneau	58.4	134.6
	26 June	Saskatoon	52.2	106.6
	28 June	Anchorage	61.2	150
	1 July	Schefferville	54.8	66.8
	3 July	Ft. Churchill	58.7	94.1
	4 July	"	"	"
	5 July	"	"	"
	8 July	Juneau	58.4	134.6
		Yakutat	59.5	139.7
	9 July	Lower Tonsina	61.5	144.5
	11 July	Aniak	61.6	159.6
	12 July	Aniak	"	"
		Anchorage	61.2	150
	13 July	"	"	"
	22 July	Sitka	57	135.4
		Juneau	58.4	134.6
		Gustavus	58.4	135.7
	25 July	Northway	63	142
	27 July	College	64.9	148
	31 July	Edmonton	53.6	113.5
		Grande Prairie	55.2	119
		Peace River	56.2	117.3
		Beatton River	57.3	121.5
		Ft. Nelson	58.8	122.7
		Watson Lake	60.2	129.2
		Ft. Simpson	62.2	121.5
	1 Aug	Watson Lake	60.2	129.2
	5 Aug	Ft. Nelson	58.8	122.7
		Smith River	59.9	126.5
		Watson Lake	60.2	129.2
		College	64.9	148

Year	Night of	Observing Station	Geographic Coordinates Lat.	Long.
1963	6 Aug	Whitehorse	60.6 N	135.3 W
		Northway	63	142
		Nenana	64.5	149.1
		College	64.9	148
		Tanana	65.2	152.1
	8 Aug	Northway	63	142
	11 Aug	Juneau	58.4	135.6
		Gustavus	58.4	135.7
		Ft. Nelson	58.8	122.7
		Yakutat	59.5	139.7
		Homer	59.6	151.5
		Watson Lake	60.2	129.2
		Whitehorse	60.6	135.3
		Kenai	60.6	151.3
		Anchorage	61.2	150
		Tonsina	61.5	145.1
		Gulkana	62.1	145.4
		Farewell	62.5	153.9
		Summit	63.4	149.1
		Minchumina	63.8	152
		Big Delta	64.3	145.8
		College	64.9	148
		Tanana	65.2	152.1
	12 Aug	Juneau	58.4	135.6
		Yakutat	59.5	139.7
		Cordova	60.5	145.5
		Whitehorse	60.6	135.3
		Bethel	60.8	161.7
		Anchorage	61.2	150
		Mayo	61.3	135.7
		Aniak	61.6	159.6
		Aishihik	61.7	137.8
		Gulkana	62.1	145.4
		Talkeetna	62.3	150.1
		Farewell	62.5	153.9
		Snag	62.5	140.3
		Northway	63	142
		McGrath	63	155.6
		Summit	63.4	149.1
		Minchumina	63.8	152
		Big Delta	64.3	145.8
		Nenana	64.5	149.1
		Galena	64.7	156.9
		College	64.9	148
		Tanana	65.2	152.1
	16 Aug	Jet Aircraft	10 W to 63 N to	80 W 66 N
	18 Aug	Nenana	64.5	149.1
		College	64.9	148
	28 Sept	College	64.9	148

Year	Night of	Observing Station	Geographic Coordinates Lat.	Long.
1964	26 April	Montreal	45.5 N	73.7 W
	28 April	College	64.9	148.0
		Coral Harbour	64.1	83.2
		Goose Bay	53.4	60.5
	30 April	Prince Albert	53.5	105.6
		Goose Bay	53.4	60.5
	3 May	Ft. Chipewyan	58.8	111.2
	9 May	Goose Bay	53.4	60.5
		Ft. Chimo	58.2	68.3
	11 May	Iliamna	59.7	154.9
	17 May	Ft. Chimo	58.2	68.3
	2 June	Ft. Churchill	58.7	94.1
	5 June	Ft. Chimo	58.2	68.3
	9 June	Calgary	51.0	114.1
		Brochet	58.1	101.6
	10 June	Goose Bay	53.4	60.5
	11 June	Juneau	58.4	134.6
		Sitka	57.1	135.3
	12 June	Ft. Chimo	58.2	68.3
	15 June	Big Trout Lake	53.8	90.1
		Lufthansa	Frankfurt - U.S.	
	20 June	Knob Lake	54.8	66.8
	21 June	Saskatoon	52.2	106.6
		Prince Albert	53.5	105.6
	23 June	Watson Lake	60.2	129.2
	24 June	Prince George	53.9	122.5
		Watson Lake	60.2	129.2
	28 June	The Pas	54.0	101.1
		Peace River	56.2	117.3
		Ft. Chipewyan	58.8	111.2
		Brochet, Man.	58.1	101.6
		Big Trout Lake	53.8	90.1
		Prince Albert	53.5	105.6
		Saskatoon	52.2	106.6
		Ft. Smith	60.1	112.2
	29 June	Cold Lake	54.5	110.1
		Edmonton	53.6	113.5
		Ft. McMurray	53.7	110.4
		Ft. Chipewyan	58.8	111.2
		Grande Prairie	55.2	119.0
		Ft. St. John	56.2	120.8
		Ft. Nelson	58.8	122.7
		Saskatoon	52.2	106.6
		Rivers	50.0	100.2
		Calgary	51.0	114.1
		The Pas	54.0	101.1
		Peace River	56.2	117.3
		Brochet	58.1	101.6
		Big Trout	53.8	90.1
		Winnipeg	50.0	97.2
		Lethbridge	49.7	112.8
		Lufthansa	Frankfurt - U.S.	

Year	Night of	Observing Station	Geographic Coordinates Lat.	Long.
1964	30 June	Whitehorse	60°.6 N	135°.3 W
		Victoria	48.4	123.2
		Edmonton	53.6	113.5
		Calgary	51.0	114.1
		Ft. Nelson	58.8	122.7
		The Pas	54.0	101.1
		Battle Harbour	52.2	55.9
		Saskatoon	52.2	106.6
		Prince Albert	53.5	105.6
		Kenai	60.6	151.3
		Homer	59.6	151.5
	1 July	Ft. St. John	56.2	120.8
		Ft. Nelson	58.8	122.7
		Prince George	53.9	122.5
		Edmonton	53.6	113.5
		Peace River	56.2	117.3
	4 July	Saskatoon	52.2	106.6
		Knob Lake	54.8	66.8
		Ft. Chimo	58.2	68.3
	5 July	Watson Lake	60.2	129.2
		Whitehorse	60.6	135.3
		Peace River	56.2	117.3
		Brochet	58.1	101.6
		Goose Bay	53.4	60.5
		Ft. Nelson	58.8	122.7
		Lufthansa	Frankfurt - U.S.	
		Nitchequon	53.2	70.8
		Knob Lake	54.8	66.8
		Big Trout Lake	53.8	90.1
		Ft. Chimo	58.2	68.3
	6 July	Edmonton	53.6	113.5
		Goose Bay	53.4	60.5
		Ft. Nelson	58.8	122.7
		Yakutat	59.5	139.7
	7 July	Knob Lake	54.8	66.8
	8 July	Ft. Chipewyan	58.8	111.2
		Edmonton	53.6	113.5
		Peace River	56.2	117.3
		Juneau	58.4	134.6
		Knob Lake	54.8	66.8
		Prince Albert	53.5	105.6
		Ft. Smith	60.1	112.2
	10 July	Ft. Nelson	58.8	122.7
	11 July	Edmonton	53.6	113.5
		Ft. Chipewyan	58.8	111.2
		Ft. Nelson	58.8	122.7
		Watson Lake	60.2	129.2
		Ft. McMurray	53.7	110.4
		Whitehorse	60.6	135.3
		Calgary	51.0	114.1
		Peace River	56.2	117.3

Year	Night of	Observing Station	Geographic Coordinates Lat.	Long.
1964	11 July	Knob Lake	54.8 N	66.8 W
		Saskatoon	52.2	106.6
		Ft. Churchill	58.7	94.1
	12 July	Saskatoon	52.2	106.6
		Calgary	51.0	114.1
		Edmonton	53.6	113.5
		Ft. St. John	56.2	120.8
		Watson Lake	60.2	129.2
		Ft. Nelson	58.8	122.7
		Beatton River	57.3	121.5
		Peace River	56.2	117.3
	13 July	Ft. Chipewyan	58.8	111.2
		Hay River	60.8	115.8
		Ft. Smith	60.1	112.2
		Ft. Nelson	58.8	122.7
		Ft. St. John	56.2	120.8
		Beatton River	57.3	121.5
		Watson Lake	60.2	129.2
		Edmonton	53.6	113.5
	15 July	Homer	59.6	151.5
		Gustavus	58.4	135.7
		Ft. Churchill	58.7	94.1
	16 July	Williams Lake	52.2	122.1
		Whitehorse	60.6	135.3
		Snag	62.4	140.4
		Watson Lake	60.2	129.2
		Saskatoon	52.2	106.6
		Pan American Airways	64 N,147 W -	55 N, 130 W
		Alaska Airlines	63	142
		Sparrevohn	61.1	155.6
		Mayo	63.6	135.9
		Prince Albert	53.5	105.6
		Gustavus	58.4	135.7
		Anchorage	61.2	150.0
		Kenai	60.6	151.3
		Homer	59.6	151.5
		Elmendorf, AFB	61.2	149.9
	17 July	Sparrevohn	61.1	155.6
		Gulkana	62.1	145.4
		Yakutat	59.5	139.7
		Talkeetna	62.3	150.1
		Nenana	64.5	149.1
	21 July	Pan American Airways	Fairbanks - Seattle	
		Alaska Airlines	Fairbanks - Seattle	
		Gulkana	62.1	145.4
		College	64.9	148.0
		Whitehorse	60.6	135.3
		Knob Lake	54.8	66.8
		Lake Minchumina	63.8	152.0

Year	Night of	Observing Station	Geographic Coordinates Lat.	Long.
1964	22 July	Ft. Simpson	61.9° N	121.3° W
		Ft. Nelson	58.8	122.7
		Watson Lake	60.2	129.2
		Knob Lake	54.8	66.8
		Beatton River	57.3	121.5
		Gulkana	62.1	145.4
		Pan American Airways	Fairbanks - Seattle	
		Ft. Chimo	58.2	68.3
	23 July	Ft. Chipewyan	58.8	111.2
		Ft. Smith	60.1	112.2
		Edmonton	53.6	113.5
		Yellowknife	62.5	114.6
		Ft. Nelson	58.8	122.7
		Nitchequon	53.2	70.8
		Ft. Chimo	58.2	68.3
		Watson Lake	60.2	129.2
	24 July	Ft. Nelson	58.8	122.7
		Watson Lake	60.2	129.2
		Beatton River	57.3	121.5
		Hay River	60.8	115.8
		Yellowknife	62.5	114.6
		Ft. Simpson	61.9	121.3
		Goose Bay	53.4	60.5
		Nitchequon	53.2	70.8
		Gulkana	62.1	145.4
		College	64.9	148.0
		Ft. Smith	60.1	112.2
	25 July	Ft. Smith	60.1	112.2
		Lufthansa	Frankfurt - U.S.	
	26 July	Yellowknife	62.5	114.6
		Ft. Simpson	61.9	121.3
		College	64.9	148.0
		Ft. Nelson	58.8	122.7
		Nitchequon	53.2	70.8
		Watson Lake	60.2	129.2
	27 July	Terrace	54.6	128.5
		Ft. Nelson	58.8	122.7
		Sparrevohn	61.1	155.6
		Watson Lake	60.2	129.2
	28 July	Kenai	60.6	151.3
		McKinley Park	63	148
		Northway	62.6	142.0
		Anchorage	61.2	150.0
		Homer	59.6	151.5
		Ft. Smith	60.1	112.2
		Watson Lake	60.2	129.2
		Ft. Chimo	58.2	68.3
	29 July	Ft. Simpson	61.9	121.3
		Gulkana	62.1	145.4
		Ft. Chipewyan	58.8	111.2

Year	Night of	Observing Station	Geographic Coordinates Lat.	Long.
1964	30 July	Ft. Smith	60.1° N	112.2° W
		Ennadai Lake	61.0	101.3
		Brochet	58.1	101.6
		Ft. Churchill	58.7	94.1
	1 Aug	Lake Minchumina	63.8	152.0
		Ft. Chimo	58.2	68.3
	2 Aug	Yellowknife	62.5	114.6
		Ft. Nelson	58.8	122.7
		Watson Lake	60.2	129.2
		Smith River	59.9	126.5
		Ft. Simpson	61.9	121.3
		College	64.9	148.0
		Big Delta	64.0	145.7
		The Pas	54.0	101.1
		Whitehorse	60.6	135.3
		Ft. Churchill	58.7	94.1
		Ft. Smith	60.1	112.2
		Lake Minchumina	63.8	152.0
		Ft. Chimo	58.2	68.3
	3 Aug	Ft. Nelson	58.8	122.7
		Beatton River	57.3	121.5
		Ft. Chipewyan	58.8	111.2
		Nome	64.5	165.4
		Pan American Airways	64.0	145.7-
		Pan American Airways	62.6	142.0
		Kotzebue	66.9	162.6
		Ft. Churchill	58.7	94.1
		Ennadai Lake	61.0	101.3
	6 Aug	College	64.9	148.0
		Reykjavik	64.1	21.9
		Eyrarbakki	63.8	21.1
		Keflavik	64.0	22.6
	7 Aug	Pan American Airways	64	145
		Sparrevohn	61.1	155.6
		Lake Minchumina	63.8	152.0
		Summit	63.3	149.1
		Keflavik	64.0	22.6
	8 Aug	Pan American Airways	64.0	145.7
		Gulkana	62.1	145.4
		Northway	62.6	142.0
		Tanana	65.2	152.1
		Kotzebue	66.9	162.6
		Fairbanks	64.8	147.9
		Ennadai Lake	61.0	101.3
		Hall Beach	68.5	82.5
	9 Aug	College	64.9	148.0
		Lake Minchumina	63.8	152.0
		Ennadai Lake	61.0	101.3
		Aniak	61.6	159.6
		Ft. Churchill	58.7	94.1

Year	Night of	Observing Station	Geographic Coordinates Lat.	Long.
1964	11 Aug	Edmonton	53.6 N	113.5 W
		Tin City	65.5	168.0
		Nome	64.5	165.4
		Kotzebue	66.9	162.6
	13 Aug	Pan American Airways	63.6	144.3
		Gulkana	62.1	145.4
		Alaska Airlines	63	143
		Wien Alaska Airlines	66.0	153.7
		Wien Alaska Airlines	64.8	147.9
		Ft. Nelson	58.8	122.7
		Whitehorse	60.6	135.3
		Barrow	71.3	156.8
		Aniak	61.6	159.6
		Nome	64.5	165.4
		Kotzebue	66.9	162.6
	20 Aug	Ft. Churchill	58.7	94.1
	29 Aug	Dawson	64.1	139.0
		Big Trout Lake	53.8	90.1
	30 Aug	Big Trout Lake	53.8	90.1
1965	1 April	Great Whale River	55.3	77.5
		Hall Beach	68.5	82.5
	28 May	Calgary	51.0	114.1
		Churchill	58.7	94.1
	3 June	Edmonton	53.6	113.5
		Whitecourt	54.2	115.7
		Smithers	54.9	127.2
		Grande Prairie	55.2	119.0
		Ft. St. John	56.2	120.8
	12 June	Ft. Nelson	58.8	122.7
	13 June	Prince George	53.9	122.5
		Whitecourt	54.2	115.7
		Grande Prairie	55.2	119.0
		Peace River	56.2	117.3
		Ft. Chipewyan	58.8	112.2
		Ft. Nelson	58.8	122.7
		Ft. Smith	60.1	112.2
	15 June	Edmonton	53.6	113.5
		Big Trout Lake	53.8	90.1
		Grande Prairie	55.2	119.0
	16 June	Grande Prairie	55.2	119.0
		Wagner	55.3	115.0
		Peace River	56.2	117.3
		Ft. Nelson	58.8	122.7
	19 June	Edmonton	53.6	113.5
		Smithers	54.9	127.2
		Wagner	55.3	115.0
	20 June	Prince George	53.9	122.5
		PAA-Annette Island	55	132
		Wagner	55.3	115.0
		Beatton River	57.3	121.5

Year	Night of	Observing Station	Geographic Coordinates Lat.	Long.
1965	24 June	Ft. Nelson	58.8° N	122.7° W
	25 June	Ft. Churchill	58.7	94.1
	26 June	Ft. Churchill	58.7	94.1
	29 June	Edmonton	53.6	113.5
		Prince George	53.9	122.5
		Smithers	54.9	127.2
		Grande Prairie	55.2	119.0
		Wagner	55.3	115.0
		Ft. St. John	56.2	120.8
		Beatton River	57.3	121.5
		Ft. Churchill	58.7	94.1
		Ft. Nelson	58.7	122.8
	30 June	Nitchequon	53.2	70.8
		Goose Bay	53.4	60.5
	1 July	Goose Bay	53.4	60.5
		Grande Prairie	55.2	119.0
		Wagner	55.3	115.0
	3 July	Brochet	58.1	101.6
		Ft. Churchill	58.7	94.1
	4 July	Goose Bay	53.4	60.5
		Knob Lake	54.8	66.8
		Grande Prairie	55.2	119.0
		Ft. Churchill	58.7	94.1
	5 July	Goose Bay	53.4	60.5
		Cold Lake	54.5	110.1
		Grande Prairie	55.2	119.0
		Ft. St. John	56.2	120.8
		Peace River	56.2	117.3
		Beatton River	57.3	121.5
		King Salmon	58.7	156.5
		Ft. Nelson	58.8	122.7
	6 July	Winnipeg	50.0	97.2
		Saskatoon	52.2	106.6
		Prince Albert	53.5	105.6
		Edmonton	53.6	113.5
		Whitecourt	54.2	115.7
		Grande Prairie	55.2	119.0
		Wagner	55.3	115.0
		Peace River	56.2	117.3
		PAA-Five Fingers Island	57.2	133.7
		Ft. Churchill	58.7	94.1
		Ft. Chipewyan	58.8	111.2
		PAA-Haines	59	130
		Ft. Smith	60.1	112.2
	7 July	PAA-Port Hardy	51	128
		Prince Albert	53.5	105.6
		Edmonton	53.6	113.5
		Sitka	57.1	135.3
		PAA-Juneau	58.4	134.6
		Ft. Chipewyan	58.8	111.2
		Ft. Smith	60.1	112.2
	8 July	Saskatoon	52.2	106.6

Year	Night of	Observing Station	Geographic Coordinates Lat.	Long.
1965	10 July	Ft. Nelson	58.8° N	122.7° W
		Whitehorse	60.6	135.3
	11 July	Lethbridge	49.7	112.8
		Prince Albert	53.5	105.6
		Edson	53.6	116.5
		Grande Prairie	55.2	119.0
		PAA-Juneau	58.4	134.6
		King Salmon	58.7	156.5
		Ft. Nelson	58.8	122.7
		PAA-Atlin	59.6	133.7
		Bethel	60.8	161.7
	12 July	Williams Lake	52.2	122.1
		PAA-Ethelda Bay	53	130
		Edmonton	53.6	113.5
		Prince George	53.9	122.5
		Whitecourt	54.2	115.7
		Grande Prairie	55.2	119.0
		Ft. St. John	56.2	120.8
		Peace River	56.2	117.3
		Beatton River	57.3	121.5
		Ft. Chipewyan	58.8	111.2
		Ft. Nelson	58.8	122.7
		PAA-Haines	59	130
		Whitehorse	60.6	135.3
	13 July	Saskatoon	52.2	106.6
		Prince Albert	53.5	105.6
		Ft. Nelson	58.8	122.7
	14 July	Sipewisk	-	-
		Boyd	56	96
		Ilford	56	95
		Peace River	56.2	117.3
		Beatton River	57.3	121.5
		Ft. Chipewyan	58.8	111.2
		PAA-Haines	59	130
		Whitehorse	60.6	135.3
		Dawson	64.1	139.0
	15 July	Calgary	51.0	114.1
		Edmonton	53.6	113.5
		Edson	53.6	116.5
		Prince George	53.9	122.5
		Grande Prairie	55.2	119.0
		Peace River	56.2	117.3
		Brochet	58.1	101.6
		PAA-Juneau	58.4	134.6
		Ft. Chipewyan	58.8	111.2
		Ft. Nelson	58.8	122.7
		PAA	61.7	139.0
	16 July	Calgary	51.0	114.1
		Knob Lake	54.8	66.8
		Grande Prairie	55.2	119.0
		Peace River	56.2	117.3
		Ft. St. John	56.2	120.8
		PAA	56.2	132.7
		Beatton River	57.3	121.5
		Churchill	58.7	94.1
		PAA-Northway	62.6	142.0

Year	Night of	Observing Station	Geographic Coordinates Lat.	Long.
			°	°
1965	17 July	PAA-Ethelda Bay	53 N	130 W
		Grande Prairie	55.2	119.0
		Beatton River	57.3	121.5
		Brochet	58.1	101.6
		Ft. Churchill	58.7	94.1
		Ft. Nelson	58.8	122.7
		Whitehorse	60.6	135.3
		Aishihik	61.7	137.5
		Ft. Simpson	61.9	121.3
		PAA-Snag	62	140
	18 July	Prince George	53.9	122.5
		Grande Prairie	55.2	119.0
		Ft. Nelson	58.8	122.7
	19 July	Grande Prairie	55.2	119.0
		Great Whale River	55.3	77.5
		Peace River	56.2	117.3
	20 July	Grande Prairie	55.2	119.0
		Great Whale River	55.3	77.5
		Peace River	56.2	117.3
		Brochet	58.1	101.6
		Ennadai Lake	61.0	101.3
		Ft. Simpson	61.9	121.3
		Yellowknife	62.5	114.6
	21 July	Cold Lake	54.5	110.1
		Great Whale River	55.3	77.5
	22 July	Ft. Churchill	58.7	94.1
		Ennadai Lake	61.0	101.3
	23 July	Beatton River	57.3	121.5
		Ft. Nelson	58.8	122.7
	25 July	King Salmon	58.7	156.5
		Aniak	61.6	159.7
	26 July	PAA-Port Hardy	51	128
		Ft. McMurray	53.7	110.4
		Terrace	54.6	128.5
		Grande Prairie	55.2	119.1
		Peace River	56.2	117.3
		Ft. St. John	56.2	120.8
		Beatton River	57.3	121.5
		Brochet	58.1	101.6
		Ft. Churchill	58.7	94.1
		King Salmon	58.7	156.5
		Ft. Chipewyan	58.8	111.2
		Ft. Nelson	58.8	122.7
		Uranium City	59.5	108.8
		Homer	59.6	151.5
		Smith River	59.9	126.5
		Watson Lake	60.2	129.2
		Kenai	60.6	151.3
		Whitehorse	60.6	135.3
		Hay River	60.8	115.8
		Aniak	61.6	159.6
		Talkeetna	62.3	150.1
		Summit	63.3	149.1
		Nenana	64.5	149.1

Year	Night of	Observing Station	Geographic Coordinates Lat.	Long.
1965	26 July	Eielson	64.6° N	147.1° W
		Fairbanks	64.9	147.9
	27 July	PAA	52	130
		PAA-Juneau	58.4	134.6
		King Salmon	58.7	156.5
		Ft. Nelson	58.8	122.7
		Smith River	59.9	126.5
		Watson Lake	60.2	129.2
		Whitehorse	60.6	135.3
		Hay River	60.8	115.8
		Bethel	60.8	161.7
		Aishihik	61.7	137.5
		Ft. Simpson	61.9	121.3
		PAA-Northway	62.6	142.0
	28 July	Beatton River	57.3	121.5
		King Salmon	58.7	156.5
		Ft. Nelson	58.8	122.7
		PAA-Haines	59	130
		Watson Lake	60.2	129.2
		Kenai	60.6	151.3
		Ft. Simpson	61.9	121.3
		PAA-Northway	62.6	142.0
	31 July	Ft. Churchill	58.7	94.1
		Ft. Nelson	58.8	122.7
		Watson Lake	60.2	129.2
		Ennadai Lake	61.0	101.3
		Ft. Simpson	61.9	121.3
		Yellowknife	62.5	114.6
	1 Aug	Grande Prairie	55.2	119.0
		PAA-Juneau	58.4	134.6
		King Salmon	58.7	156.5
		Ft. Nelson	58.8	122.7
		Ft. Chipewyan	58.8	111.2
		Smith River	59.9	126.5
		Ft. Smith	60.1	112.2
		Watson Lake	60.2	129.2
		Whitehorse	60.6	135.3
		Hay River	60.8	115.8
		Ft. Simpson	61.9	121.3
		Yellowknife	62.5	114.6
		Northway	62.6	142.0
		Summit	63.3	149.1
		Big Delta	64.0	145.7
		Dawson	64.1	139.0
		Fairbanks	64.8	147.9
		Norman Wells	65.3	126.5
	2 Aug	PAA-Haines Junction	60.8	137.5
		Ft. Smith	60.1	112.2
		Watson Lake	60.2	129.2
		Whitehorse	60.6	135.3
		Ft. Simpson	61.9	121.3
		PAA-Big Delta	64.0	145.7

Year	Night of	Observing Station	Geographic Coordinates Lat.	Long.
1965	3 Aug	PAAKetchikan	55°3 N	131°7 W
		Juneau	58.4	134.6
		Yakutat	59.5	139.7
		Watson Lake	60.2	129.2
		Teslin	60.2	132.7
		Whitehorse	60.6	135.3
		Anchorage	61.2	150.0
		Aishihik	61.7	137.5
		Gulkana	62.1	145.4
		Northway	62.6	142.0
		Mayo	63.6	135.9
		PAA-Big Delta	64.0	145.7
		Dawson	64.1	139.0
		Fairbanks	64.9	147.9
		Stevens Village	66.0	149.1
	4 Aug	Juneau	58.4	134.6
		Ft. Nelson	58.8	122.7
		Yakutat	59.5	139.7
		Northway	62.6	142.0
		Summit	63.3	149.1
		Big Delta	64.0	145.7
	6 Aug	Smith River	59.9	126.5
		Watson Lake	60.2	129.2
		Dawson	64.1	139.0
		Fairbanks	64.8	147.9
		Stevens Village	66.0	149.1
	7 Aug	Watson Lake	60.2	129.2
		Teslin	60.2	137.2
		Ft. Simpson	61.9	121.3
		Yellowknife	62.5	114.6
		Dawson	64.1	139.0
	11 Aug	Anchorage	61.2	150.0
		Fairbanks	64.9	148.7
		Livengood	65.5	148.5
		Bettles	67.2	150.4
	15 Aug	Watson Lake	60.2	129.2
		Ft. Yukon	66.6	145.3
	30 Aug	Knob Lake	54.8	66.8
		Goose Bay	53.4	60.5

histogram using the smoothing relation N=(a+2b+c)/4, where b is the frequency on the period in question, and a and c are the frequency for the adjoining periods. This smoothing relation serves to correct at least partially for cloudy nights and other factors and should represent the relative frequency with greater accuracy than the histogram. Table 3.2 and Fig. 3.3 show that:

1. NLC occur over North America more frequently than previously supposed, and that the NLC activity here is comparable to that observed in Europe and the USSR.

2. The earliest and latest dates that NLC were observed over North America are April 1 and September 28 respectively.

3. Ninety-two percent of the displays occur during the months of June, July, and August.

4. The peak of activity occurs around July 20, about one month after the summer solstice.

5. Eighty-two percent of the displays were observed after the summer solstice.

6. Seventy-seven percent of the displays were observed during the 2 month period, 21 June - 20 August.

It can also be added that the brightest and most extensive NLC displays occur during the 2 month period 15 June - 15 August.

It is of interest to compare these North American results with those obtained in Scotland, the USSR, and with all northern hemisphere data. To make this comparison, the NLC observational data from Scotland for the years 1885 -1965 (see Paton, 1964, 1965a, 1965b), from the USSR for the years 1957-1961 (see Bessonova, 1963), and for all the northern hemisphere for the years 1885-1965 (see Fogle and Echols, 1965), were analysed using the same procedure as that used for the North American data. The results are shown in Fig. 3.3, and Fig. 3.4. The

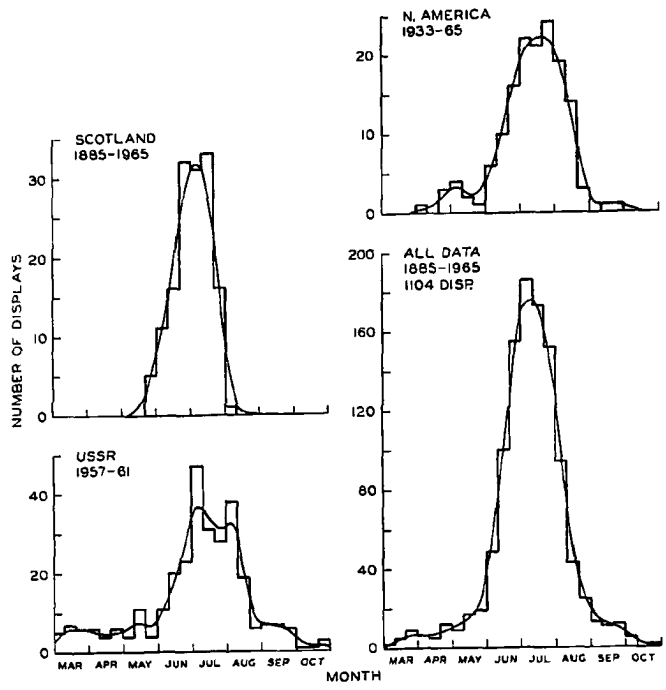

Fig. 3.3. Comparison of the frequency of observed occurrence of NLC with season over Scotland, the U.S.S.R., North America, and over all the northern hemisphere.

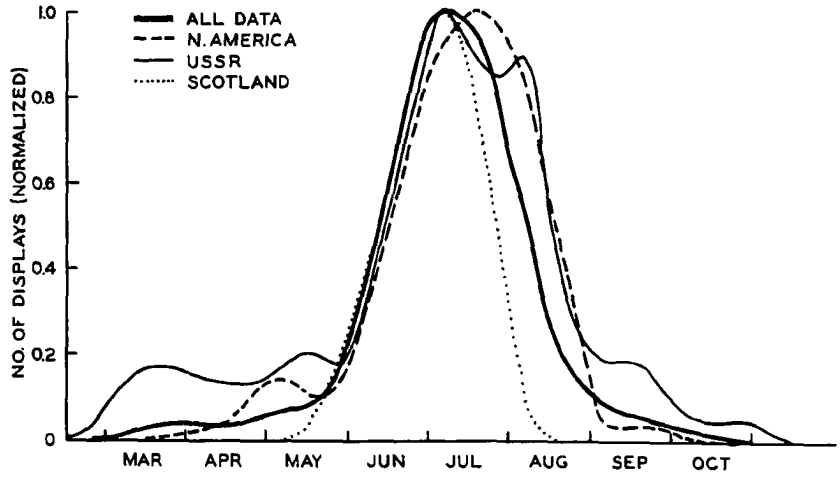

Fig. 3.4. Normalized frequency of observed occurrence of NLC from Scotland, the U.S.S.R., North America, and for all the northern hemisphere.

Scotland observations made from stations at about 56°N, show a peak of activity around July 10; the earliest and latest sightings were made on the nights of May 26 (1889) and August 2 (1960) respectively. The USSR observations, made from stations over a latitude range of 45°-80°N, show a broad irregular peak of activity spread, over the period July 1 - August 10, the earliest and latest reported sightings were made on the nights of March 5 (1959) and October (1959). A careful examination of the USSR data suggests that a number of the reported displays, particularly those in March, September, and October, may well have been aurora or sunlit high cirrus rather than NLC, (these perhaps questionable sightings were made when the SDA was less than 3° or greater than 16° during which times NLC are not visible). The curve for all observations shows a peak of activity on July 12 with the earliest and latest reported observations on March 5, and October 29, respectively. The curve is biased to some extent by the fact that the majority of the sightings were made in the latitude range of 45°-58°N, where NLC are not observed as late in the summer as at higher latitudes. The observational data indicates that the peak of NLC activity occurs earlier at lower latitudes (below 58°N). This points to a possible latitudinal shift of NLC toward the pole as the summer progresses. (NLC have not been observed in Scotland at 56°N after August 2, but a number of displays have been observed in North America, Sweden, and Russia at latitudes 60°-70°N in late August).

To investigate the possibility of a latitudinal shift of NLC with season, simultaneous observations were made from aircraft at

Barrow, Alaska (71.3°N) and at Fairbanks, Alaska (65°N) during the period periods 1 - 14 April 1965, and 25 August - 9 September 1965. The Arctic Research Laboratory at Barrow provided the ground and aircraft facilities for the observations at that location. Pilots of the Pan American aircraft flying between Fairbanks and Seattle conducted the observations in the vicinity of Fairbanks. No displays however were observed from either location during the above mentioned observation periods.

To examine the possibility of there being certain days during the year when NLC are more likely to occur, the number of times NLC have been reported on a given day during the period 1885 - 1964 was determined (see Fogle and Echols, 1965 for listing of dates on which NLC were reported during this period). These results, shown in Fig. 3.5 give no indication that there are preferred nights for NLC occurrence.

The earliest and latest dates on which well-documented NLC observations have been made over North America are April 10 and September 28 respectively. Reports of NLC earlier and later than these dates have been made, but these reports are not well enough documented to say with certainty that they were NLC. Hamilton (1964) reports seeing NLC at Lerwick (60.1°N 1°W) as early as 5 January (1964), but no photos were taken and Paton (1964a) has suggested that what Hamilton saw was not NLC but a long enduring meteor trail.
L. R. Pitwell (1963) reports seeing NLC from Addis Ababa (9°N, 39°E) on the night of 17 January 1963, but no photographs were taken, and based on the reported color (reddish) structure (dome shaped) observing time, and the latitude of observation, it seems unlikely

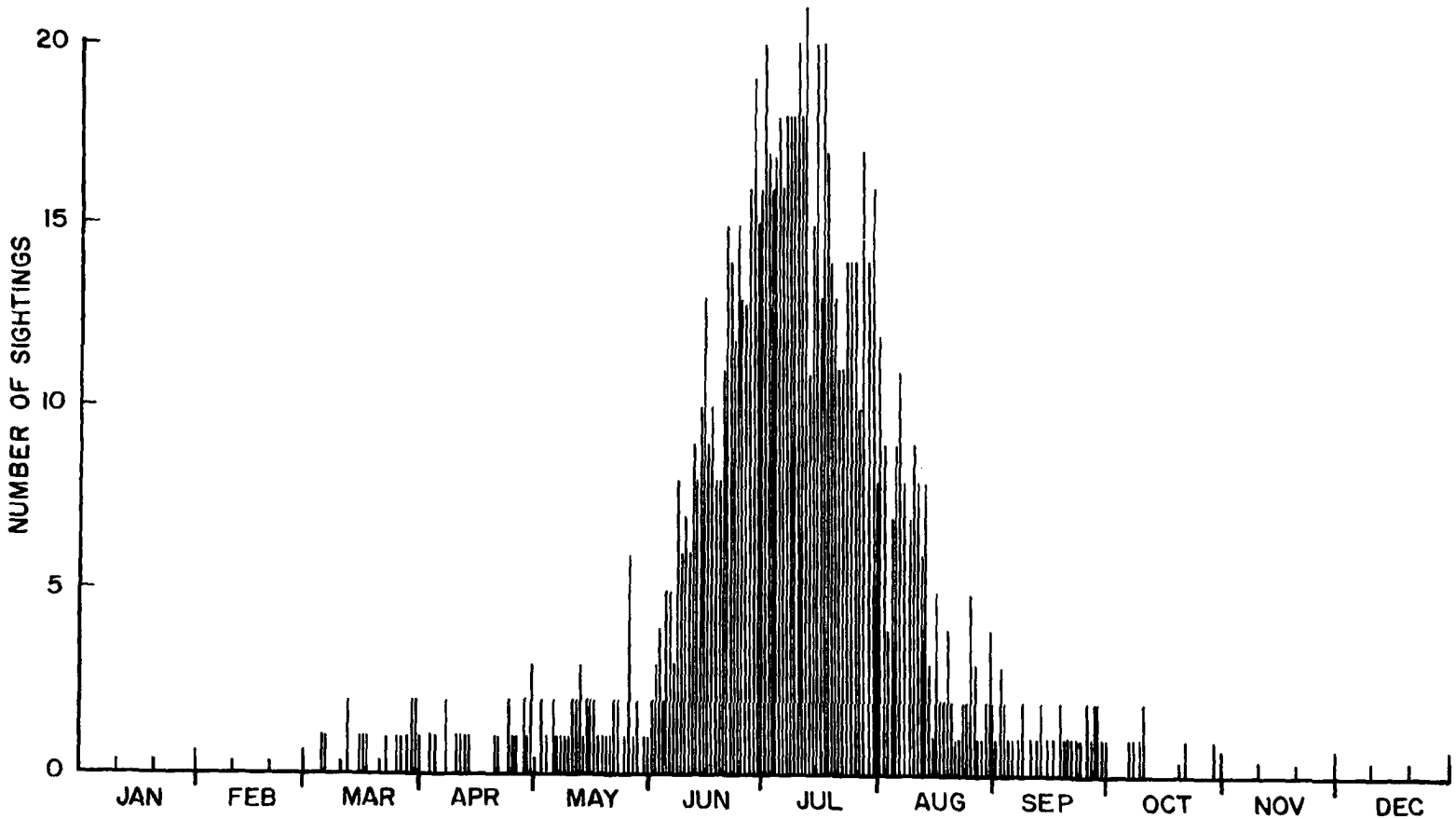

Fig. 3.5. Number of times NLC have been reported on a given night during the period 1885-1964.

that they were NLC. Hanson (1965) reports seeing NLC on the night of 12 November 1964 from an ice island off the north coast of Alaska (location 79.6°N, 138°W), but in view of the time of observation (solar depression angle of around 7°), the tropospheric cloud cover (broken clouds at lower level, high thin overcast above), the lack of structure characteristic of NLC, and the color of the clouds observed (pale yellow and pink), it seems unlikely that these were really NLC. The fact that no NLC have been observed during over 500 cloudless nights in the period October - March at College, Alaska, despite a careful watch kept by experienced observers favors the conclusion that NLC do not occur during this period.

3.3.2: Variation of NLC Observations with Latitude of Observer

The North American observational data (Table 3.2) shows that the lowest and highest latitudes from which NLC have been reported over North America are 45.5°N and 77°N respectively. Using the data given in Table 3.2, the number of displays observed per 5° latitude range was determined. The results (Fig. 3.6) show that NLC over North America were most frequently observed in the latitude range 50° - 65° N, and that the optimum latitude is around 60°N. The USSR data (Bessonova, 1963) gives similar results; the lowest and highest latitude observations reported there are 45°N and 71.5°N and the optimum latitude was around 55°-60°N. The decrease in the number of displays observed per year in latitudes north of 60° is primarily because as one proceeds polewards from 60°, there are increasingly longer periods, centered around the summer solstice, when the sky background is too bright for NLC to be observed even if present.

Using the North American observational data for 1964 and 1965, the percentage of nights on which NLC are seen at different times of the year at latitudes 45°, 55°, and 60° was determined. These results (Table 3.3) show that at 55°N, one might expect to see NLC on about 55% of the clear nights during the period July 1-20, and at 60°N, one should see NLC on 70-85% of the clear nights during the period July 1-31.

TABLE 3.3

THE VARIATION WITH LATITUDE AND TIME OF YEAR OF THE PERCENTAGE OF NIGHTS ON WHICH NLC ARE SEEN

Period	45°N	55°N	60°N
June 1-10	10%	20%	30%
11-20	0	35	50
21-30	10	40	45
July 1-10	10%	55%	70%
11-20	10	55	85
21-31	0	35	70
August 1-10	0%	15%	60%
11-20	0	10	20
21-31	0	5	5

No reliable reports of naturally occurring NLC from places below 45°N have been reported.* Astapovich (1958) reported that a watch

*Artificial Noctilucent Clouds

Over the past few years there have been over a dozen sightings of artificial NLC (Meinel, 1963) at latitudes below 45°. These clouds have been associated with rocket launchings from the point Magu Missile Range at 34°N, 118°W. Most of the sightings have been correlated with launchings of the SCOUT missile, which has a solid propellant and burns high into the atmosphere. The exhaust products of the SCOUT missile are rich in water vapor and solid particles, and it appears that these substances are introduced into the mesopause region in sufficient amount to create artificial NLC. When the winds are toward the east, the clouds drift over Arizona where Meinel has observed them.

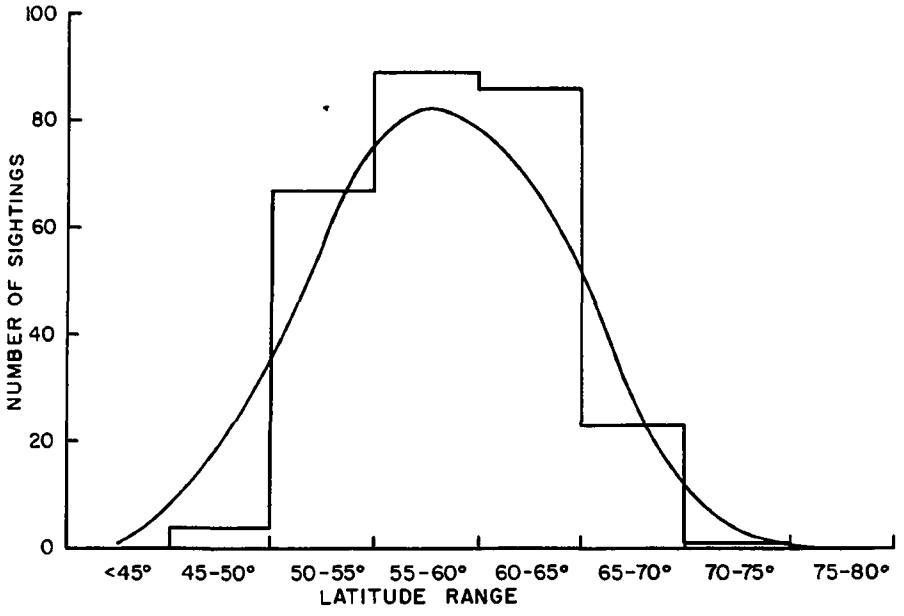

Fig. 3.6. Frequency of observed occurrence of NLC over North America with respect to latitude of observer.

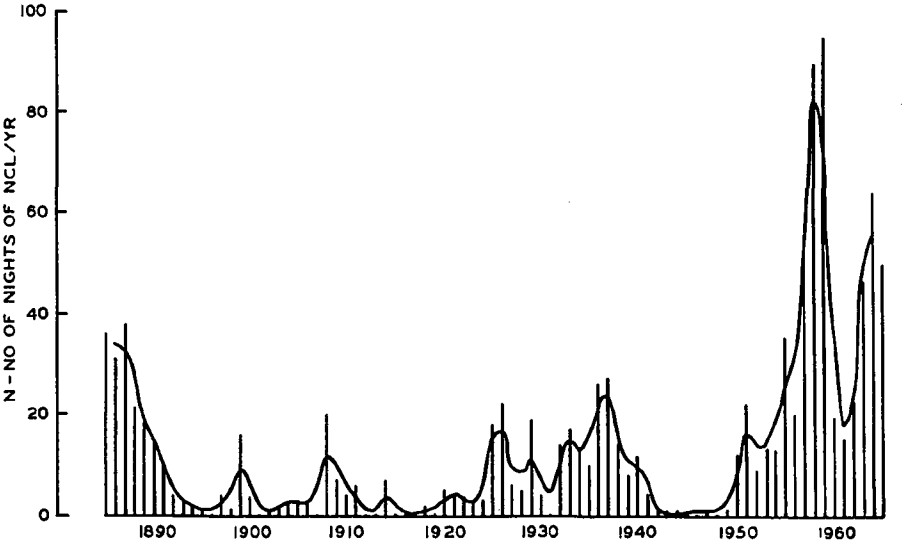

Fig. 3.7. Yearly variation of NLC activity.

for NLC during 700 cloudless summer nights from Ashkabad, Russia (37.5°N, 58.3°E) gave no sightings, and a careful watch kept at Hanover, New Hampshire (43°N) by Keith D. Baker, an experienced NLC observer, also gave no sightings. No NLC were sighted from Boston, Massachusetts (42.4°N) during a three year (1959-1961) watch of the twilight sky by F. Volz (1966). In view of these considerations, it seems unlikely that NLC are formed at latitudes below about 50°N; otherwise they would be visible at latitudes below 45°N.

As NLC are most often observed at elevation angles of 3°-10° above the observer's northern horizon this corresponds to the clouds being from 4.5° to 7°N of the observer (see Fig. 2.18), the range of latitudes over which NLC are formed is from about 50°N-80°N, and the observed latitude of maximum formation is around 65°N.

3.3.3: Longitudinal Distribution of NLC Occurrence

The longitudes from which most NLC reports have been made coincides with regions of high population density and the number of persons making NLC observations. Relatively few observations are reported from sparsely populated regions. For this reason it is not possible at this time to determine whether or not there is any asymmetry in the longitudinal distribution of NLC occurrence.

There may be a real longitudinal effect, particularly at those longitudes (approximately 10°E and 120°W) where the auroral zone crosses the maximum zone of NLC occurrence. If a low mesopause temperature of around 135°K is needed for NLC formation (as suggested by the evidence now available), and if during years of high sunspot activity the mesopause in the auroral zone frequently experiences

considerable heating, one would expect to have fewer NLC displays present at longitudes of around 10°E and 120°W than at other longitudes. The observational data so far available does not allow this question to be adequately examined, but more and better data for this purpose should be obtained over the next few years.

3.3.4 Year to Year Variation of NLC Activity

Using a complete listing of the NLC observations reported during the years 1885-1964 (see Fogle and Echols, 1965) plus the data for 1965, the apparent yearly variation of NLC activity was determined. These results (Fig. 3.7) show that the years of maximum NLC reports were 1887, 1899, 1908, 1926, 1937, and 1959, but the apparent variation in the number of NLC reported per year may mainly indicate fluctuating interest in NLC.

3.3.5 Daily Variation of NLC Appearance

The NLC data for the period 1889-1894 indicates that the clouds are seen more often after than before midnight (the clouds were observed on 6 occasions before and on 33 occasions after midnight), but this feature is not corroborated by the NLC data from North America and Sweden. In North America, 83% of the displays reported were first sighted before midnight, and all of Ludlam's (1957) observations in Sweden in 1954 and 1955 were first sighted before midnight. In general, the NLC displays observed over North America were found to be brightest and most extensive after midnight. This feature of NLC may account for their being reported more often after than before midnight during the period 1889-1894.

3.4 Area of NLC

Sometimes the whole boundary of a NLC display can be seen and its area estimated; this may be only a few tens of thousands of km^2. The extent of the sky at the level of 82 km visible from the ground is a circular region about 1000 km in radius and of an area about 3 million km^2; but only a part of this can be illuminated by sunlight against a dark sky (see Section 2.5). The nine most widely observed NLC displays over North America (Table 3.4) were too extensive to be all visible from any one place; combination of data from many observers indicates that each of these displays covered more than 2 million km^2. Maps of the widespread displays occuring in 1963 and 1964 are given by Fogle (1964a) and Fogle, Chapman and Echols(1965). The approximate extent of the 5/6 July 1964 , and 26/27 July 1965 displays over North America is shown in Fig. 3.8.

TABLE 3.4

ESTIMATED AREA OF WIDESPREAD NLC DISPLAYS OVER NORTH AMERICA

Date	Area
11/12 August 1963	2.5 million km^2
12/13 August 1963	2.0 million km^2
29/30 June 1964	3.0 million km^2
5/6 July 1964	3.6 million km^2
11/12 July 1964	2.5 million km^2
16/17 July 1964	2.0 million km^2
24/25 July 1964	2.5 million km^2
2/3 August 1964	2.0 million km^2
17/18 July 1965	3.0 million km^2
26/27 July 1965	3.5 million km^2
1/2 August 1965	2.0 million km^2

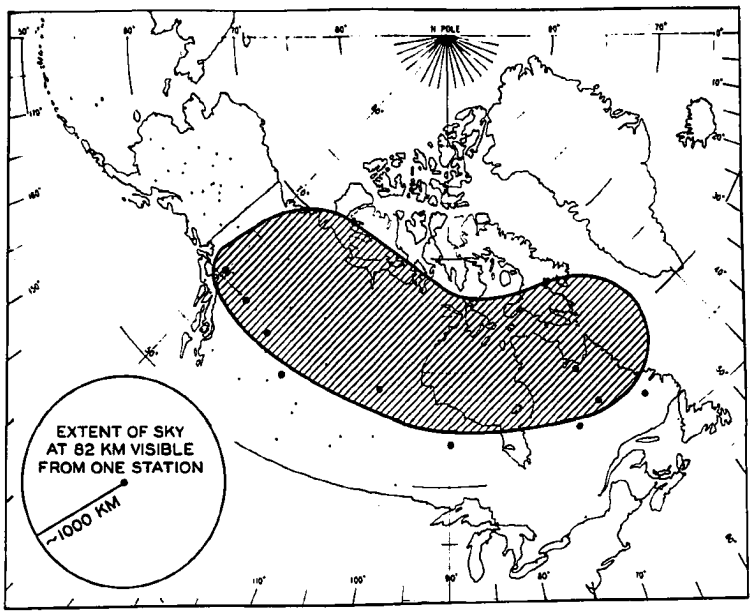

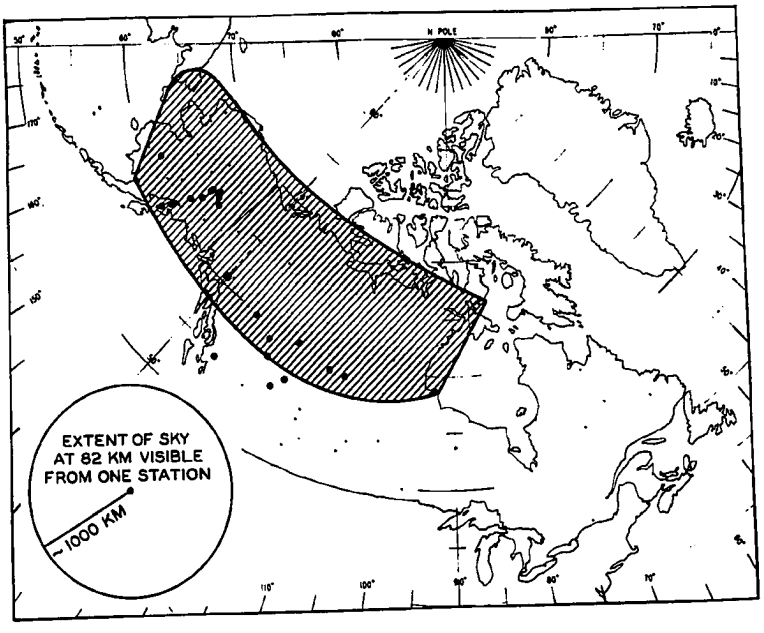

Fig. 3.8. Approximate area over North America covered by NLC on the night of (A) 5 July 1964, (B) 26 July 1965.

The 2/3 August 1964 display was observed by 13 stations in Alaska and Canada and by the pilots of 2 BOAC aircraft off the south coast of Iceland. This display, if continuous, extended in longitude from 25°W to 150°W. Since NLC can be seen at any one time only within a sector of about 120° longitude, it cannot be said with certainty that this display was continuous over the range of latitudes from which it was observed. It is possible that NLC might at times cover all longitudes around the pole and have an area of $10^8 km^2$, but this, if true, would be difficult to establish by observations of the kind so far available because of the difficulties just mentioned.

During the summer of 1964, there were 14 nights on which NLC were widely observed over North America, Europe and the USSR (see Table 3.5). Of these, the most widely observed were on the nights of 5/6 July, 24/25 July, and 2/3 August.

On several occasions during 1964, NLC were widely observed over North America but were not seen at all over the USSR (on July 16/17 , 21/22, 26/27, and on August 13/14). The nights in 1964 when NLC were widely observed over the USSR but not seen over North America were: June 8/9, 25/26, 26/27, and July 3/4, 9/10, 14/15, and 19/20.

These facts indicate that on some nights in the northern hemisphere, NLC are present over a wide range of longitudes (possibly circumpolar) while on other nights they are less widespread.

3.5 Drift Motion of NLC

Observations of the drift motion of NLC provide information on the wind velocity at the mesopause. Interpretation of the wind observations at this altitude is complicated by the presence of irregular components

Table 3.5

Dates During 1964 on which NLC were Widely Observed over the Northern Hemisphere

Date (1964)	Region	No. of Observing Stations	Latitude range of observing stations	Longitude range of observing stations
15/16 June	North America	1	53.8°N	90.1°W
	USSR	1	56	92 E
	North Atlantic	2	-	30-55 W
28/29 June	North America	8	52.2-60.1	90.1-117.3W
	USSR	4	56-58.3	24.1-92.9E
	Western Europe	2	56	0-10E
29/30 June	North America	16	49.7-58.8	90.1-122.7W
	USSR	3	55-69	82.9-101.1E
	Western Europe	2	56-58	0-20 E
	North Atlantic	1	-	30 -55 W
30 June/1 July	North America	11	48.4-60.6	55.9-151.5W
	USSR	2	54.9-57.0	23.9-24.1E
	Western Europe	2	53	5 E-60 W
5/6 July	North America	10	53.2-60.6	60.5-129.2 W
	USSR	5	52.3-59.4	24.8-117.7E
	North Atlantic	1	55 -57	0-70 W
6/7 July	North America	4	53.4-59.5	60.5-139.7 W
	Western Europe	1	55	0
	USSR	3	55.5-59.4	24.1-65.4E
15/16 July	North America	3	58.4-59.6	94.1-151.5W
	USSR	1	57	24.1E
	Western Europe	2	56-60	15 E-25 W
24/25 July	North America	11	53.2-64.9	60.5-148.0W
	USSR	9	52.0-61.9	37.6-159E
25/26 July	North America	1	60.1	112.2W
	USSR	6	59.4-61.8	24.8-60.4E
	North Atlantic	2	56-60	25-38 W
	Western Europe	1	56	0 -5 E
1/2 Aug	North America	2	58.2-63.8	68.3-152.0W
	USSR	4	59.4-62.4	24.8-60.9E
	Western Europe	1	58	10 E
2/3 Aug	North America	13	54.0-64.9	68.3-152 W
	USSR	1	59.9	82.0E
	Western Europe	1	60	10 E
3/4 Aug	North America	8	57.3-64.5	94.1-162.6W
	USSR	1	62.4	60.9E
	Western Europe	1	63	15 E
8/9 Aug	North America	8	61.0-68.5	82.5-162.6W
	USSR	1	61.2	46.6E
	Western Europe	1	63	15 E
9/10 Aug	North America	5	58.7-64.9	94.1-152.0W
	USSR	1	67.1	59.4E
	Western Europe	1	63	15E

with a time scale of two or three hours and a vertical scale of several kilometers and by diurnal and semidiurnal oscillations associated with atmospheric tides (see Craig, 1965). Since NLC are observed in summer months at high latitudes and usually around midnight, little information can be gained about latitudinal,seasonal and vertical variations of wind, or on the tidal component. There is also some question as to whether the observed motion of NLC features represents the true wind or a wave motion.

To determine the true wind at NLC heights, one must measure the velocity of the NLC system as a whole rather than the velocity of individual bands, or of bright knots caused by the intersection of two bands. Measurements based on the movement of the bands or knots generally yield values that are improbably high (200-300 m/sec) and in a direction opposite to the true wind. Motion pictures provide the most reliable velocity determinations. They clearly show the motion of the bands relative to the cloud system.

A survey of the literature reveals 97 determinations of NLC velocity (Jesse, 1890; Archenhold, 1928; Störmer, 1933; Vestine, 1934; Störmer, 1935, Khvostikov, 1952; Ludlam, 1957; Witt, 1962; Fogle, 1964a). A plot of these results (Fig. 3.9) shows that in northern latitudes the motion is generally towards the southwest; speeds of 40 m/sec are common and values up to 200 m/sec have been reported. A plot of the direction of motion of the NLC as a function of local mean time (Fig. 3.10), indicates an apparent change of direction of NLC drift from generally toward the SW before midnight to towards the WSW after midnight. This apparent change

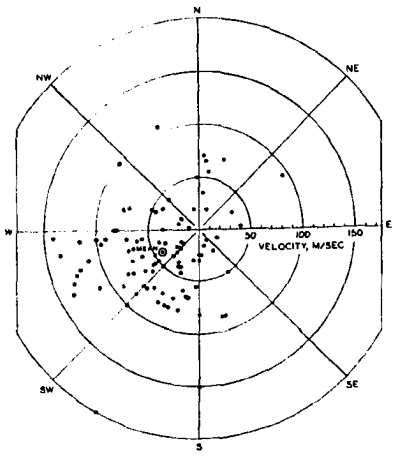

Fig. 3.9. Vectorial distribution of NLC velocities. A total of 97 measurements made during the period 1885-1963 give a mean speed of 40 m/sec towards 240° azimuth.

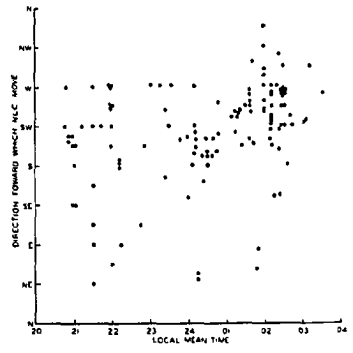

Fig. 3.10. Distribution of the drift motion of NLC as a function of local mean time.

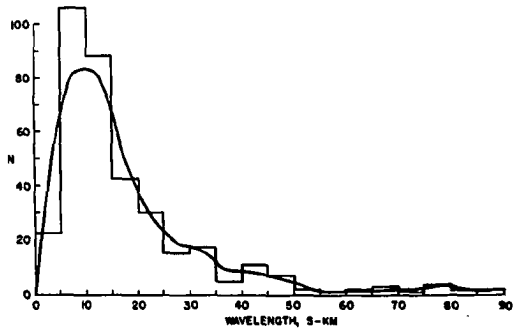

Fig. 3.11. Distribution of measured wavelengths in NLC.

may be fortuitous. A drift of the NLC from the sunlit atmosphere towards the earth's shadow does however appear to be a real effect.

3.6 Wave Structure in NLC

A prominent feature of many NLC displays is the presence of well-defined parallel bands. These have been identified with systems of waves of various wavelengths. Only a few wavelengths have been measured in the past; they range between 7 and 100 km (Witt, 1962 ; Störmer, 1935). Over the past year we have developed a simple method for measuring the wavelengths from individual photographs of NLC. The method assumes a constancy of the height of NLC at 82 km and requires good photographs which contain several well-defined features whose elevation and azimuth angles are independently measured. From the photographs, the elevation angles to the pair of bands in question is measured as well as the incremental angle between them. A knowledge of these two quantities is sufficient to determine the cloud wavelengths. The relation of the wavelength to the elevation angles and to the angle between the bands is shown in Fig. 2.17. Photographs of three NLC displays observed over North America have been analysed by this method so far. A total of 248 wavelengths, ranging from 5 to 100 km, was determined from these photographs by measuring the distance between each two adjoining wave crests. The frequency distribution of the wavelengths is shown in Fig. 3.12, the most frequent value being about 10 km. In considering this curve, it must of course be kept in mind that the closely spaced crests are much more numerous than the crests separated by large distances; thus the short waves predominate in Fig. 3.11.

Two mechanisms have been suggested to account for the wave structure in NLC: (1) Internal gravity waves (Hines, 1959), and (2) interface waves (Haurwitz, 1961). A comprehensive discussion of these mechanisms by Haurwitz (1964) suggests that the short waves of about 10 km may be interface waves, and the longer waves may be internal gravity waves. More data on the temperature distribution and wind shear at the mesopause, as well as simultaneous velocity and wavelength measurements are needed to determine with more certainty the cause of the waves.

3.7 Influence of Aurora on NLC

Prior to 1965 there were only four reports of simultaneous NLC and aurora (Vestine, 1934; Paton, 1953; Witt, 1957; and Schröder,, 1965) indicating that this may be a rare event.

Vestine (1934) saw aurora with NLC on the night of 20 July 1933 at Meanook, Alberta (54.6°N, 113.3°W) from 2345-0334 (105°W Meridian Time) At 2400, a dull auroral arc consisting of several dull scattered rays was seen above the NLC display and showed the green auroral line. The aurora lasted about 5 minutes. Between 2400 and 0030, the intensity and extent of the NLC diminished giving the impression that the display was about over. However, after 0030 the NLC began to increase in intensity and extent, and was observed until 0334.

Paton (1953) saw NLC and aurora together on the night of 24 July 1950 at Edinburgh, Scotland (56°N, 3.2°W) from 2355 (GMT) to 0050. The aurora ceased at 0050, and by 0205 evidence of turbulence was clearly visible in the NLC. The NLC vanished at 0309. Paton suggested that the turbulence was due to considerable vertical motion at the mesopause caused in some way by the aurora.

On the night of 13 August 1956, Witt (1957) observed an intense and extensive NLC display beginning around 2150 (15°E Meridian time). After midnight the display diminished considerably and at 0115, a faint aurora was observed.

On the night of 30 July 1963, NLC and aurora were seen at Lerwick in the Shetland Islands by Byrne (1964) and at Ronnebeck, Germany by Schröder (1965). At Lerwick the aurora and the NLC occurred in different parts of the sky and no unusual changes were detected in the NLC.

On our NLC expedition to western Canada during the summer of 1965 we observed NLC with aurora on 13 occasions, (Table 3.6). Also see Fig. 3.12 for photographs of two of these displays. On 7 of the thirteen occasions, the aurora occurred in the same region of the sky as the NLC. Interesting changes were observed in the NLC after onset of the aurora on 6 of these 7 nights. The general effects observed were a reduction of the NLC intensity and extent and a transformation of their well-ordered structure into swirls and formless veils. On two occasions, the NLC vanished completely within an hour after onset of the aurora.

The changes in brightness and form of NLC after onset of aurora point to a possible auroral-induced heating at or below the mesopause. There are a few other data which point to this same possibility, but more data, in particular temperature measurements in the mesosphere during and after onset of aurora in the presence of NLC, is needed to establish this feature with certainty.

Additional experimental evidence pointing to auroral induced heating below the mesopause is given by Murcray (1957). He finds

A

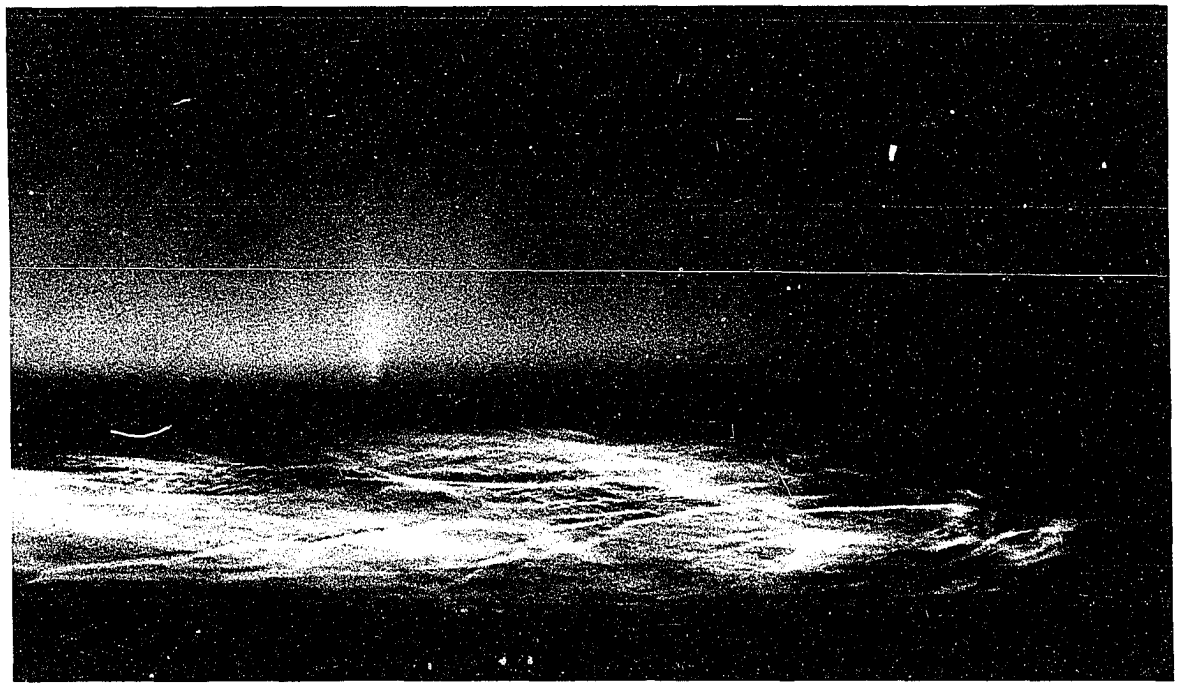

B

Figure 3.12. Photographs of NLC and Aurora (A) from Grande Prairie, Alberta on 18/19 July 1965, and (B) from Watson Lake, Y. T. on 1/2 August 1965.

Table 3.6

Nights when NLC and Aurora were Observed During 1965 Expedition to Western Canada

Station	Night of	NLC		Aurora		Remarks
		Brightness	Observed from (LMT)	Brightness	Observed from (LMT)	
Grande Prairie, Alberta (55°2N, 118°9W)	15 June	Moderate	0000-0200	faint	2300-0030	Aurora near zenith, far from NLC. No change in NLC.
	16	faint	2200-2300	bright	2210-0100	Brilliant aurora over most of northern sky. Widespread but faint NLC vanished completely within 50 minutes of onset of aurora.
	29	moderate	2315-0130	moderate	0012-0030	Aurora near NLC at horizon, NLC lost intensity & structure after onset of aurora.
	5 July	bright	2205-0215	faint	0100-0200	Aurora near zenith. No changes in NLC.
	15 "	bright	2145-0230	faint	2335-2340	Faint auroral arc near NLC for about 2 minutes. No visible change in NLC.
	18 "	faint	2230-0100	bright	2200-0215	Aurora near NLC. Intensity of NLC diminished after onset of aurora & vanished about 2 hours before civil twilight.
	19 "	faint	0045-0115	moderate	0040-0050	NLC vanished 35 min. after onset of aurora.
Watson Lake, Y.T. (60°2N, 128°8W)	27 July	moderate	2200-0200	bright	2300-0100	Well defined structure in NLC decayed & some reduction in intensity after onset of aurora in the same region as the clouds. NLC moved rapidly to SW after auroral onset.
	28 "	moderate	0045-0150	faint	0030-0055	Aurora in different part of sky from NLC. No change in NLC.
	1 Aug	bright	2150-0230	bright	2150-2200	Aurora near horizon close to NLC. Within 1 hr after onset of aurora, turbulence observed in NLC, and NLC brightness decreased.
	2 "	faint	0120-0140	faint	2230-2315	Aurora in diff. part of sky from NLC. No change in NLC.
	3	moderate	2145-0200	faint	2250-2330	" " "
	6	moderate	2230-0230	moderate	2215-2300	" " "

that the 9.6 micron band of O_3 may be enhanced by the aurora. If this observation is confirmed, it might signify heating of the mesosphere.

Nordberg (1965) finds that the high latitude winter temperature measurements made during the IGY (1956-58) show considerably higher temperatures than more recent measurements (1962-64), and on this ground suggests that there may be a relationship between solar activity and high temperatures. Furthermore the summer mesopause temperatures over Ft. Churchill (59°W) during the IGY were around 165°K (Nordberg and Stroud, 1961), whereas during the IQSY in the presence of NLC the high latitude summer mesopause temperature was about 130°K (Nordberg, 1966). At this time it is not clear how auroral induced heating of the mesopause could occur. The observed lower border of aurora is generally around 100 km, but pulsating aurora often extend down to 90 km, (Campbell and Rees, 1961). Thus it seems unlikely that heating at the mesopause could be caused by particle bombardment in situ. The possibility of hydromagnetic wave heating at the mesopause can be ruled out since this heating is confined to higher altitudes--around 200 km, (Chamberlain, 1961). Maeda and Watanabe (1964) have suggested that pulsating auroras are sources of infrasonic waves, and that these infrasonic waves may possibly provide some heating at or below the mesopause. According to London (1956), increased H_α and L_α radiation associated with solar flares might possibly be responsible for initially heating the top of the stratosphere, producing a weak circulation and resulting in slight ascending motion at subsolar latitudes. London states that "this could be amplified by the appearance of temporarily increased amounts of ozone at upper levels, causing the level of maximum absorption and heating, due to normal Hartley-Huggins radiation from the sun, to lift thereby further decreasing the static stability in the region of 50 to

80 km. This decreased static stability would aid in the vertical exchange of momentum and could affect the horizontal circulation patterns below."

3.8 Spectrum and Polarization of NLC

The first indication that the light from NLC was scattered sunlight was obtained by Helmholtz (1889). He observed the clouds through a spectroscope and found the spectrum to be continuous with no emission lines and with the intensity stronger in the blue than in the red. These results were confirmed by Størmer (1933) who obtained a spectrum of a NLC display on the night of 24 July 1932 and found that it resembled that of daylight with Fraunhofer lines clearly present and no emission lines.

One of the basic problems connected with NLC is the composition and size distribution of the cloud particles. Prior to 1962, when direct samples of the particles were collected (see Section 3.9), the only way to infer the particle size was by optical methods such as spectroscopic or polarization measurements.

A serious difficulty in the analysis of spectral measurements is the selective atmospheric extinction on both incident and scattered light. This effect is particularly marked at the low elevation angles (0 to 10°) where the clouds are usually observed. The uncertainty as to the respective contributions of the singly and multiply scattered light to the total measured light further complicates spectral measurements. These complications can be lessened by taking a calibration spectrum of the twilight sky and subtracting this from the NLC spectrum, but the procedure is involved and time consuming.

In contrast to the problems encountered in determining the spectral intensity distribution, the state of polarization of the scattered light is not appreciably altered by selective atmospheric extinction, and the degree of polarization is a readily measured quantity and is sensitive to the presence of large particles, especially at large scattering angles (greater than 90°).

Since the diameter of NLC particles is roughly comparable to the wavelength of visible light, the Rayleigh approximation cannot be used in interpreting the spectral and polarization data,instead one must use the Mie theory (see Van de Hulst, 1957;. Witt, 1960). The application of the Mie theory to NLC particles is discussed in detail by Chao (1965).

Polarization measurements by Witt (1960a,b) and Villmann (1962) show that:

(1) The average diameter of NLC particles is between 0.2 and 0.36 microns.

(2) There is no appreciable proportion of particles with diameter larger than 0.48 microns.

(3) The particle size distribution is of the form $N(d) = \text{Const} \times d^{-p}$, where d is the diameter and p is greater than 3.

Witt's data on the measured degree of polarization as a function of the scattering angle is shown in Fig. 3.13.

The theoretical analysis of the scattering of sunlight by NLC particles made by Chao (1965) indicates that one should be able through polarization measurements to determine whether NLC are made visible by an increase of the particle size due to condensation of water vapor on them. Thus, further polarization measurements should provide additional

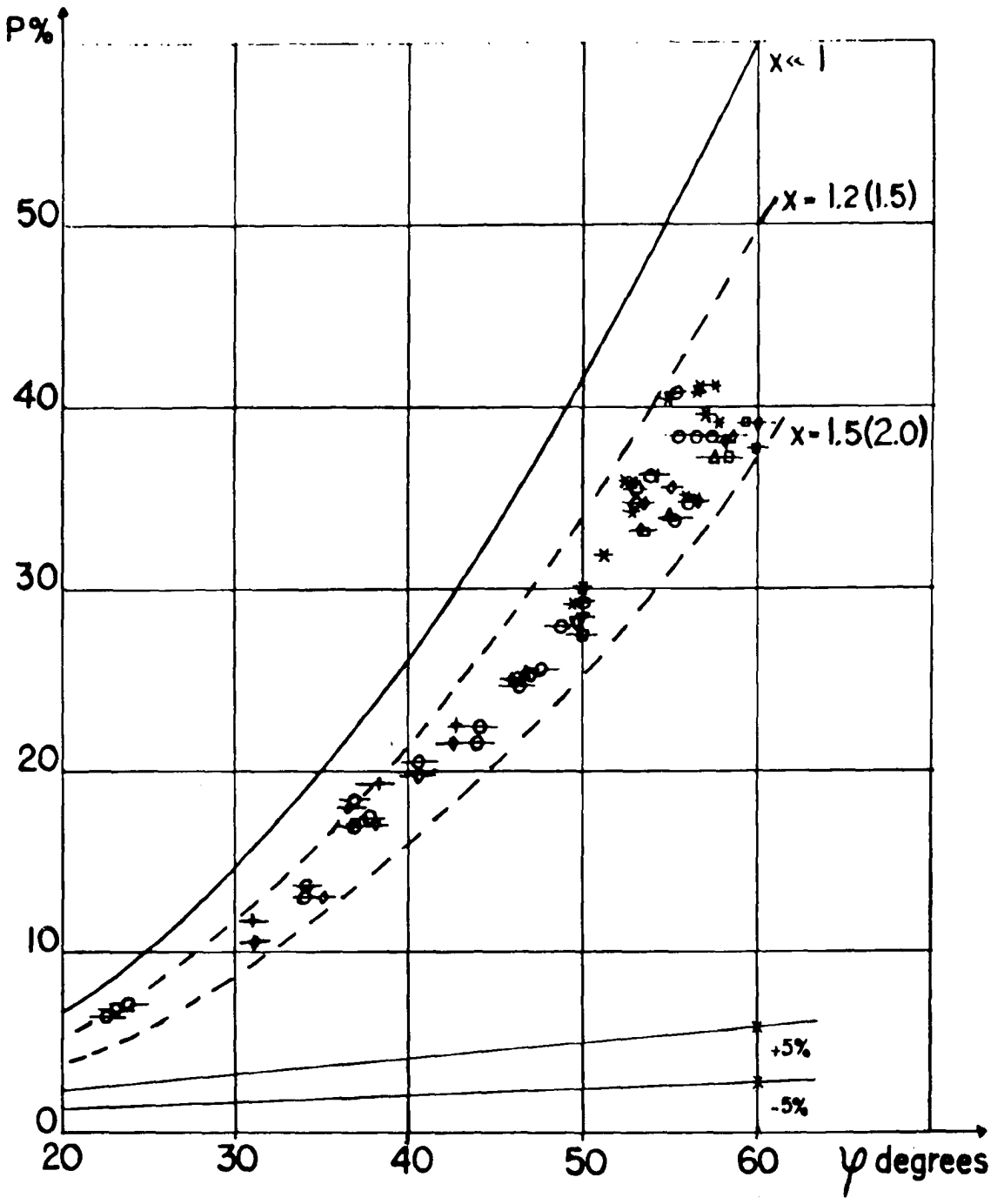

Fig. 3.13. Measured degree of polarization as a function of the scattering angle for λ = 4700 A. The size parameter X = 2 πr/ λ, where r is the particle radius and λ is the wavelength. X << 1 corresponds to Rayleigh scattering. The broken lines show the degree of polarization for particles with X = 1.2 and 1.5, as indicated, and a refractive index of n = 1.55. Corresponding values for particles with n = 1.33 (water) are given in parentheses. The magnitude of a 5% error is also indicated (Witt, 1960a).

valuable information on the nature and size on NLC particles.

Grishin (1956) published the first continuous spectra of NLC. He obtained 15 spectra on 3 NLC displays during the summer of 1951 from a station near Moscow. He used a prism spectrograph and panchromatic film for recording the spectra. Deirmendjan and Vestine (1958) interpreted these spectra as being due to single scattering of sunlight by spherical dielectric particles with a maximum diameter of 0.8 microns. This result was in general agreement with earlier estimates of NLC particle size (Vestine, 1934; Astapovich, 1939; Ludlam, 1957; Witt, 1957).

To obtain additional spectral data on NLC, we had a fast diffraction grating spectrograph designed (by Dr. G. Romick) and constructed for use on our NLC field expedition to western Canada during the summer of 1965. A Bausch and Lomb plane transmission grating with 600 grooves/mm and a blaze angle and blaze wavelength of 28.7° and 5500A respectively was used. A 58 mm f/1.2 Canonflex lens was employed to focus the NLC on the slit, whose opening was kept constant at 0.25 mm. The spectra were recorded on Kodak 103 a-f spectrographic film in a Canonflex RM camera with a 100 mm f/2.0 lens. Using this instrument several hundred usable spectra were obtained from 15 NLC displays observed on our field expedition to Canada in the summer of 1965. The analysis of this large body of data is only partially complete at this time and a comprehensive discussion of the final results will be described later this year. The preliminary results show several interesting features. A few of the unreduced spectra are shown in Fig. 3.14 in the form of densitometer traces. Figure 3.14 A and B are spectra

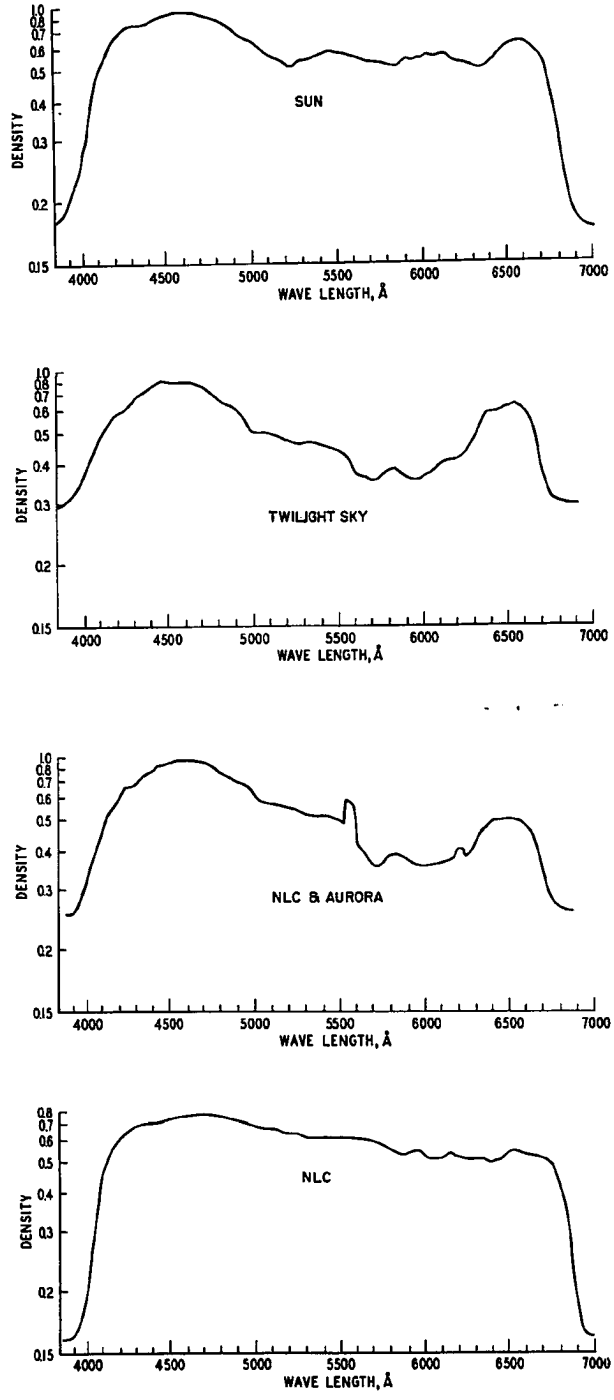

Fig. 3.14. Densitometer traces of spectra of (A) the sun, (B) the twilight sky on 2/3 July 1965, (C) NLC and aurora on 29/30 June 1965, and (D) very bright NLC on 26/27 July 1965.

of the sun and twilight sky respectively. The spectra of a weak NLC display and a simultaneous aurora which occurred on the night of 29 June 1965 is shown in Fig. 3.14C. Figure 3.14D is a spectrum of the very bright and well developed NLC display observed on the night of 26 July 1965 from Watson Lake, Yukon Territory. The relative intensity versus wavelength for the 26 July spectrum shown in Fig. 3.14D is given in Fig. 3.15 along with a photograph of the display taken at the same time as the spectrum. This spectrum shows that the light from NLC is most intense at shorter wavelengths and indicates that the average NLC particle diameter is comparable with or slightly smaller than the wavelength of visible light, i.e. a few tenths of a micron.

The technique employed in reducing the spectra is that developed by C. S. Deehr (1961), a brief description of which is given below. Kodak 103 a-F spectrographic film (35 mm) of the same age and emulsion number was used for both the NLC and the calibration spectra. The processing was kept as uniform as possible. A calibration spectrum was made for each NLC spectrum, with the same exposure time and scattering angle. Microdensitometer traces of each spectrum were made using a Leeds and Northrup densitometer. The spectral sensitivity of the film was determined by first taking a spectrum through a step wedge of a standard source calibration lamp, and then running this spectrum through the microdensitometer. The first step in the reduction was to subtract the density of the background chemical fog from the NLC and calibration spectra. Then the relative intensities of these spectra were determined from the curve of density versus relative intensity determined for the calibration lamp. The final step was to subtract the relative intensities at different wavelengths of the calibration

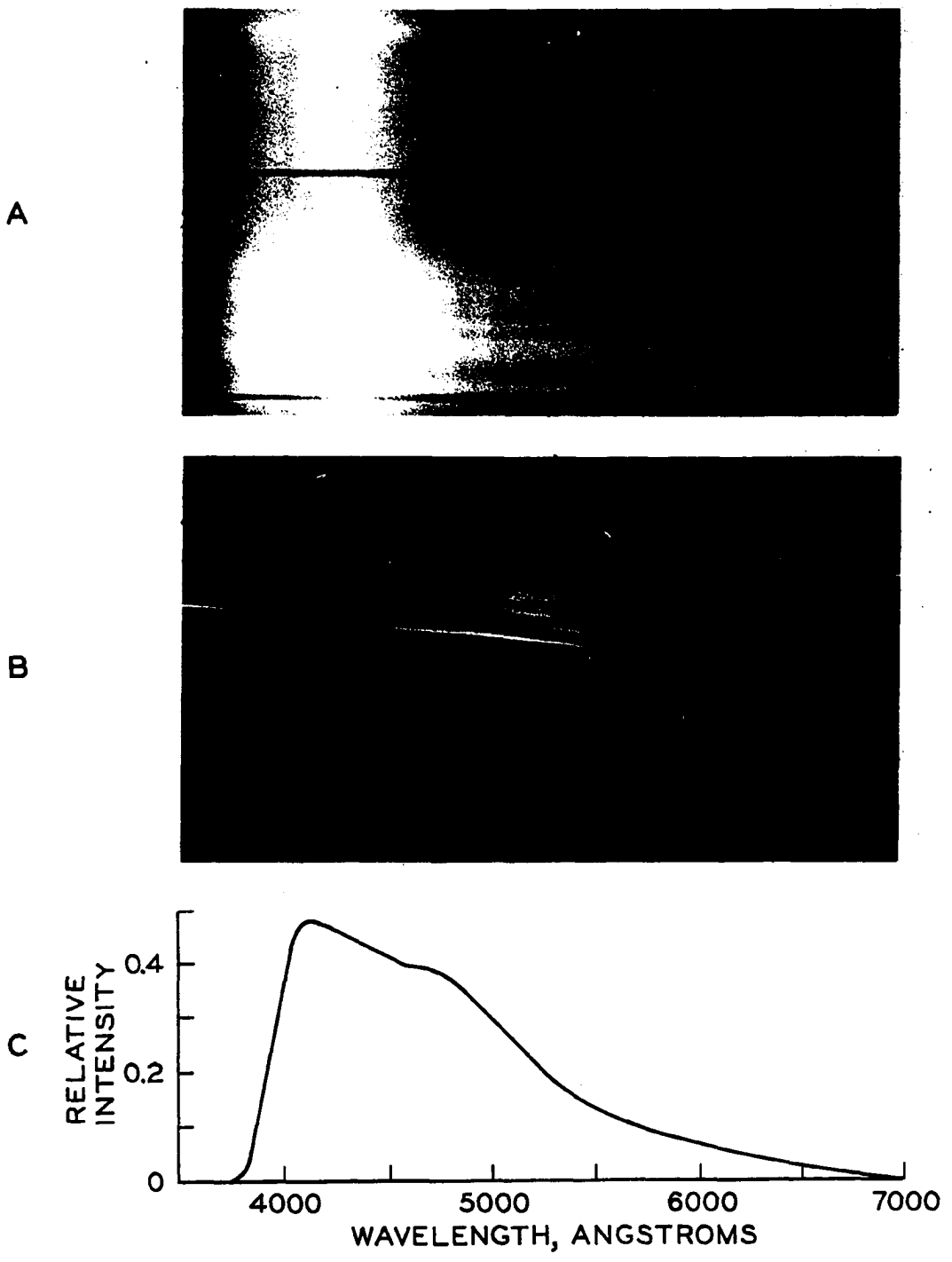

Fig. 3.15. Reduced spectrum of bright NLC on 26/27 July 1965. (A) NLC spectrum, (B) Photograph of NLC taken at same time as spectrum, (C) Reduced spectrum.

(i.e. twilight sky) spectrum from that of the NLC spectrum.

3.9 Size, Concentration and Composition of NLC Particles

For many years there was much uncertainty as to the distribution in size, concentration, and the composition of NLC particles. In order to find the real nature of these particles, Hemenway, Soberman, and Witt organized an international cooperative research program to attempt sampling of the particles *in situ* using high altitude rocket sampling techniques developed by Hemenway and Soberman (1962). The results obtained on this program are described in detail in a series of papers which appeared in Tellus 16, 34-117, 1964. These are summarized below. Four sampling rockets were launched during August, 1962 from the Kronogard rocket range (66°N, 19°E) in northern Sweden. Two of the rockets were fired in the presence of NLC and two when no NLC was present. Two of the flights were successful, one in the presence and one in the absence of NLC. Each sampling payload contained four different surfaces. The first was nitrocellulose coated with a thin layer of aluminum. The second surface was also of nitrocellulose but covered with a layer of fuchsin dye. The third surface was a lucite slide covered with a thin layer of pure indium metal. The fourth surface was of calcium metal on lucite protected by evaporated coatings of paraffin, aluminum and silicone oil. The purpose of these different surfaces was (1) to retain non-volatile particles, (2) to show whether a volatile coating had been present on the particles, and (3) to retain craters in the event that the particles were composed entirely of a volatile substance. The total area available for particle impaction was 648 mm^2.

The collecting surfaces were exposed between the altitudes of approximately 75 to 98 km during ascent of the Nike Cajun solid propellent rocket. From the range-altitude curves (Fig. 13, Soberman, et al, 1964) it appears that the rocket trajectory over the 75-98 km region was inclined at about 30° from the vertical, making the path length of the exposed collecting surfaces approximately 30 km.

The results of these sampling experiments, as described by Hemenway, Soberman, and Witt (1964) are as follows:

(1) The nuclei of NLC particles contain traces of nickel and iron and are of extraterrestrial origin.

(2) These nuclei have an integral size distribution of the form $N = \text{Const} \times (\text{Diameter})^{-p}$, where $3<p<4$.

(3) The size distribution of nuclei cuts off sharply at about 0.05 microns.

(4) The particle concentration in the sampled layer (75-98 km) is at least one thousand times greater in the presence of NLC than when they are absent.

(5) A significant fraction of the particles had a volatile coating when collected. This coating was inferred to be ice formed from water vapor of terrestrial origin.

(6) The particle concentration in a vertical column through the NLC was greater than 8×10^{10} particles per square meter.

(7) If the number density of particles decreases exponentially with height, then the scale height is about 2 km.

The integrated size distribution of NLC particles and the percentage of particles having a volatile coating are shown in Figs. 3.16 and 3.17. Photographs of a few of the NLC particles collected

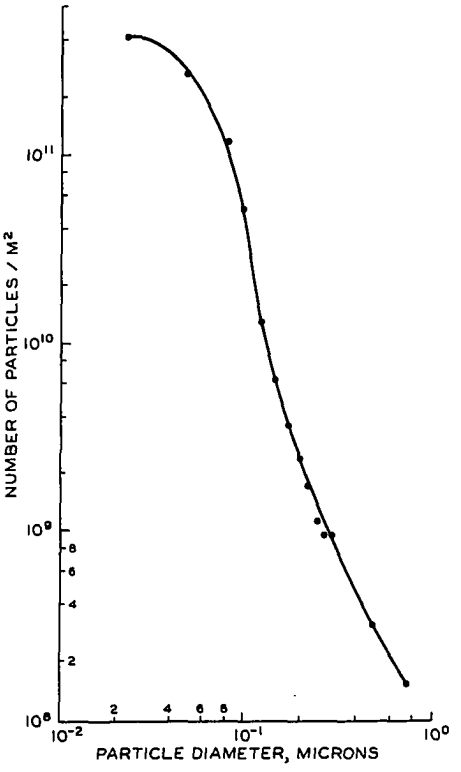

Fig. 3.16. Integrated size distribution of NLC particles (Hemenway, et al., 1964).

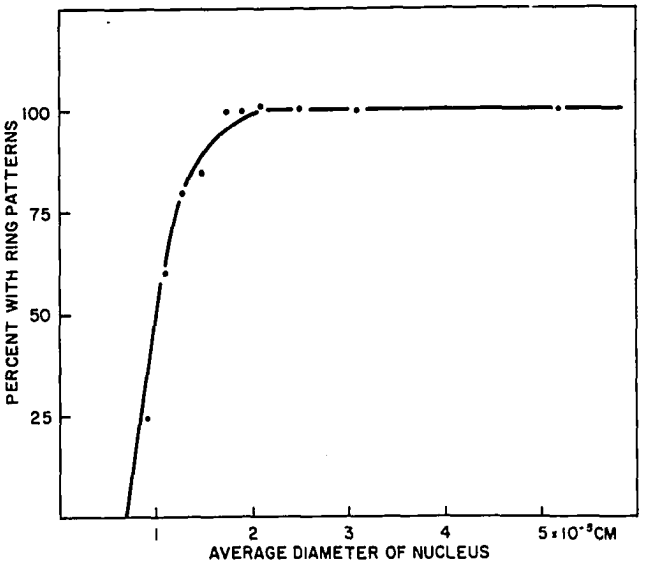

Fig. 3.17. Per cent of particles with volatile coating as a function of particle diameter (Hemenway, et al., 1964).

are shown in Fig. 3.18.

One interesting feature of the above sampling experiments is that no uncoated particles with diameters above about 0.20 microns were found, indicating that particles of this size are absent in the regions above and below the cloud layer. This suggests that the larger particles may be formed in the NLC layer by coagulation of the smaller particles. A second feature is that the diameter of the haloes surrounding the particles was from 2 to 5 times larger than that of the particles themselves. The ratio of halo diameter to particle diameter was greatest for the smaller particle diameters (0.1 to 0.2 microns) indicating that these particles had relatively thicker coatings of volatile material (Fig. 3.19).

Laboratory experiments by Linscott, Hemenway, and Witt (1964) suggest that an average haloed NLC particle had approximately 3×10^{-12} grams of water associated with it.

3.10 Artificial Cloud Experiments

The recent observations (Meinel, 1963) of artificial NLC induced by rocket exhausts point to another method of determining whether particle growth is responsible for the formation of NLC. If the missing ingredient at the mesopause is water vapor, then an injection of a sufficient supply of water there should serve to create NLC over a limited region. If an increase in the concentration of dust at the mesopause is all that is required for the formation of these clouds, then an injection of dust particles with diameter about 0.3 μ should form a small noctilucent-type cloud.

Four experiments of the first kind were carried out in August 1964

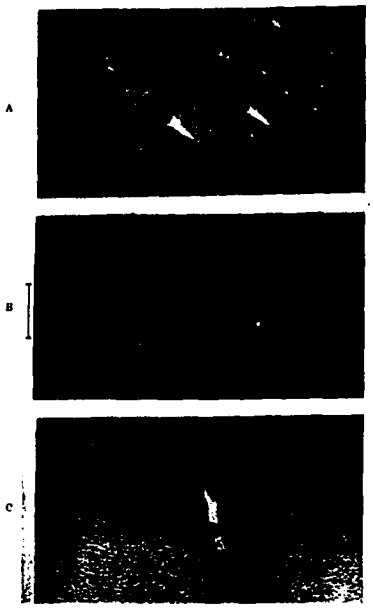

Fig. 3.18. Samples of NLC particles. (A) Cloud collecting surface showing particles with haloes, (B) Non-cloud collecting surface, and (C) Control surface. Scale = 1 micron. (Hemenway, et al.,1964).

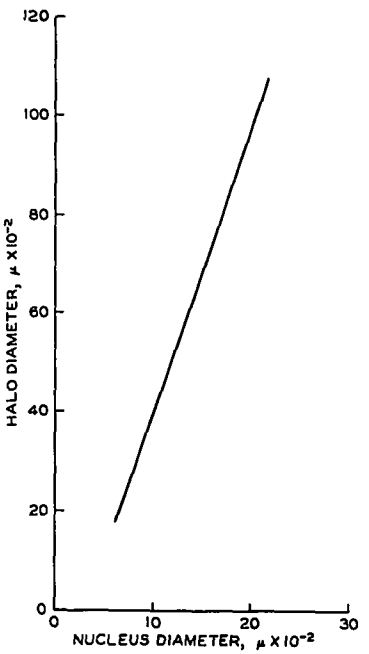

Fig. 3.19. Variation of halo diameter with diameter of the nucleus for particles collected on the cloud flight. (Hemenway, et al, 1964).

from the Meterological Rocket Network range at Ft. Greely, Alaska, but as we were unable to locate a source of dust particles of diameter $\sim 0.3\mu$, no dust injection experiment was planned. Two water injections were to be tried in the presence of NLC when we know the mesopause conditions are suitable, and two, in the absence of NLC. Boosted Arcas rockets were to be used to carry the water canisters to the mesopause. Calculations of the amount of water necessary and the size of the cloud that might be produced were made. These indicated that a release of 2 kg (about 100 moles) of water at the mesopause should yield a cloud of about 0.5 km in radius, providing the water was not instantaneously turned into ice on release.

Two field stations, equipped with phototheodolites of long focal length K-24 cameras, spectrographs, and a polarimeter were set up about 200 km south of the Ft. Greely range to observe the results of the water releases. These stations were located at the Gulkana F.A.A. landing field and at the Tolsona White Alice Site on an approximately east-west base line of about 40 km.

During the period 25 July-15 August when the firings were to take place, only 5 nights were clear. No NLC were present over Ft. Greely during these 5 nights, so it was not possible to inject the water into existing displays. The two clear-sky injections were made, however, on 5/6 and 8/9 August at approximately 2300 LMT. No visible clouds were formed from these releases. Because of the difficulty of tracking the rockets, we did not know at what altitude the water was released. Hence it is uncertain whether any water was released at the proper altitude, or whether the water did not vaporize and rapidly expand before freezing, but turned into ice instantaneously on release,

or whether water vapor is not necessary for the formation of NLC.

Further experiments along these lines, with better rocket tracking arrangements, are being planned for 1967-1968.

CHAPTER 4

NOCTILUCENT CLOUDS IN THE SOUTHERN HEMISPHERE

4.1 Early History

The existence of NLC in the southern hemisphere was uncertain until recently; over the period 1885-1964, during which over a thousand nights of NLC were reported from the northern hemisphere, only three observers have reported seeing NLC in the southern hemisphere (Fogle, 1964), and none of these reports supported by photographs. Stubenrauch (see Vestine, 1934) reported seeing NLC from Punta Arenas, Chile (53.1°S, 71°W) on two nights during the southern summer of 1888, but did not give exact dates, times, directions and characteristics of the displays observed. A ship's captain reported seeing NLC on 10 out of 31 clear nights from his ship located off Puerto Williams (54.5°S,68°W) in the Beagle Channel during the southern summer of 1888 (Vestine 1934) but again no information on the dates, times, directions, and characteristics were given. The third report was made by Mr. W. Holman (private communication). His observation was made on the night of 4/5 December 1962 from the USNS ELTANIN, which at the time of the observation was located southeast of Tierra del Fuego at 55°S, 58.8°W. Mr. Holman attempted to photograph the clouds, but was unsuccessful.

4.2 Formation of Southern Hemisphere Network of NLC Observers

In 1964, after our work on NLC over North America was underway, we began making plans to investigate NLC in the southern hemisphere. During that year, arrangements were made to have the personnel at the U.S. Antarctic bases make NLC observations, and an observation manual

(Fogle, 1964) was prepared and sent to them. In late 1964 it was arranged with the help of WMO that the personnel at the meteorological stations in South America and on the islands in the latitude range 45°-70°S should make NLC observations. No reliable observations were received from these stations prior to 1965, however.

4.3 Inferences on Southern Hemisphere NLC from Northern Hemisphere Data

Based on the observational data from the northern hemisphere, one would expect that if NLC occur in the southern hemisphere, they would most likely be observed in the southern summer months of December, January, and February with the peak of activity in January, observed from stations in the latitude range of 50°-60°S (the times for observing NLC from these latitudes are shown in Figs. 4.1 and 4.2.) But there is little habitable land in the zone 50°-60°S (see Fig. 1.6) and a corresponding scarcity of people. Further complicating NLC observations in this zone is the considerable tropospheric cloud cover experienced there.

4.4 Confirmation of the Existence of Southern Hemisphere NLC

After careful study of the locations and tropospheric cloud cover of the inhabited areas in the 50°-60°S zone, Punta Arenas, Chile, the southernmost city on the South American continent at 53.1°S, 71°W., was selected as the best place to make ground based observations of NLC. I went to Punta Arenas for the period January 8-17, 1965 when the NLC activity should be at its maximum there. During these 9 nights, 7 of which were clear enough to see NLC if they were present, one display was observed on the night of 9 January 1965. The display was

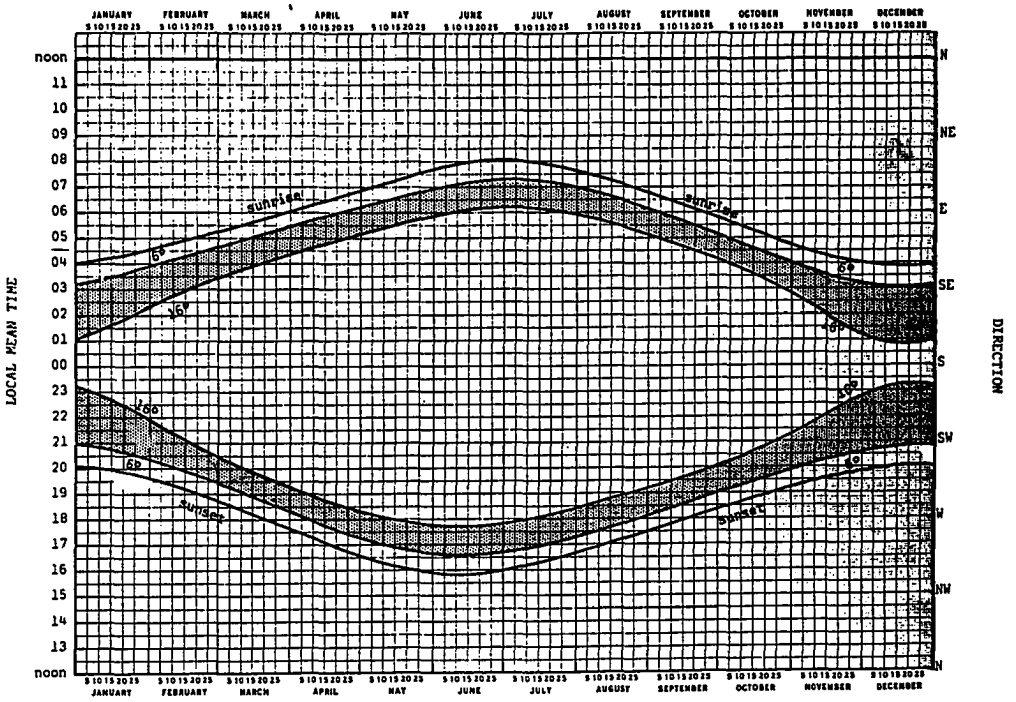

NOCTILUCENT CLOUD OBSERVATION PERIODS (SHADED AREA) FOR 50° S.

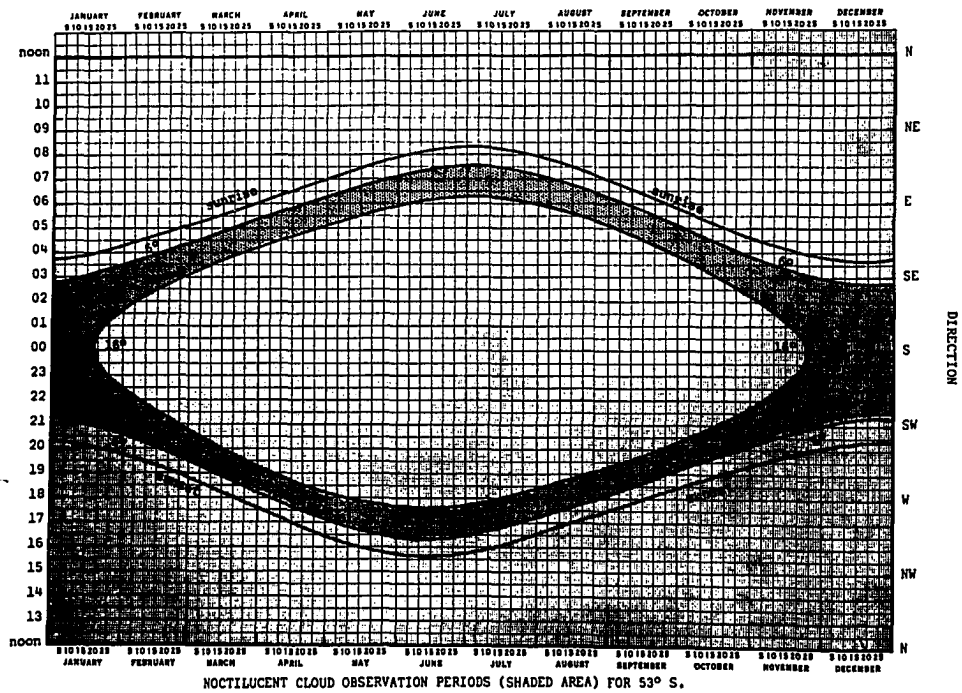

NOCTILUCENT CLOUD OBSERVATION PERIODS (SHADED AREA) FOR 53° S.

Fig. 4.1. NLC observation periods for 50°S and 53°S.

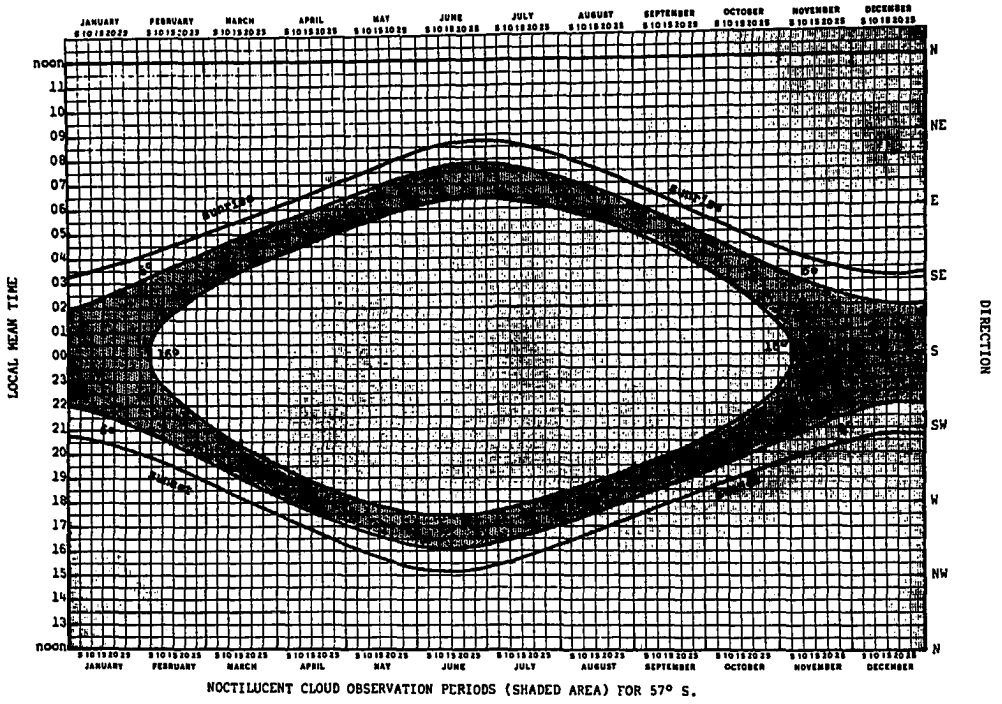

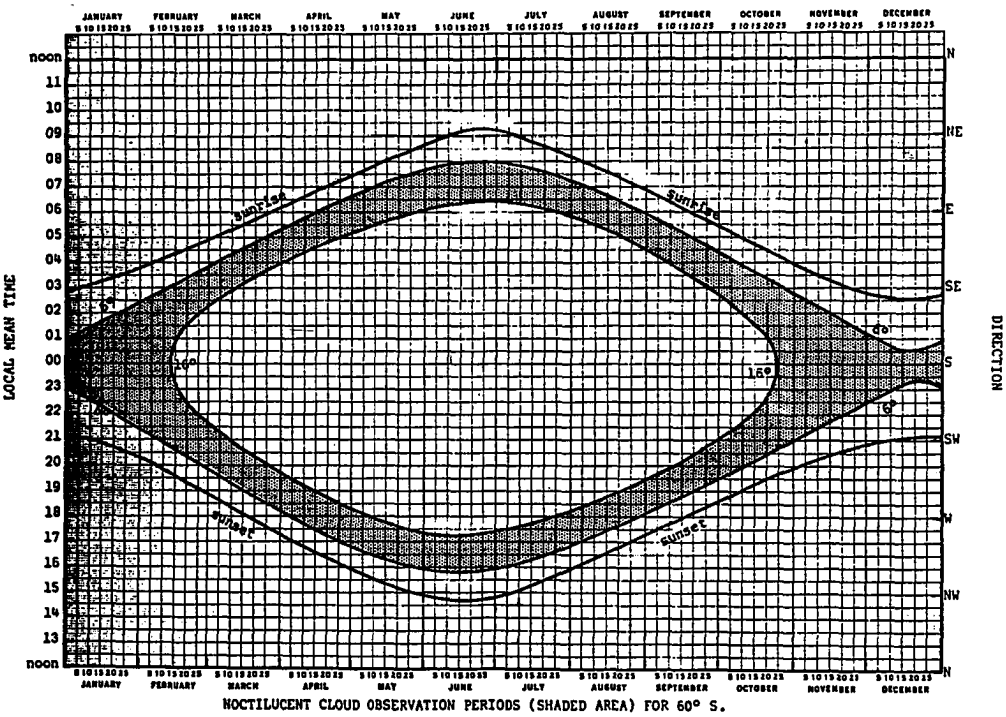

Fig. 4.2. NLC observation periods for 56°S and 60°S.

moderate in intensity, it extended up to about 8° above the horizon, and in azimuth from about southwest to southeast. It was first observed at 2200 LMT and was obscured by low tropospheric cloud at 2245 LMT (Fogle, 1965a). The range of solar depression angles corresponding to this observing period is 10.0°-12.6°. A photograph of this display is given in Fig. 4.3.

4.5 The NLC Expedition to Punta Arenas, Chile During the Austral Summer of 1965-66

Having this confirmation that NLC exist in the southern hemisphere, we began preparations to investigate their characteristics (frequency of occurrence, height, velocity). The National Science Foundation provided us with an additional grant for this work and made arrangements for the Chilean Air Force to furnish air support for the investigation. Our plans were to set up two ground stations near Punta Arenas for height and velocity determinations and to have one of our observers fly every night at 20,000 ft down to 58°S, to obtain data on the frequency of occurrence and spatial extent of the NLC.

This past November (1965), we went to Punta Arenas and established our ground stations. The main station was located at the Chilean Air Base, Bahia Catalina, approximately 4 km north of the city of Punta Arenas. The auxiliary station was set up at Las Mercedes, a Salesian agricultural school located approximately 15 km SSE of the town of Porviner on Tierra del Fuego, across the Straits of Magellan from Punta Arenas (see Fig. 4.4). The geographic coordinates of these two stations are:

Bahia Catalina: 53°7' 30"S, 70°52'42"W
Las Mercedes: 53°24'30"S, 70°18'22"W
Length of Base Line: 49.872 km.
Orientation: approximately NW-SE

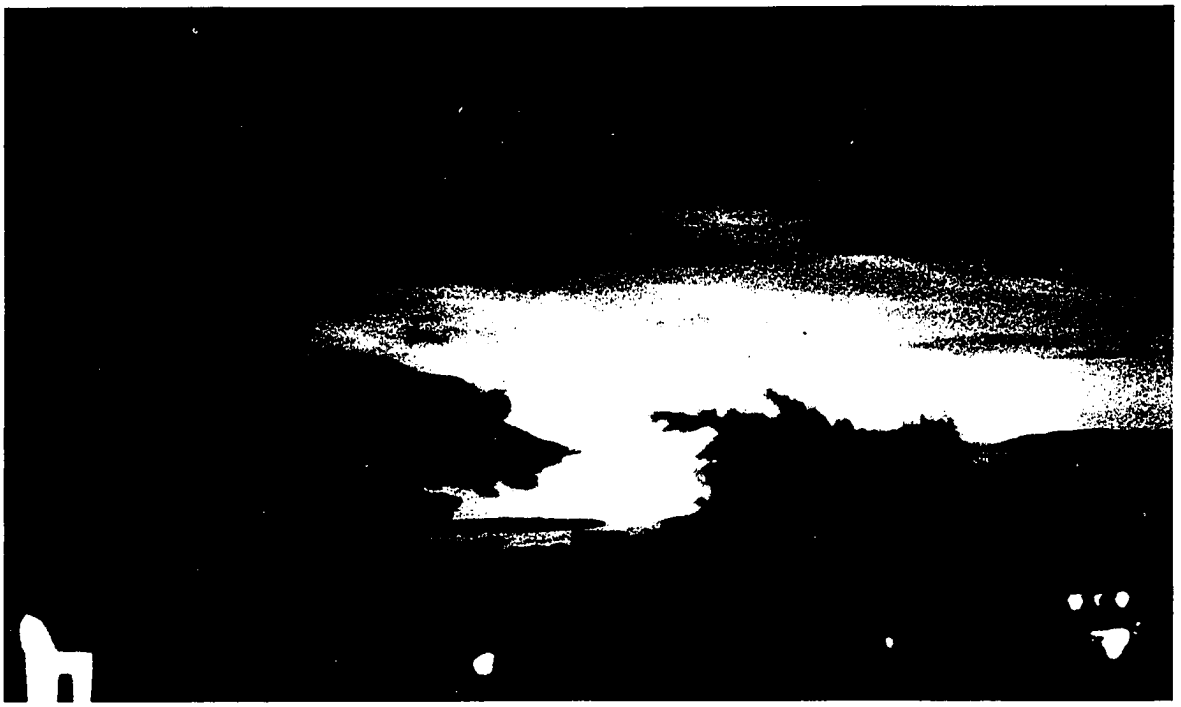

A

B

Figure 4.3. Photographs of NLC displays from Punta Arenas, Chile. (A) 9/10 January 1965, (B) 3/4 January 1966

NLC observations from the ground stations commenced on 27 November 1965 and were continued until 17 February 1966. The airborne observations did not begin until 14 December; they were made on 15 nights (December 14, 19, 25, 26, 27, 29, and January 1, 2, 17, 18, 19, 20, 22, 24, 26)during the 82 day expedition. The limited range of our aircraft (a B-26), prevented flights further south than 56°; on most of the 13 nights, the flight was within a 30 mile radius of Punta Arenas. The lack of de-icing equipment on the aircraft prevented flights being made on nights when there was ground rain or icing conditions in the lower clouds.

4.6 Results of the Punta Arenas Expedition

NLC were seen on 9 nights during the expedition (see Table 4.1). Three of these were seen only from the aircraft, two of them only from the ground, and four from both ground and aircraft. These displays were observed to drift generally towards the WNW. Using the observational data in Table 4.1, the percentage of clear nights with NLC was determined (Table 4.2). The results (Fig. 4.5) indicate that the peak of NLC activity at 53°S occurs some 20-30 days after the austral summer solstice.

The brightest and most widespread displays observed occurred during the period January 1-4 with the best display occurring on the night of January 3. It is of interest to note that the intense Quadrantids meteor shower occurs on these same days and has its maximum on January 3. No displays, however, were observed during the intense Geminids meteor shower which occurs during the period December 9-15 and peaks on December 13, but this could be due to the relatively poor observing conditions (only three of the nine nights were clear

enough for NLC observations) rather than the lack of NLC. Photographs of one of these displays is shown in Fig. 4.3.

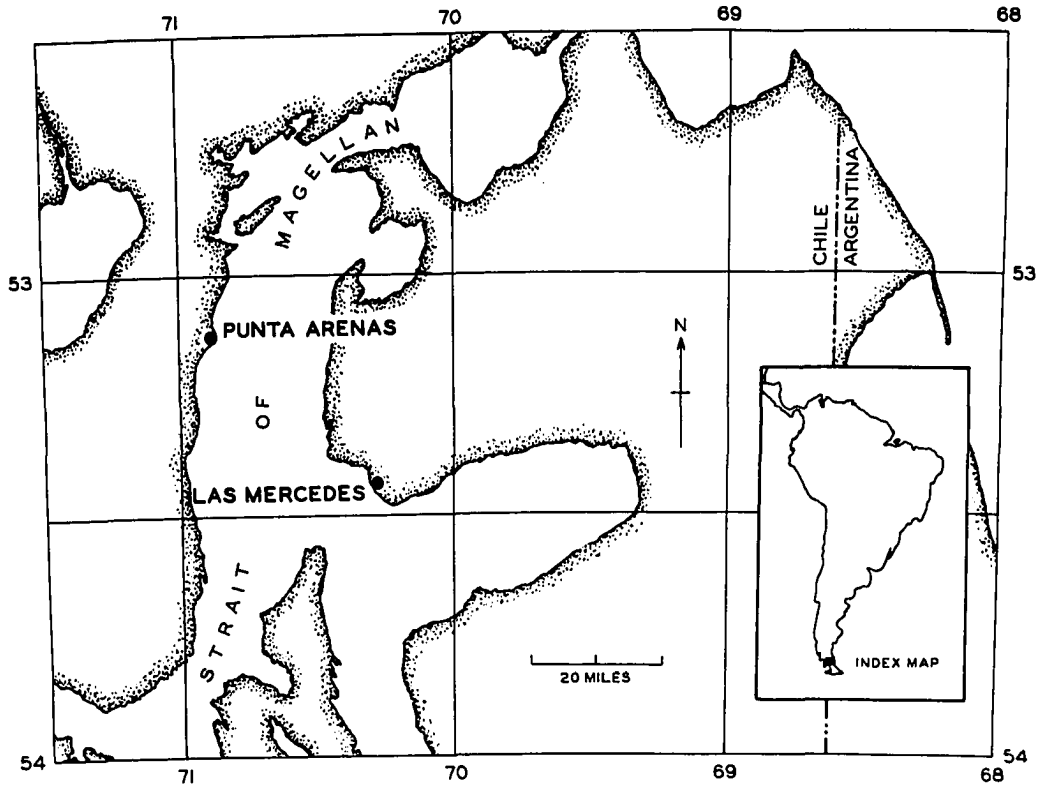

Fig. 4.4. Location of field stations near Punta Arenas, Chile.

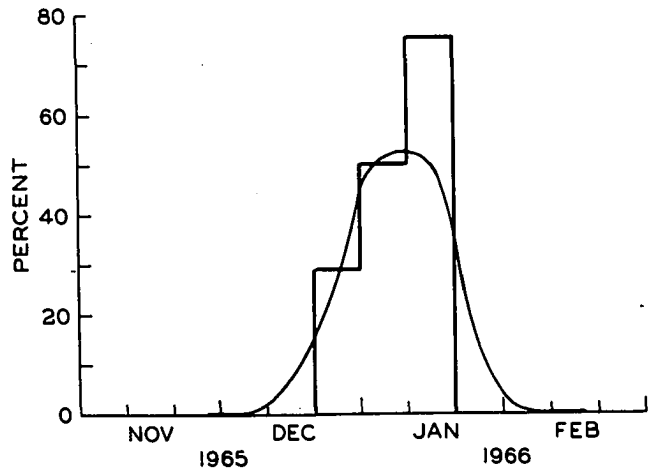

Fig. 4.5. Per cent of clear nights with NLC at Punta Arenas, Chile, during Austral summer of 1965-66.

Table 4.1

Summary of NLC Observations from Punta Arenas during the Austral Summer of 1965-66

(1) Date	(2) Presence of NLC (G)(A)*	(3) Flight	(4) Cloud Cover in Twilight Sector**	(5) Period NLC Observed (LMT)	(6) Range of SDA when NLC Observed	(7) Brightness †	(8) Forms Present	(9) Extent of NLC in Azimuth	(10) Extent of NLC in Elevation
27 Nov '65	No		B	-					
28	-		D	-					
29	No		B	-					
30	No		B	-					
1 Dec	-		D	-					
2	No		B	-					
3	-		B	-					
4	No		B	-					
5	No		B	-					
6	-		D	-					
7	-		D	-					
8	No		B	-					
9	-		D	-					
10	No		B	-					
11	-		D	-					
12	No		B	-					
13	-		D	-					
14	No	Yes	D	-					
15	-		D	-					
16	-		D	-					
17	-		D	-					
18	No		A	-					
19	No	Yes	C	-					
20	-		D	-					
21	-		D	-					
22	No		B	-					
23	-		D	-					
24	-		D	-					
25	Yes (A)	Yes	D	2350-0015	13°	1	Veil, Whirls	182°-184°	0°-2°
26	No	Yes	D						
27	No	Yes	B						

Table 4.1 (Continued)

Summary of NLC Observations from Punta Arenas During the Austral Summer of 1965-66

(1)	(2)	(3)	(4)	(5)	(6)	(7)	(8)	(9)	(10)
Date	Presence of NLC (G)(A)*	Flight	Cloud Cover in Twilight Sector**	Period NLC Observed (LMT)	Range of SDA when NLC Observed	Brightness †	Forms Present	Extent of NLC in Azimuth	Extent of NLC in Elevation
28 Dec '65	-		D						
29	Yes (A) (G)	Yes	C	2240-2355	11.9°-13°	2	Veils & Bands	165°-240°	8°-35°
30	No		B						
31	No		B						
1 Jan '66	Yes (G) (A)	Yes	C	2345-0220	8°-13.5°	3	Bands & Billows	184°-227°	3°-10°
2	Yes (G) (A)	Yes	B	2230-0145	11°-13.5°	2	Veil, Billows, Bands, Whirls	158°-191°	4°-7°
3	Yes (G)		B	2145-0230	8°-14°	3	Veil, Billows, Bands, Whirls	160°-244°	3°-10°
4	Yes (G)		C	2352-0005	14°	1	Bands	175°-185°	2°-4°
5	No		A						
6	-		D						
7	No		B						
8	-		D						
9	No		B						
10	No		B						
11	-		D						
12	-		D						
13	-		D						
14	-		D						
15	-		D						
16	-		D						

Table 4.1 (Continued)

Summary of NLC Observations from Punta Arenas During the Austral Summer of 1965-66

(1) Date	(2) Presence of NLC (G)(A)*	(3) Flight	(4) Cloud Cover in Twilight Sector**	(5) Period NLC Observed (LMT)	(6) Range of SDA when NLC Observed	(7) Brightness†	(8) Forms Present	(9) Extent of NLC in Azimuth	(10) Extent of NLC in Elevation
17 Jan '66	Yes (A) (G)	Yes	C	0156-0205	12°	1	Veil	160°-190°	5°-8°
18	Yes (A)	Yes	C	0110-0150	13°-14.5°	2	Bands	135°-165°	1°-3°
19	No	Yes	D						
20	Yes (A)	Yes	C	2240-2250	14°-14.5°	1	Bands	165°-185°	2°-4°
21	-		D						
22	No	Yes	B						
23	-		D						
24	No	Yes	B						
25	No		B						
26	No	Yes	B						
27	-		D						
28	No		B						
29	No		B						
30	-		D						
1 Feb	-		D						
2	-		D						
3	-		C						
4	-		D						
5	-		D						
6	No		B						
7	No		B						
8	-		C						
9	No		B						
10	-		D						
11	-		C						
12	No		B						
13	No		B						
14	-		D						
15	No		B						
16	-		D						
17	-		D						

* (G) - Visible from ground stations
(A) - Visible from aircraft

NLC present - (Yes), NLC absent - (No)
No observation possible due to overcast skies - (___)

** Denotes which nights NLC observations were made from aircraft flying above tropospheric clouds

*** As seen from ground stations: A-completely clear, B-scattered clouds, C-broken clouds, D-overcast

† NLC brightness scale: (1) Very weak NLC, barely discernable,
(2) NLC easily detected but of low brightness,
(3) bright NLC,
(4) exceptionally bright NLC

Table 4.2

Observed Frequency of Occurrence of NLC at Punta Arenas During the Austral Summer of 1965-66.

Period	No. of Nights of Observations	No. of Nights when NLC could be Observed	No. of NLC	% of Nights clear	% of Clear Nights that NLC were Observed
1965					
Nov 20-30	4	3	0	75	0
Dec 1-10	10	5	0	50	0
11-20	10	3	0	30	0
21-31	11	7	2	67	29
1966					
Jan 1-10	10	8	4	80	50
11-20	10	4	3	40	75
21-31	11	7	0	67	0
Feb 1-10	10	3	0	30	0
11-20	7	3	0	43	0

CHAPTER 5

CHARACTERISTICS OF THE MESOSPHERE

In this chapter the physical and chemical properties of the earth's atmosphere are reviewed. A knowledge of these properties is important to the understanding of the NLC phenomenon.

5.1 Atmospheric Properties

Most of the data on atmospheric properties presently available was obtained at mid latitudes rather than at high latitudes where NLC occur. Until high latitude data on these properties is available, these mid-latitude data have to suffice. Using the mid-latitude data, Minzner, Champion and Pond (1959) have prepared a "model atmosphere". The variation of the temperature, pressure, density, molecular weight, scale height, number density, mean free path, and viscosity with altitude for this model atmosphere are reproduced here in Table 5.1 and Figs. 5.1 and 5.2.

Over the past ten years, there have been several dozen measurements of the temperature up to and beyond the mesopause at high latitudes. These measurements were made using the rocket-grenade technique in which 4 lb. high explosive charges are detonated approximately every 3km, and the temperatures and winds are determined by measuring the velocities of sound and the deflections of the sound waves from the successful explosions. This technique provides values of the temperature and wind up to a maximum altitude of around 90 km averaged over 3 km height intervals. Larger grenades and more sensitive microphones are required to extend these measurements to higher altitudes (Stroud, Nordberg, Bandeen, Bartman, and Titus, 1960).

Table 5.1

Properties of Model Atmosphere from 0-100 km*
(Minzner, Champion, and Pond, 1959)

Height (km)	Temperature (°K)	Mean Molecular Weight	Pressure (mb)	Mass Density (kg/m^3)	Scale Height (km)	Number Density (m^{-3})	Mean Free Path (m)	Kinematic Viscosity (m^2/sec)	Coefficient of Viscosity ($kg\ m^{-1}\ sec^{-1}$)
0	288.16	28.97	1.01+3	1.22+0	8.43	2.55+25	6.63-8	1.46-5	1.79-5
5	255.69	28.97	5.40+2	7.36-1	7.49	1.53+25	1.10-7	2.21-5	1.63-5
10	223.26	28.97	2.65+2	4.13-1	6.55	8.60+24	1.96-7	3.52-5	1.46-5
15	216.66	28.97	1.21+2	1.95-1	6.37	4.05+24	4.17-7	7.30-5	1.42-5
20	216.66	28.97	5.53+1	8.89-2	6.38	1.85+24	9.14-7	1.60-4	1.42-5
25	216.66	28.97	2.53+1	4.06-2	6.39	8.45+23	2.00-6	3.50-4	1.42-5
30	231.24	28.97	1.18+1	1.79-2	6.83	3.71+23	4.55-6	8.40-4	1.50-5
35	246.09	28.97	5.83+0	8.26-3	7.28	1.72+23	9.83-6	1.91-3	1.58-5
40	260.91	28.97	3.00+0	4.00-3	7.73	8.32+22	2.03-5	4.13-3	1.65-5
45	275.71	28.97	1.60+0	2.02-3	8.18	4.20+22	4.02-5	8.55-3	1.73-5
50	282.66	28.97	8.78-1	1.08-3	8.40	2.25+22	7.50-5	1.63-2	1.76-5
55	275.78	28.97	4.84-1	6.11-4	8.21	1.27+22	1.33-4	2.83-2	1.73-5
60	253.68	28.97	2.56-1	3.52-4	7.57	7.33+21	2.30-4	4.59-2	1.61-5
65	231.62	28.97	1.28-1	1.93-4	6.92	4.02+21	4.20-4	7.77-2	1.50-5
70	209.59	28.97	6.02-2	1.00-4	6.27	2.08+21	8.12-4	1.38-1	1.38-5
75	187.60	28.97	2.59-2	4.82-5	5.62	1.00+21	1.68-3	2.61-1	1.26-5
80	165.7	28.97	1.01-2	2.12-5	4.97	4.41+20	3.83-3	5.31-1	1.13-5
85	165.7	28.97	3.69-3	7.76-6	4.98	1.61+20	1.05-2	1.45+0	1.13-5
90	165.7	28.97	1.35-3	2.85-6	4.99	5.92+19	2.85-2	3.96+0	1.13-5
95	179.9	28.94	5.12-4	9.92-7	5.43	2.06+19	8.19-2		
100	199.0	28.90	2.14-4	3.73-7	6.02	7.78+18	2.17-1		

*In this table, a one or two-digit number (preceded by a plus or minus sign) following the initial entry indicates the power of ten by which that entry should be multiplied.

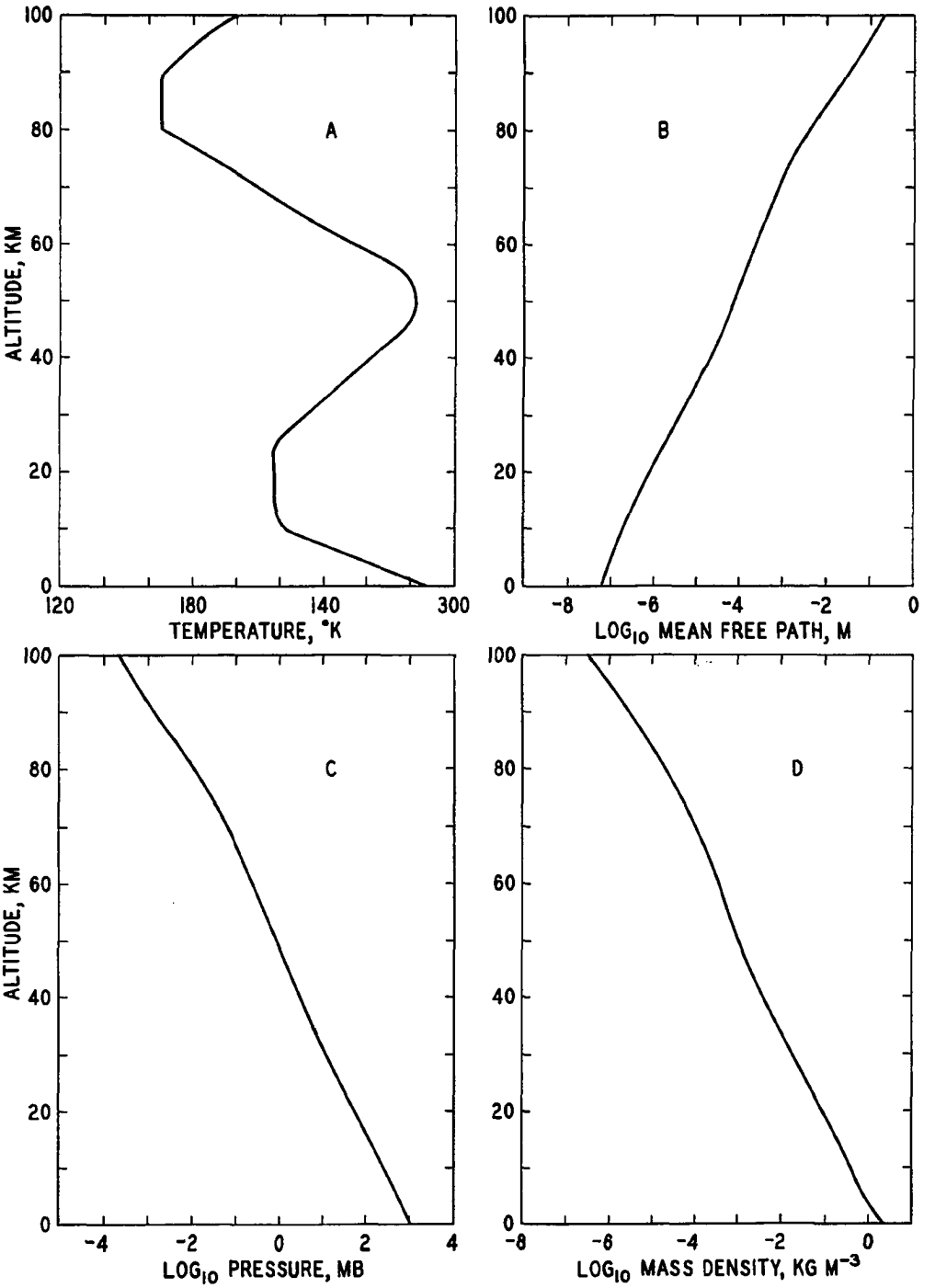

Fig. 5.1. Model atmosphere (Minzner, et al. 1959).

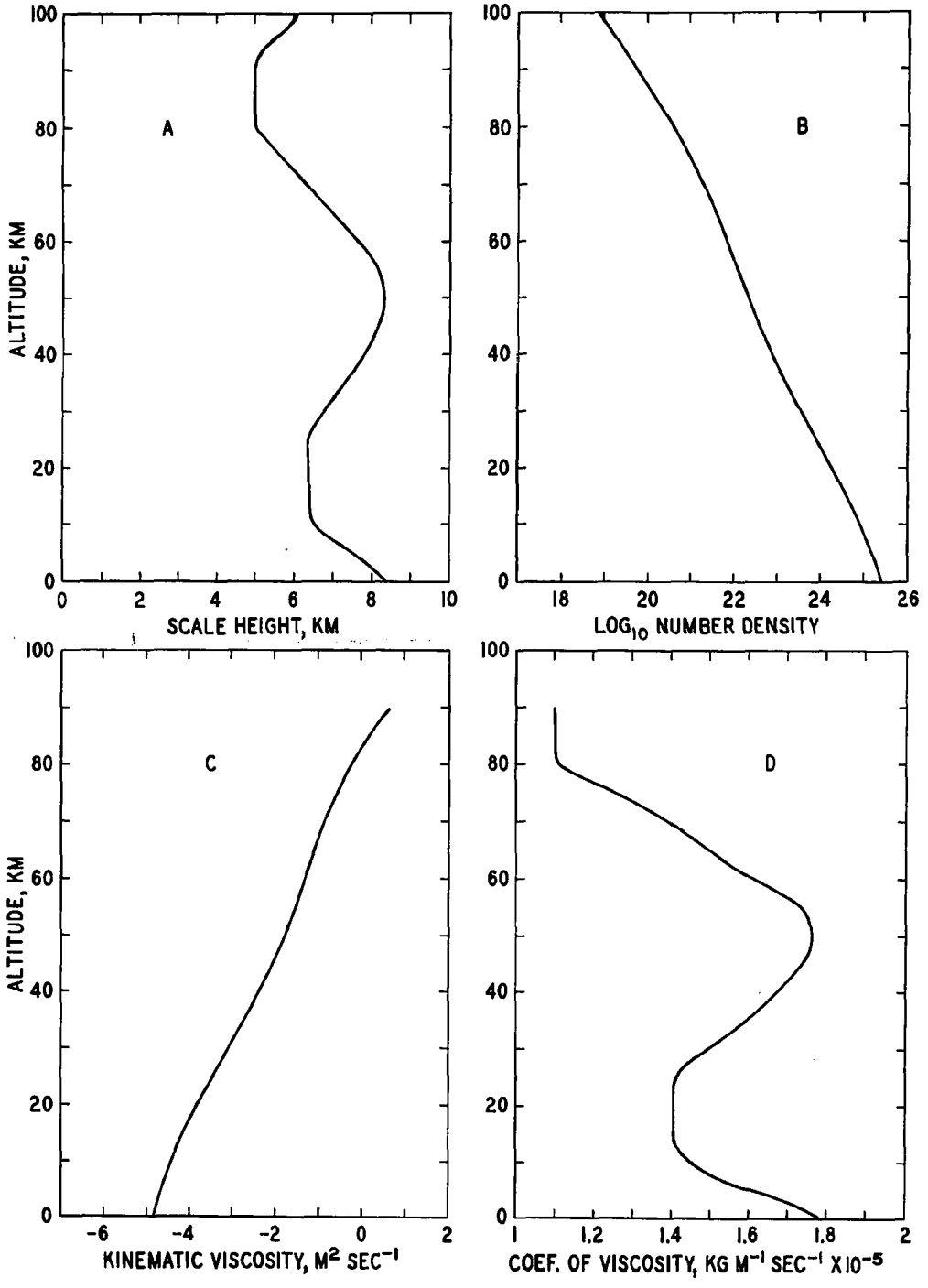

Fig. 5.2. Model atmosphere (Minzner, et al. 1959).

As the temperature at the mesopause appears to be an important parameter for NLC formation and as NLC form in a thin layer, it would be of great interest to obtain continuous temperature measurements over the height range 75-85 km.

High latitude mesopause temperature measurements were first made from Ft. Churchill, Manitoba (59°N) during 1956-1958, years of high sunspot activity. The results of these measurements confirmed the deductions of Kellogg and Schilling (1951), Pant (1956) and Murgatroyd (1957) that the mesopause is warmer in winter than in summer at high latitudes and is also warmer in winter at high latitudes than at low latitudes. Kellogg (1961), in his discussion of this winter warming of the high latitude mesosphere, points out that this warming could be explained by adiabatic heating due to very rapid subsidence generated by the large-scale meridional circulation (about 1 km per day or more), but if the downward motion does take place, then another much more effective source of energy - the energy of recombination stored in atomic oxygen - would be released between 80 to 100 km. The required amount of heating could be produced by this mechanism with a subsidence rate as low as 42 meters per day.

The summer and winter temperature profiles obtained from the above-mentioned measurements (Fig. 5.3) show an average summer mesopause temperature of 170°K and an average winter mesopause temperature of 230°K.

Over the past three years (1963-1965), during which the sunspot activity was low, other high latitude temperature measurements were made from Pt. Barrow, Alaska (71°N), Ft. Churchill, Canada (59°N) and

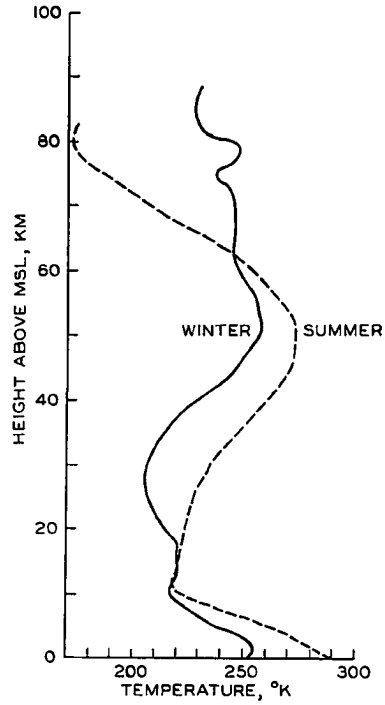

Fig. 5.3. Average summer and winter temperature profiles over Ft. Churchill (59°N) during 1956-58. The averages are based on 5 winter and five summer firings, (Stroud, et al., 1960).

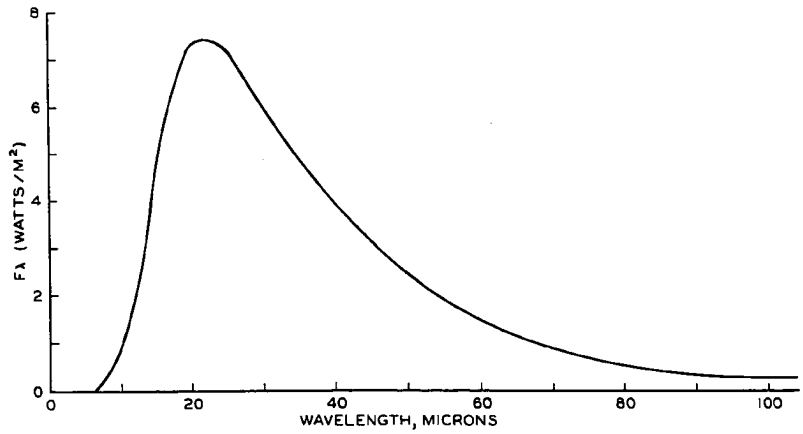

Fig. 5.4. Variation of the radiation flux from a black body at T = 130°K (λ_{max} = 22.3 microns.)

Kronogard, Sweden (66°N). Detailed results of these firings are not yet available, but a general discussion of them has recently been presented by Nordberg, Katchen, Theon, and Smith (1965). The preliminary results are as follows: (1) the winter warming of the upper mesosphere over Churchill is much less intense during IQSY than it was during IGY (average seasonal temperature excursions at 80 km during IQSY are about 45°K compared with 65°K during the IGY). (2) IQSY summer mesopause temperatures were around 140°K both in the presence and the absence of NLC. These results suggest a relationship between solar activity and high mesopause temperatures and lend some support to the possibility of auroral induced heating of the mesosphere.

In NLC displays one often observes two intersecting groups of long parallel bands which move in different directions. This has led to the speculation that on occasion there may be two layers of NLC separated by a sharp shear region. Schilling (1964) in a discussion of latitudinal variation of mesopause height as inferred from eclipse observations, conjectures that a double mesopause may exist and that the two minima may differ in height from 20 to 30 km over the equator, the difference decreasing to zero at the poles.

Assuming the NLC particles to have an emissivity of 1 and taking their temperature to be 130°K, the variation of the radiation flux as a function of wavelength was determined (Fig. 5.4). The peak of the curve is at $\lambda_{max} = 22.3\mu$.

5.2 Chemical Composition

Due to mixing, the chemical composition of the atmosphere is fairly uniform up to around 80 km, as shown in Fig. 5.5. Above this altitude

photo-dissociation of O_2 produces a marked increase of atomic oxygen.

5.3 The Ionosphere

The ionosphere (defined as the part of the earth's atmosphere where ions and electrons are present in quantities sufficient to affect the propagation of radio waves) usually extends from about 50 km up to great heights but may sometimes extend lower down. The part of the ionosphere below 90 km is called the D region, that between 90 and 160 km the E region, and that above 160 km the F region (Fig. 5.6), (Ratcliffe, 1961). The D region is of particular interest to us, as the NLC are formed in this altitude range. According to Houston (1958) the electrons in the D region arise mainly from the ionization of NO by Lyman-alpha radiation.

Parthasarathy and Rai (1966) have examined the effect of dust particles on the steady state distribution of electrons and ions in the D region and find that the presence of dust causes an increase in the effective recombination coefficient due to electron attachment to the particles. Their results suggest that if the dust concentration is sufficiently high in NLC, a sharp drop in the electron density could be produced at that altitude. Aikin, Kane, and Troim (1964) have found such sharp drops in the electron density profile near the mesopause on two occasions (March 9, 1963 and April 9, 1963 - see Fig. 5.7) over Wallops Island, Virginia (38°N); they suggest that this drop in the electron density may be caused by electron attachment to dust. According to Parthasarathy (private communication), a dust concentration at the mesopause of about 100 particles per cc would be required to produce this effect.

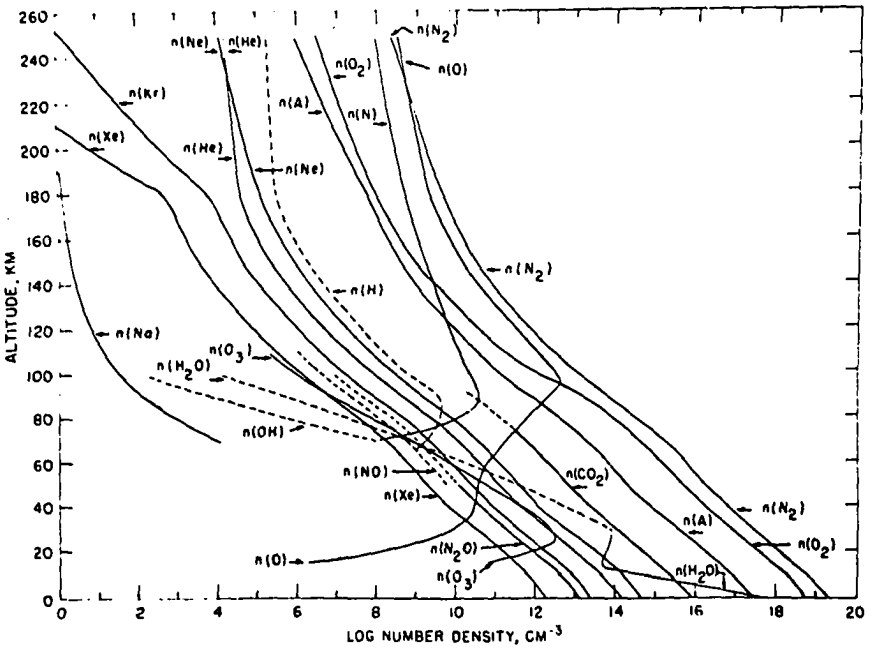

Fig. 5.5. Vertical distribution of atmospheric constituents from the earth's surface to 250 km. (Handbook of Geophysics, 1957).

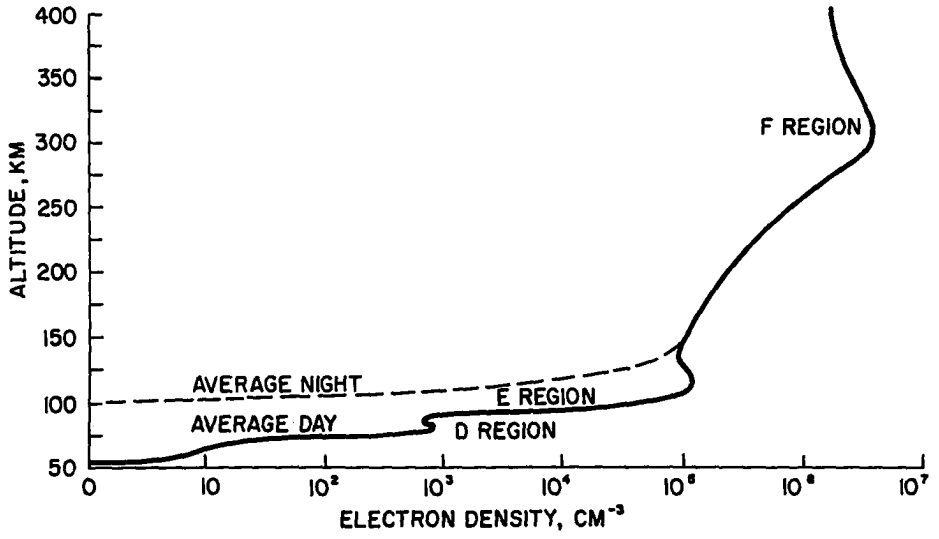

Fig. 5.6. Electron density model of the ionosphere. (Handbook of Geophysics, 1957).

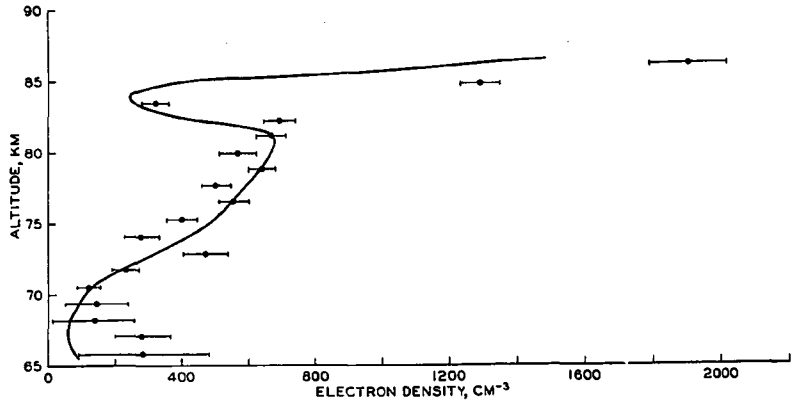

Fig. 5.7. Sharp drop in the electron density at around 84 km over Wallops Island, Virginia on 8 March 1963. Each point is the average electron density in an interval of approximately 1 km. The horizontal bar indicates the uncertainty due to the standard deviation in the scatter of the data used to determine this average value. (Aiken, et al., 1964).

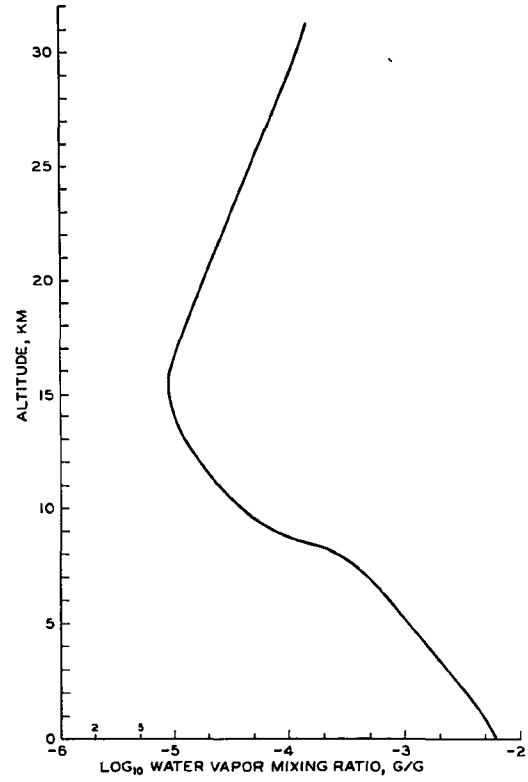

Fig. 5.8. Variation of the water vapor mixing ratio with height. (Gutnick, 1962).

5.4 Water Vapor Concentration

Owing to the difficulties encountered in measuring the water vapor content of the atmosphere, considerable uncertainty exists as to its concentration and the degree of photodissociation of H_2O by Lyman-alpha radiation near the mesopause.

Several humidity measurements up to a height of about 30 km (see Gutnick, 1962) show that the proportion of water vapor to dry air increases from around 0.01 g/kg at 15 km to around 0.1 g/kg at 30 km (Fig. 5.8).

To explain this increase of water vapor concentration with height above 15 km, Hesstvedt (1964) suggests that sufficiently strong vertical motions exist near the tropical tropopause to transport water substance in the form of ice crystals (with radii less than 3 microns) into the stratosphere and that this air mass is transported by atmospheric circulation to middle and high latitudes at heights of 25 km or more. Applying his circulation model (Fig. 5.9) to a newly computed photochemical oxygen-hydrogen model atmosphere, Hesstvedt calculated the water vapor concentration as a function of height for different latitudes and seasons; his results are shown in Fig. 5.10. The sharp drop above about 75 km is due to the high dissociation rate of H_2O by Lyman-alpha radiation and by the continuum at 1500-1900A. Hesstvedt's results for 82 km (a concentration of 0.05 g/kg, corresponding to a frostpoint of 159°) does not exclude the possibility that NLC consist of ice particles, because temperatures as low as 130 °K are observed in NLC. More information on circulation in the stratosphere and mesosphere and on the water vapor content of the

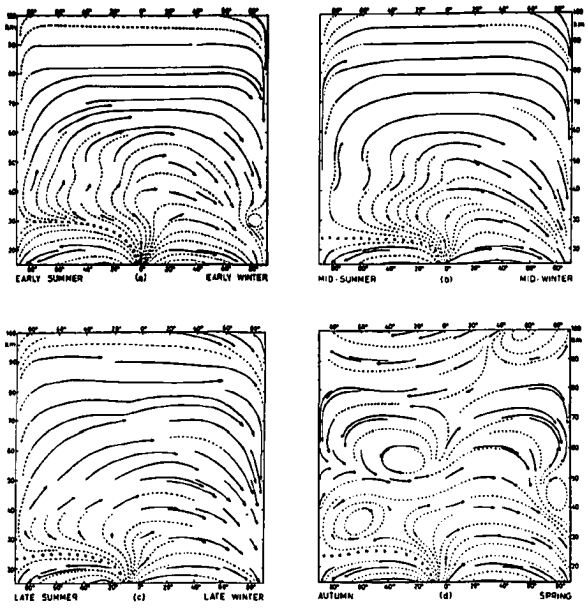

Fig. 5.9. Mean motion in the upper atmosphere as inferred from the data of Murgatroyd and Singleton (1961). The arrows indicate the distance traveled by air particles in 6 weeks (Hesstvedt, 1964).

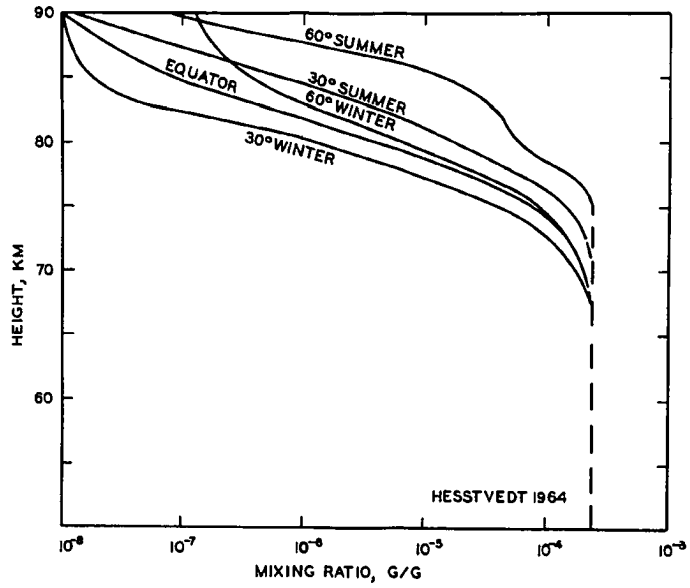

Fig. 5.10. Water vapor mixing ratios in an atmosphere with motion in accordance with figure 5.9 (Hesstvedt, 1964).

mesosphere are needed to test the validity of Hesstvedt's results. The possibilities that water substance embedded in meteoroids may be deposited in the mesosphere, and that water vapor be formed in situ at that altitude by the reaction $H + OH \rightarrow H_2O$, also need further consideration.

5.5 The Distribution of Dust in the Atmosphere

Much data has been obtained on the concentration of particulate matter in the atmosphere below 30 km (see Chagnon and Junge, 1961; Junge, 1961; Junge, Chagnon, and Manson, 1961; Junge and Manson, 1961). They show a maximum density of particles in the range 0.1 to 1.0 microns at about 20 km altitude, with a concentration of around 0.1 particles/cc (Figs. 5.11 and 5.12), they suggest that these particles consist primarily of ammonium sulfate or sulfuric acid formed by local heterogeneous chemical reactions. Recent photometric studies of the twilight (Volz and Goody, 1962) and balloon-borne coronograph measurements (Newkirk and Eddy, 1964) have corroborated in the existence of the 20 km dust layer.

Junge and his collaborators distinguish three kinds of particle in the stratosphere: (1) Aiken nuclii of terrestrial origin with radii less than 0.1 microns and concentration of the order of 10^3 per cc in the middle troposphere, the concentration falling off sharply with increasing altitude, (2) aerosols with radii between 0.1 and 1 micron of stratospheric origin, with concentrations of the order of 1 per cc at 0.1 micron, and (3) extraterrestrial particles with radii greater than 1 micron with nearly negligible concentrations. Newkirk and Eddy (1964) find evidence of thin layers of increased concentration

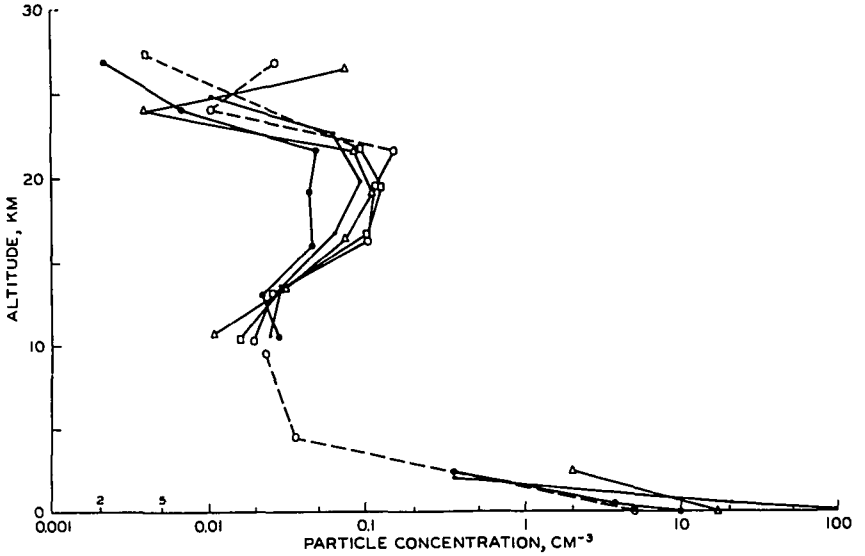

Fig. 5.11. Comparison of five vertical profiles of particle concentration in the 0-30 km region. (Chagnon and Junge, 1961).

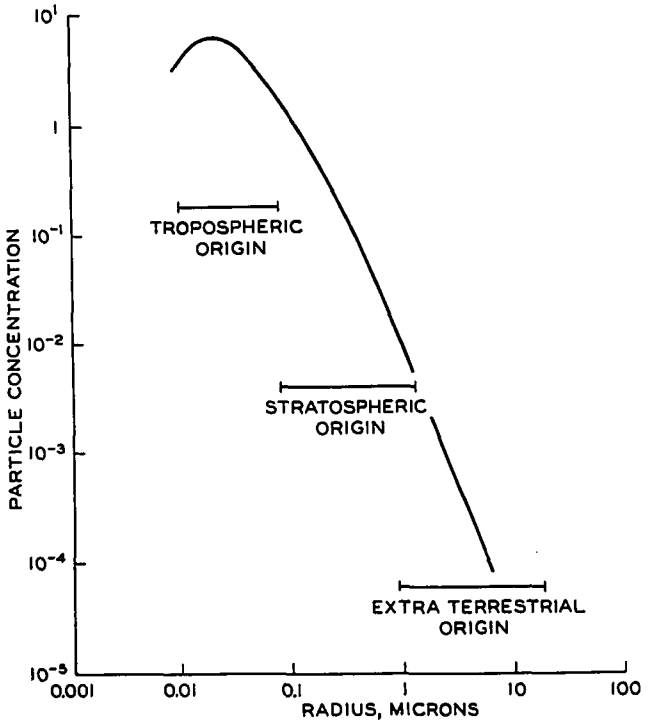

Fig. 5.12. Average size distribution of stratospheric aerosols with indication of their most likely origin (Junge, et al., 1961).

of dust in the stratosphere, confirming the results of Volz and Goody (1962) and others.

Volcanic eruptions greatly increase the concentration of dust and other aerosols in the troposphere and lower stratosphere. The classical and well studied case is the series of eruptions of Krakatoa (6.1°S, 105.4°E) in Java, which began in May, 1883 and ended in February, 1884; the most violet eruptions took place in August, 1883. The Krakatoa dust cloud reached heights above 30 km and was composed of particles with radii between 0.05 and 0.2 microns. Dust from this cloud spread across the earth and within three months was visible in western Europe even in full daylight. Estimates of the primary glow stratum ranged from about 10 to 30 km. The higher values were obtained in the early history of the cloud and the lower values after several years (Ludlam, 1957). According to Kiessling (1888), the cloud sank at the rate of 0.1 cm/sec over a period of 5 months.

The eruption of Agung volcano (8.4°S, 115.5°E) on the island of Bali on March 17, 1963 produced effects similar to Krakatoa. According to Meinel and Meinel (1963), the Agung dust cloud, which had reached 30°N by September, 1963, had a primary glow stratum at a height of 22 km and some indication of a secondary one at 53 km. There is some dispute as to whether the secondary layer was real, or caused by reflections of the primary glow. There appears to be no measurement of the concentration or composition of the material in these clouds.

The formation of NLC at 82 km has for a long time been taken as evidence of the presence of dust at the mesopause. The turbidity measurements of Volz and Goody (1962) show that dust is present at all

levels up to 65 km. Estimates of the particle concentration in NLC range from 0.01 to 1/cc (Ludlam, 1957). Hemenway, Fullum, Skrivanek and Soberman (1964) have determined from rocket sampling experiments that when NLC are present, the dust particles in the 75-98 km region range in diameter from 0.05 to 0.5 microns and have a distribution given by $N \propto (\text{diameter})^{-p}$, where p is between 3 and 4 (see Fig. 3.16).

The particulate matter in the 30-100 km region is generally believed to be of extraterrestrial origin. Recent estimates of the accretion of extraterrestrial material by the earth range from about 10^9 grams/day (Newkirk and Eddy, 1964), to 10^{11} grams/day (Dole, 1962) but the actual amount may be higher. The distribution in size, composition, and speed of this material on entry into the atmosphere varies widely. Chemically, the particles are of two known types: metallic and stony, the stony ones being by far the most predominant (90-95% of the total). The possibility of a third type - particles composed of or containing solid "ices" of H_2O, NH_3, CO_2, etc. has also been suggested, but according to Belton (1966) these are unlikely to be very numerous if they exist. Estimates of the characteristic densities of these particles range from about 0.01 g/cc for "fluffy" dustball structures to about 8 g/cc for compact metallic particles. They arrive from interplanetary space with speeds ranging from about 12-75 km/sec (Millman and McKinley, 1963).

Much of this extraterrestrial material enters the earth's atmosphere as meteors, which are observable from the ground by various means (visual, optical, or radio). Estimates of the accretion of extraterrestrial material by the earth are based on the influx of these

meteors, and the contribution due to the entry of low speed submicron size dust which may be quite large, is ignored because of difficulties in measuring it. Observation shows that the contribution of material from the well known meteor showers (Table 5.2) is relatively small compared to that of the sporadic meteors (Lovell, 1954; Whipple and Hawkins, 1956; Millman and McIntosh, 1962).

TABLE 5.2

LIST OF ANNUALLY RECURRING METEOR SHOWERS

Shower	Date of Maximum	Extreme Limits	Stream Hourly Rate at Maximum		
			Radio	Visual	Photo.
Quadrantids	Jan. 3	Jan. 1-4	95	30	1.9
Aurigids	Feb. 9	5 days?	--	5	--
Virginids	Mar.13	16 days?	--	1?	--
Lyrids	Apr.22	2 days	9	5	--
η Aquarids	May 4	10 days	15	5	--
Arietids	June 8	May 29-June 18	66	--	--
ζ Perseids	June 9	June 1-16	42	--	--
β Taurids	June 30	June 24-July 6	27	--	--
δ Aquarids	July 28	July 24-Aug. 7	34	10	--
Perseids	Aug.12	July 29-Aug.17	50	37	2.5
Orionids	Oct.22	Oct. 18-26	18	13	2.9
Southern Taurids	Nov. 1	Oct. 27-Nov. 22	--	5	--
Northern Taurids	Nov.12	Oct.17-Dec.2	14	5	--
Leonids	Nov.17	5 days	9	6	--
Geminids	Dec.13	Dec.7-15	80	55	5.6
Ursids	Dec.22	Dec.22-23	13	15	--

Visible meteors are produced by particles whose diameter exceeds 300 microns and which enter the atmosphere at speeds of tens of km/sec. These particles are subjected to extremely high pressures and undergo considerable heating owing to the impact of air molecules, causing fragmentation of the particles and vaporization from their surface. The vaporized material subsequently recondenses into smaller particles which settle slowly through the atmosphere. Since the visible paths of most meteors lie between heights of 65-100 km (Fig. 5.13), their condensation products are distributed over a layer extending from below the NLC level up to about 20 km above it.

The seasonal variation of the inflow of visible, photographic, and radar meteors (Fig. 5.14) shows a considerable increase in the influx of material during the northern hemisphere summer months of June-August.

According to Whipple (1954), most of the small particles producing photographic meteors (both shower and sporadic) are derived from cometary debris. Studies of the zodiacal light and the solar corona have shown the existence of a cloud of interplanetary particles disposed as a rather thin disc lying in the plane of the ecliptic. According to Allen (1946) the average diameter of the interplanetary particles is around 10 microns, and their concentration (which he assumes to fall off inversely as the distance from the sun) is about 3×10^{-15} per cc at 1 astronomical unit, corresponding to a space density of about 6×10^{-23} g/cc. Van de Hulst (1947), using different assumptions, obtained a space density at 1 astronomical unit of 5×10^{-21} g/cc.

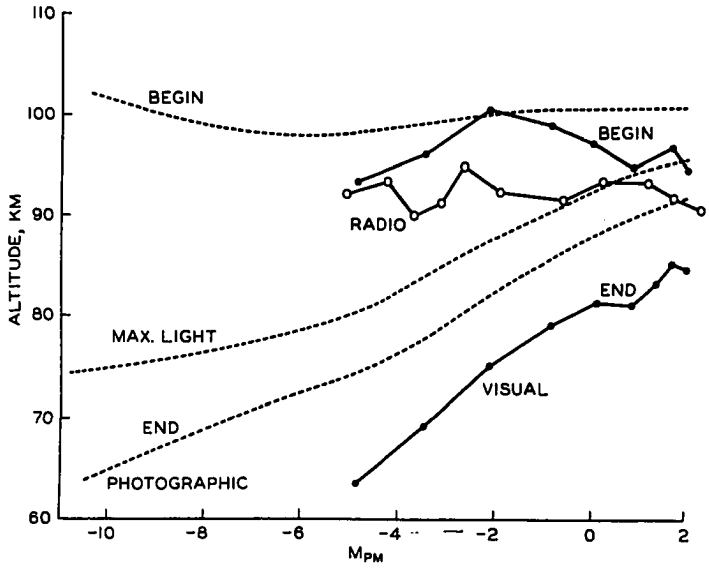

Fig. 5.13. A comparison of meteor heights measured by three basic techniques, M_{PM} is the absolute magnitude of maximum light. (Millman and McKinley, 1963).

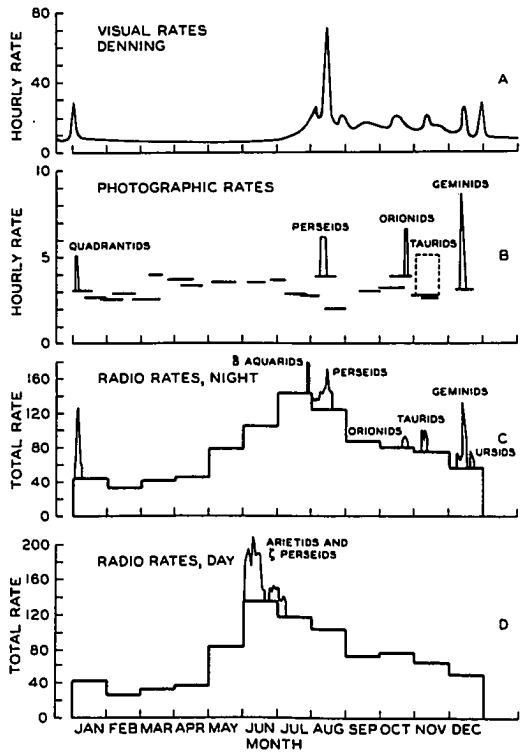

Fig. 5.14. Variation of inflow of visible, photographic and radar meteors with season. (Whipple and Hawkins, 1956).

Recent rocket and satellite data have shown the existence of a dust cloud encompassing the earth (Kaiser, 1962). These data indicate that the particles are captured in geocentric orbits from the interplanetary dust cloud rather than being produced by impact of meteorites on the moon as suggested by Whipple (1961). Dole (1962) finds that the steady state concentration of the earth's dust cloud is approximately 10^{-18} g/cc at an altitude of 1800 km above the earth and that the concentration varies as $1/r^{1.14}$ where r is the distance from the earth's center. The particle flux was found to vary as $1/r^{1.66}$.

The Particles in geocentric orbits are apparently short-lived (Alexander, McCracken, Secretan, and Berg, 1962). They can be classified into two groups--one destined to impact on the earth, and the other moving in circular loops around the earth and then returning to heliocentric orbits. Dole (1962) computes the median residence time of the particles in orbit around the earth to be about 12 days, if aerodynamic drag effects are neglected, and points out that if drag effects are considered then an additional concentration of particles should appear in the upper reaches of the atmosphere between 120 and 80 km where very small particles are slowed down without being vaporized. The average cumulative mass distribution of interplanetary dust near the earth as determined by rocket and satellite data (Fig. 5.15) shows an increase in the number of particles toward smaller sizes. Estimates of the equilibrium electrostatic potential on interplanetary dust particles range from "strongly negative" to +200 volts. Belton (1966), in a detailed treatment of the question, finds the particles to be positively charged with an equilibrium potential of around +30 volts.

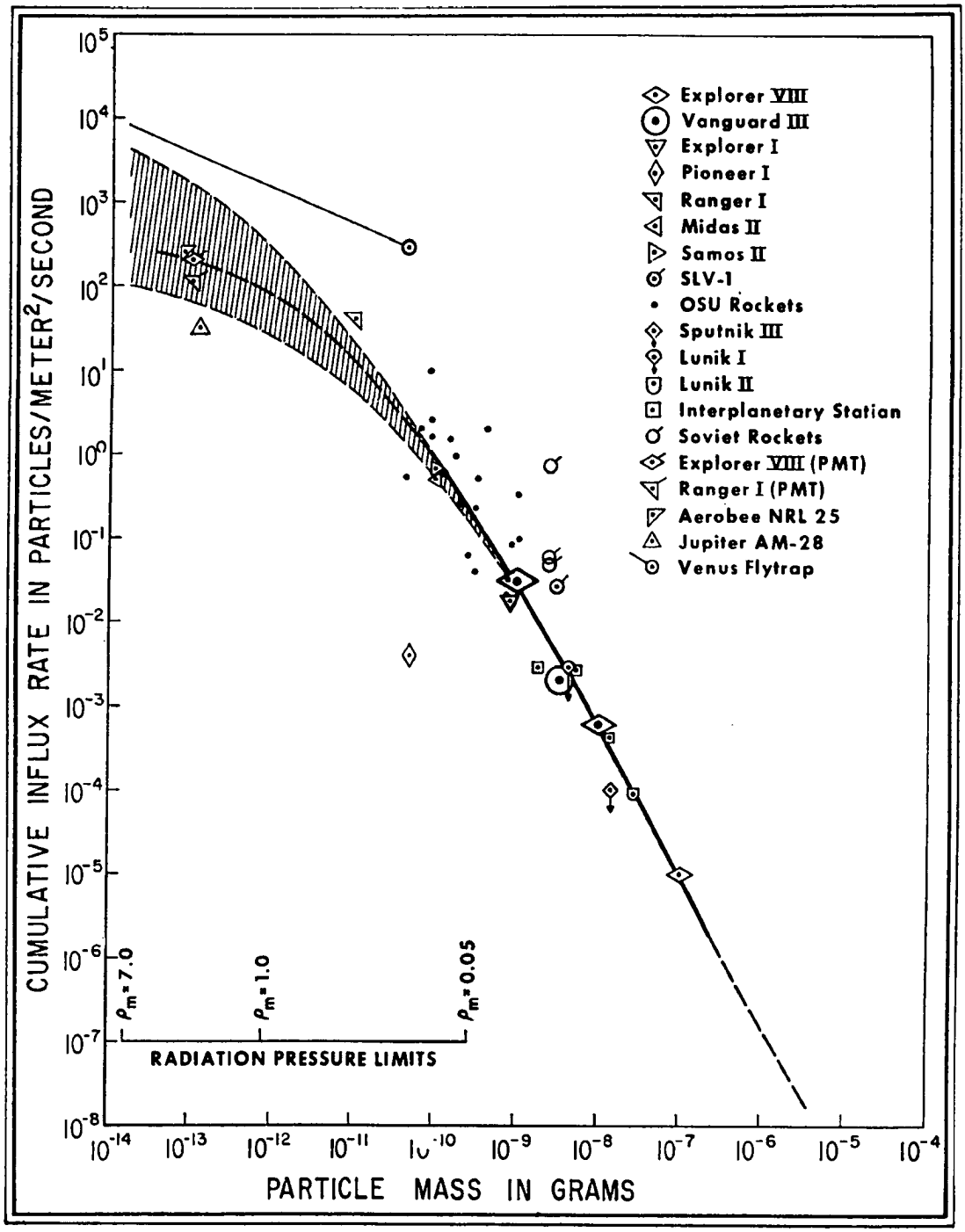

Fig. 5.15. Average cumulative mass distribution of interplanetary dust near the earth. (Alexander, et al., 1962).

5.6 Sedimentation Speed of Particles in the Atmosphere

An important consideration for dust particles in the atmosphere is their sedimentation velocity or fall speed. Due to the wide range of mean free path values in the 0-100 km region, no one equation is everywhere applicable.

The well known Stokes equation, given by

$$V = \frac{2 g r^2 (\rho - \rho')}{9 \eta}$$

where V = fall speed of particle
g = acceleration of gravity
r = radius of particle
ρ = particle density
ρ' = density of medium
η = coefficient of viscosity

is valid for spheres whose radii is very large compared to the mean free path, L(i.e. $L/r \ll 1$).

In the case of a sphere falling through a gas, the density of which is small in comparison, the Stokes equation predicts a terminal velocity independent of pressure because of the constancy of the viscosity. When the gas is at a sufficiently low pressure, it can no longer be regarded as a continuous medium with respect to the sphere, which then falls more rapidly than suggested by hydrodynamic theory. This is attributed to slip of the gas at the surface due to the molecular mean free path being comparable to or greater than the size of the sphere, contrary to one of Stokes' basic assumptions.

Various workers have empirically determined slip correction factors which applied to Stokes equation allow it to be used over a wider range of pressures and particle sizes. Knudsen and Weber (1911)

determined a slip correction factor of the form

$$F = 1 + (L/r)[A + B \exp(-cr/L)]$$

where A, B, and c are constants and L and r are the mean free path and the particle radius respectively.

This slip correction factor is more accurate than the one ($F = 1 + A\ L/r$) theoretically derived by Cunningham (see Dryden, Murnaghan, and Bateman, 1956). Davies (1945) determined the most appropriate values of the constants A, B, and c from the experimental data of Knudsen and Weber, Millikan, et al to be:

$$A = 1.257,\ B = 0.400,\ c = 1.10$$

The slip correction factor combined with the Stokes equation is often called the Stokes-Cunningham equation; it can be expressed in the following form (Junge, 1961):

$$V_{sc} = 2\ r^2(\rho-\rho')g\alpha/9\eta$$

where

V_{sc} = Stokes-Cunningham fall speed

r = particle radius

ρ = particle density

ρ' = air density

g = acceleration of gravity

η = coefficient of viscosity of air

$\alpha = 1 + \beta\ L/r$

β = $1.257 + 0.400 \exp(-1.10\ r/L)$. β varies only slightly with L/r. It is 1.65 for $L/r = 10$ and 1.25 for $L/r = 0.1$

L = mean free path length

n = number of air molecules per cc

With $L/\eta = (\pi/8mkT)^{1/2}/2n$ and for $L/r \gg 1$ and $\rho \gg \rho'$,

$$V_{sc} = (2\pi/kT\ m)^{1/2}\ r\rho g\beta/9\eta$$

As the constants in the slip correction term were only determined for $0.5 \leq L/r \leq 200$ (corresponding to Reynolds Numbers of 4 to 10^4), the Stokes-Cunningham equation is valid for spherical particles with radii of 0.1 micron only up to an altitude of around 50 km.

Higher in the atmosphere, in the 80-85 km region where the mean free path is of the order of 1 cm, the ratio of L/r for 0.1 micron particles is about 10^5, far beyond the range for which the Stokes-Cunningham equation was intended to apply. At such large L/r values, it is more appropriate to use the diffusion equation (Lettau, 1951; Chapman and Cowling, 1952; Junge, 1961). For static equilibrium the diffusion equation may be written:

$$\gamma = n_1 V_D = -nD_{12}\left\{\frac{d}{dh}\left(\frac{n_1}{n}\right) + \frac{n_1 n_2 (m_2 - m_1)g}{kn^2 T} - \frac{\rho_1 \rho_2}{P\rho}(F_1 - F_2) + \frac{n_1 n_2 \alpha_{12}}{n^2 T}\frac{dT}{dh}\right\}$$

where

γ = flux of particles

$n = n_1 + n_2$ = number of particles and molecules/cc

n_1 = number of dust particles/cc

n_2 = number of molecules/cc

V_D = diffusion velocity of particles

$m_1 = \frac{4}{3}\pi r_1^3 \rho_1$ = mass of particles

m_2 = mass of air molecules

ρ_1 = density of particle

ρ_2 = air density

P = Ambient pressure

F_1F_2 = forces acting on particles and molecules

k = Boltzmann's constant = 1.38×10^{-16} ergs/°K

T = temperature (°K)

12 = thermal diffusion coefficient = $\frac{5}{16\sqrt{2}} \left(\frac{r_1}{r_2}\right)^2$

D_{12} = diffusion coefficient = $\frac{3}{8n_2r_1^2} \left(\frac{kT}{2\pi m_2}\right)^{1/2}$ for elastic spherical particles

The four terms on the right of this equation correspond respectively to 'ordinary' diffusion or particle transport caused by a gradient in concentration, pressure diffusion causing the heavier gas to fall and the lighter gas to rise, diffusion due to external forces, and thermal diffusion. This equation is greatly simplified for application to the NLC problem because the first term is zero since the air is supposedly uniformly mixed, the third term is zero since $F_1 = F_2 = -g$, and the contribution of the fourth term is negligible compared to that of the pressure diffusion term. Under these conditions, the equation reduces to:

$$V_d = \frac{g\, r_1 \rho_1}{2n_2} \left(\frac{\pi}{2\, k\, m_2\, T}\right)^{1/2}$$

At 80 km, the following values apply:

$m_2 = 29\ m_o = 4.81 \times 10^{-23}$g

$r_2 = 1.85 \times 10^{-8}$cm

$n_2 = 2 \times 10^{14}$/cc

g = 957 cm/sec^2

T = 130°K (when NLC present)

so

$$V_D \approx 3 \times 10^6 \, r_1 \rho_1$$

whereas the Stokes-Cunningham equation gives

$$V_{sc} \approx 2 \times 10^6 \, r_1 \rho_1$$

The diffusion fall speeds for particles of different sizes and densities which might occur in NLC are given in Table 5.3. The particle sizes chosen are representative for NLC--the smallest, average, and largest size particles in NLC are r = 0.025, 0.15, and 0.2 microns, respectively.

Large fall speeds of tens of cm/sec are inconsistent with the observed persistence of NLC for periods of 5 hours or more and their continued appearance for as many as 6 consecutive nights. This points to a fairly low NLC particle density of less than 1 g/cc. If sufficient ice forms on the dust particles in needle or flaky form, the average particle density (if they are initially of solid stone with density about 3.0) could be reduced to this value and the observed vertical motion of about 1 cm/sec at 80 km in high latitude summer could assist in concentrating the particles at the mesopause.

TABLE 5.3

FALL SPEED, V_D(cm/sec), AT 80 km FOR PARTICLES OF DIFFERENT SIZES AND DENSITIES

	V_D(cm/sec)		
ρ_1 \ r_1	.025μ	0.15μ	0.2μ
0.10g/cc	0.75cm/sec	4.5cm/sec	6.0cm/sec
1.0	7.5 "	45.0 "	60.0 "
3.0 (stone)	22.5 "	135.0 "	180.0 "
8.0 (iron)	60.0 "	360.0 "	480.0 "

CHATPER 6

THE FORMATION OF NLC

Important to the understanding of how NLC form is a knowledge of what other natural phenomena such as volcanic eruptions, meteor shower, etc. may be associated with the appearance of these clouds. This Chapter deals with the possible correlation of NLC activity with volcanic eruptions, meteors and meteoroids, the sunspot cycle, and meteorological conditions at sea level. The theories of NLC formation are also reviewed.

6.1 NLC and Volcanic Eruptions

The fact that NLC were first reported in 1885, two years after the eruption of Krakatoa, led Jesse (1890) and others to suggest that NLC were caused by condensation of material hurled up to the mesopause by volcanic eruptions, but Vestine (1934) found that there was a considerable increase in the influx of extraterrestrial material during the years 1880-1887 which could also explain the high incidence of NLC occurrence during that period. He also pointed out that no increase in NLC activity followed the major eruption of Katmai volcano in Alaska in 1912, and that NLC are observed in years when no major volcanic eruptions take place. Hence he concluded that NLC are not associated with volcanic eruptions, and that an extraterrestrial source of material is more likely.

6.2 NLC and the Influx of Extraterrestrial Material

An examination of Fig. 3.5 which gives the number of times NLC have been observed on a given date shows no significant increase in NLC activity on the nights of meteor showers such as the Arietids (June 8), Perseids (June 9), Aquarids (July 28),

and Perseids (August 12). The peak of NLC activity falls around July 10, when no major meteor shower occurs. But it is not surprising that NLC has little or no relation to meteor showers since meteors are known to be the primary source of extraterrestrial material in the earth's atmosphere.

Although NLC are observed most frequently in the northern hemisphere during the months June-August, when the total meteor activity (mainly sporadic) also has its maximum, this is not evidence of a strong dependence of NLC activity on an increased flux of meteors, since NLC are observed in the southern hemisphere during the months of December-February when the total meteor activity is relatively low. However, there is some evidence indicating that NLC activity increases during years of abnormally large meteor activity--the years 1885-1887 and 1963, in which unusually brilliant, widespread and frequent NLC displays were observed, were also years of greatly enhanced meteor activity. In 1963, two radar stations at almost opposite ends of the earth observed an anomalous increase in meteor activity (McIntosh and Millman, 1964; Ellyett and Keay, 1964). Some fifty percent more echoes were reported during May through November, 1963 near Ottawa, Canada than for the same period in the preceding 5 years. At Christchurch, New Zealand, the numbers in May to August were double those for the corresponding months over the previous three years.

Additional evidence in favor of an extraterrestrial source of NLC material is the NLC display which occurred after the fall of the great meteorite (estimated mass = 4×10^7 kg) which fell in Siberia at 61°N, 101.3°E at 0700 local mean time on the morning of 30 June 1908

(see Whipple, 1960). The unusually brilliant NLC display which occurred on the night of 30 June 1908 was reported by many observers in Russia, Denmark, Sweden, Germany, and England (Ludlam, 1957), and it was on this occasion that the lowest latitude (45°N in Russia) observation of NLC was reported (Vestine, 1934). Assuming the clouds to have originated from the dust trail of the meteorite, Whipple (1930) estimated the speed of the dust cloud to be 85 m/sec towards the west. It now seems to be well established that much of the material which vaporizes from meteoroids recondenses into particles of the right size to form NLC. Observers of meteors which are large enough to be seen during daylight report seeing light-bluish trails, which are indicative of sub-micron particles. Fessenkov (1949), examined the properties of the trail left by the large meteorite which fell in Siberia on 12 February 1947 and found that the cloud of particles in the trail was more transparent to red than blue light and that the diameter of the particles must have been less than 0.1 micron.

The above results suggest that (1) the dust particles in NLC are of extraterrestrial origin, (2) some mechanism other than an increased flux of meteors is responsible for the increased concentration of particles at the mesopause, and (3) when there is a very large increase in meteor activity during summer months, NLC are brighter, more extensive and more frequently observed.

6.3 NLC and the Sunspot Cycle

The possibility that NLC activity might be correlated with reduced solar activity was suggested by Vestine (1934). At the time of his paper, it appeared that the years 1887, 1899, 1911, and 1932 were times

of the greatest frequency of occurrence of NLC, and these were years near a sunspot minimum. Vestine pointed out that this apparent correlation with low sunspot activity was not entirely satisfactory and might be fortuitous, since the number of NLC observers and the degree of interest in these clouds have varied widely over the years. Using a complete list of the reported NLC sightings for the period 1885-1964, this question was re-examined (Fogle, 1965b) and no meaningful correlation of NLC with solar activity was found (Fig. 6.1). A physical relationship between the two is however not entirely improbable, since a low mesopause temperature appears to be one of the requirements for NLC formation, and the IGY and IQSY rocket measurements suggest that the mesopause temperature in high latitudes during summer months is higher in years of high solar activity than in years of low solar activity. An extended series of NLC observations over a few sunspot cycles by the existing large network of stations may yet show some dependence of NLC activity on solar activity, but the existing data indicates that if such a dependence exists, it is not pronounced.

6.4 NLC and Surface Meteorological Conditions

Grishin (1960) compared the occurrence of over a hundred NLC displays during the period 1922-1959 with meteorological conditions at sea level, and found a strong correlation between the two. His conclusions as summed up by Paton (1964) are: (1) for a quite lengthy period before each display, there is a rapid increase in mean sea level pressure over the region underlying the display; the speed of displacement of the isobars is of the order of 800 to 1800 km per day, the higher pressure occurring in the direction of the noctilucent

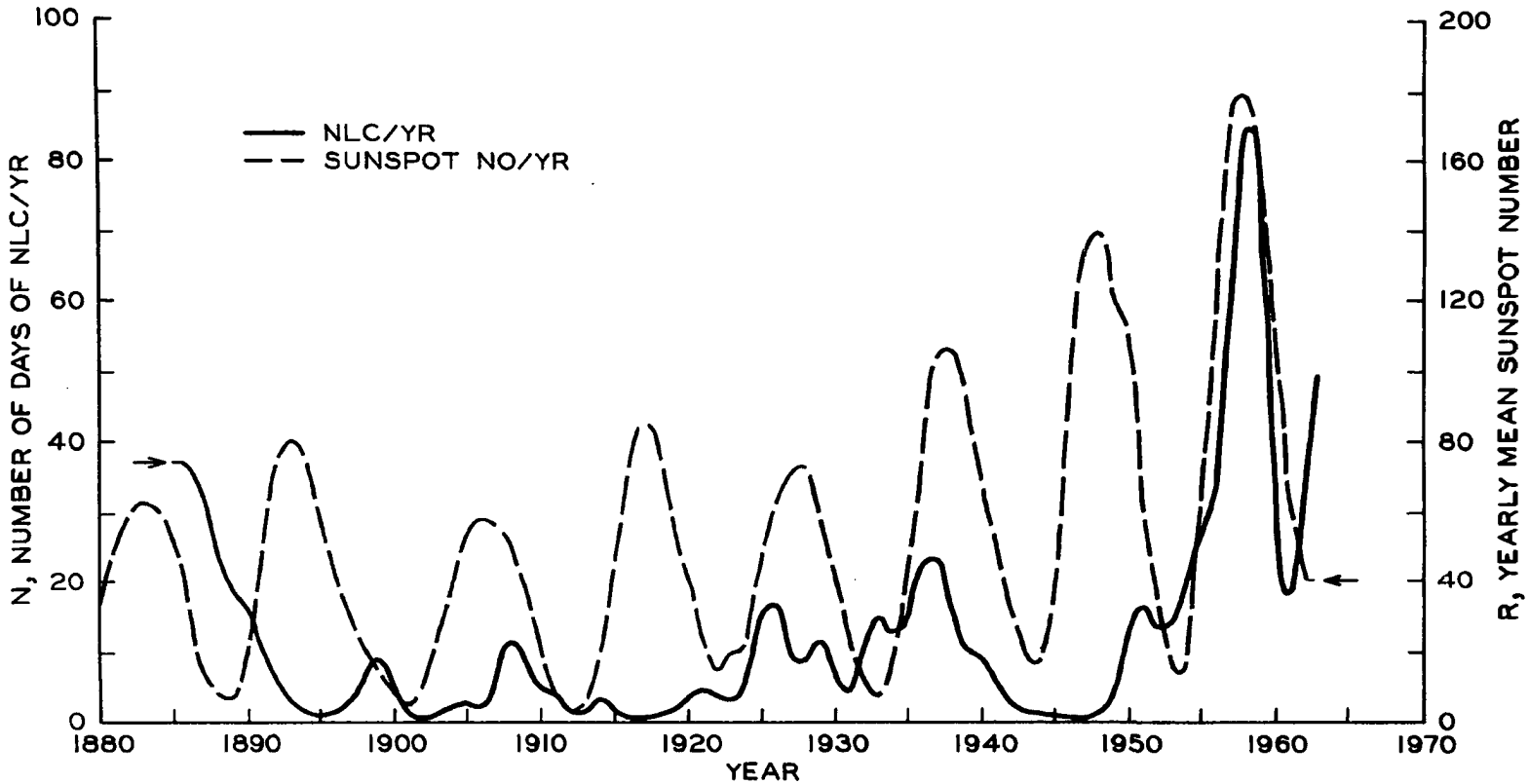

Fig. 6.1. Yearly variation of NLC activity compared to sunspot activity.

clouds, independently of the general direction of anticyclonic movement during the period. The intensity and the geographical extent of the region of this pressure change are directly proportional to the brightness and the area of the subsequent noctilucent clouds; also, in the case of bright and well defined displays, the cloud striations are in general oriented approximately in the same direction as the underlying mean sea level isobars. (2) A period of unusually frequent occurrence of NLC is always associated with abnormally high seasonal temperatures over a wide area of the earth's surface, especially during the month preceding the displays.

Grishin's results are disputed by Paton (1964) who similarly analysed over a hundred NLC displays occurring over Scotland, and found no significant correlation with surface pressure and temperature of the kind found by Grishin. In view of the great height of NLC above the troposphere, it would seen unlikely that their formation would be associated with variations in surface meteorological conditions, and Paton's results on this question are to be favored.

6.5 Theories of NLC Formation

A satisfactory complete explanation of NLC must show why they occur at or near the mesopause, mainly during summer in latitudes polewards of 50°; how they are formed, why they are present on some nights but not on others; and why they are thin, of wavy structure, and often have a duration of at least some hours.

Over the past 80 years, many speculations as to the nature and cause of NLC have been made; they are described in summary form below. They can be generally divided into the following groups--those favoring

dust clouds of (1) volcanic origin or of (2) extraterrestrial origin, and those favoring (3) ice or ice-coated dust particles.

Dust Clouds of Volcanic Origin

The proximity of the great volcanic eruption of Krakatoa to the first reporting sightings of NLC led Jesse (1890) and others to suggest that NLC were caused by condensed vapors from volcanic eruptions but statistics do not support this view. (see Section 6.1).

Dust Clouds of Extraterrestrial Origin

After a careful analysis of the data then available, Vestine (1934) concluded that NLC were not formed of volcanic dust but were dust clouds of extraterrestrial origin. He ruled out the possibility of ice clouds because of the high temperature thought to exist at the mesopause at that time.

Ludlam (1957) suggested that NLC are dust clouds in the form of a haze top at the 80 km inversion, with the dust (either volcanic or extraterrestrial) ascending to the mesopause from below due to very steep lapse rates caused by solar heating of the ozone layer. Undulations in the haze top due to wave motion could cause variations in the optical thickness, visible to an observer on the ground as billows or bands. To explain the only occasional occurrence of the clouds in high latitudes, Ludlam suggested that the large vertical motions required to form the haze top are present on some days but not on others, and only in summer in high latitudes.

Deirmendjian and Vestine (1959) examined the possibility of NLC being composed of ice-coated dust, and concluded that it cannot be

justified on physical grounds--their main objections were that it is difficult for enough water vapor to collect at the mesopause to supersaturate the region, and scattering theory shows that dust particles of 0.2 to 0.8 microns diameter needed for condensation nuclei can alone explain the formation of NLC. They suggest a silicaceous or similar composition and an interplanetary origin for the NLC particles.

According to Hoffmeister (1961), NLC are formed in the following manner: On entry into the atmosphere, micrometeorites are concentrated in low latitudes at about 150 km altitude, and as they settle slowly they are transported polewards by high altitude winds. These clouds of micrometeorites are supposed to collect eventually at the mesopause in high latitudes. To explain the sudden appearance and disappearance of cloud features and the rarity of occurrence of the clouds, Hoffmeister argues that the formation of well defined cloud layers is possible only when large-scale turbulence is absent.

Ice Clouds

Wegener (1926), Jardetzsky (1926), Vegard (1933), Humphreys (1933), and Khvostikov (1952) suggested that NLC are ice clouds, but this suggestion was rejected for many years because the mesopause temperature was thought to be much too high for the formation of ice crystals.

The low mesopause temperature (about 165°K) observed in high latitudes during the IGY caused a resurgence of interest in the possibility of NLC being composed of ice crystals. Hesstvedt (1961, 1962) extending his work on nacreous clouds to NLC, developed a detailed model of NLC as ice clouds. His results indicated that NLC could very

well be ice clouds, and his model explained several of the observed characteristics of NLC. Shortly after Hesstvedt's paper, several important rocket experiments were made which provided valuable information on NLC formation. These were the particle sampling experiments over Sweden in 1962 and the NLC temperature measurements in 1963. The results of these experiments showed that when NLC were present,

(1) the mesopause temperature was around 130°K

(2) the dust particle collected had traces of nickel and iron indicating an extraterrestrial origin

(3) the larger particles were coated with a volatile substance believed to be ice

(4) the particle concentration was much greater in the presence than in the absence of NLC.

These results led Paton (1964) to conclude that the appearance and persistence of NLC is most readily accounted for by assuming that they consist of ice coated dust particles of extraterrestrial origin and that the formation of the clouds is largely controlled by the temperature at the mesopause.

Rosinski and Pierrard (1964) attribute the appearance of NLC to the absorption of water vapor and nitric oxide on small dust particles of meteoric origin. They suggest that the small particles (about 10 Angstroms diameter) coagulate together into larger particles as they fall through the atmosphere, and that the larger particles (0.05-1 micron) generate a sharply defined concentration profile which falls progressively slower as it enters deeper into the earth's exponential atmosphere. Due to the presence of nitric oxide, the particles are supposed to acquire a positive charge, and under the influence of the

Lorentz force these charged particles converge toward high latitudes where NLC form.

Webb (1965) derives a stratospheric circulation system from Meteorological Rocket Network Data which he argues accounts for the transportation of moist air from equatorial regions to higher latitudes, where vertical motions of tens of cm/sec are supposed to raise the moist air to the mesopause and impede the downward motion of dust particles in that region; thus a concentration of particles is produced, and ice forms on them, producing observable NLC. Webb states that this circulation system is favorable for NLC formation only during the period May to mid August.

Charlson (1965) also suggests that NLC are composed of ice-coated dust particles, and computes a simple model of such a cloud, using the most recent experimental results on temperature, water vapor concentration, and particle sizes. He argues that the smaller particles have much thicker ice coatings than the larger ones, and can be expected to dominate the mass budget of the cloud, due to their greater number as well as their thicker coating; he concludes that upward motions of around 20 cm/sec are needed to sustain an ice cloud at the mesopause.

The results of the rocket experiments described earlier suggest that there may be three requisites for NLC formation: a low temperature and the presence of adequate water vapor and dust nuclei at the mesopause. Chapman and Kendall (1965) have recently proposed a theory of NLC formation based on these considerations. In their theory, the water vapor is supposed to be raised up to the mesopause from below by vertical motions of the order of 1 cm/sec as suggested by Murgatroyd and Singleton (1961). To explain the increased concentration of dust

at the mesopause when NLC are present, Chapman and Kendall propose that extraterrestrial dust entering the earth's atmosphere assumes an exponential distribution that cuts off at the turbopause (the level above which turbulence ceases) due to the effects of turbulence below that level. At times during the summer months in high latitudes the turbopause level (which in low latitudes is around 105 km) is assumed to descend to the mesopause at 82 km. This lowering of the turbopause to 82 km serves to increase greatly the dust concentration there, within a few hours, and when the temperature is low and the water vapor concentration is high, NLC are formed. Chapman and Kendall do not attempt to explain why the turbopause should occasionally fall to the mesopause in high latitudes, but they point out that with a low mesopause temperature, a strong temperature increase can be expected above the mesopause. The greater stability due to the temperature increase upwards contribute to the reduction of turbulence. Their calculations show a scale height of about 2 cm for the dust population, whereas, Hemenway, Soberman and Witt (1964) estimate the scale height to be about 2 km.

The question of how NLC are formed is a complex one, and a satisfactory explanation must await more and better data on NLC and the region in which they form. The two major assumptions employed in the above theories--vertical motions of tens of cm/sec and a lowering of the turbopause by 20 km--seem unrealistic in view of the large area (ten degrees of latitude and 100 degrees of longitude)over which NLC are sometimes observed.

CHAPTER 7

CONCLUSIONS AND RECOMMENDATIONS

Over the past ten years, our knowledge of the characteristics of NLC has advanced considerably, but much remains to be done before we obtain a satisfactory understanding of how these clouds are formed.

The results of our four year study of NLC over North America show that:

(1) NLC occur over North America as frequently as over Europe and the USSR.

(2) They are observed during nautical and part of astronomical twilight when the sun is between 6° and 16° below the observer's horizon.

(3) Sunlight passing closer than about 20 km to the earth's surface is greatly attenuated in the 4000A-7000A range and cannot adequately illuminate the clouds.

(4) Spectra of NLC obtained during the summer of 1965 show that the light from NLC is scattered sunlight and that the cloud particles scatter light best at shorter wavelengths (around 4500A) than at longer ones (6500A).

(5) The earliest and latest dates of NLC displays over North America were April 1 and September 28 respectively.

(6) The peak of NLC activity falls around July 20, one month after the summer solstice.

(7) Ninetytwo percent of the displays were observed during the months of June-August.

(8) Eightytwo percent of the displays were observed after the summer solstice.

(9) No NLC were seen in winter, although a careful watch for them was kept by experienced observers.

(10) NLC displays occurring before the summer solstice were faint and covered small areas, whereas after the solstice they were bright and extensive.

(11) NLC have been observed over North America from geographic latitudes as low as 45°N and as high as 71°N, but the optimum latitude for NLC observations is around 60°N.

(12) NLC displays are generally first seen before midnight but are brightest and most extensive after midnight.

(13) Occasionally NLC displays extend over an area of millions of square kilometers and are observed on the same night by many observers over North America, Europe, and Russia.

(14) NLC occur more often than previously supposed. During the month of July they are seen nearly every night in some part of the northern hemisphere. An observer at 60°N might expect to see NLC on about 75% of the clear nights during the month of July.

(15) The wavelengths of the well-defined wave structure often observed in the clouds range from several to more than 100 km with the billow structure having wavelengths of around 10 km.

(16) NLC displays are generally quite persistent and last for periods up to and greater than 5 hours, but individual parts (particularly the billow structure) often form and decay within a few minutes or tens of minutes.

During our expedition to western Canada in the summer of 1965, simultaneous NLC and aurora were observed on 13 occasions. On 6 of the seven occasions when the aurora occurred in the same part of the sky as the NLC, interesting changes were observed in the NLC within 30 minutes to an hour after onset of aurora. The general effects observed were a reduction of NLC intensity and extent and a transformation of their well-ordered structure into swirls and formless veils. The changes observed in the NLC suggest heating at or below the mesopause.

Our work on NLC in the southern hemisphere has resulted in the proof of the existence of NLC there and the determination of some of their characteristics. Our first well-documented sighting of NLC in

the southern hemisphere was made on the night of 9 January 1965, from Punta Arenas, Chile (53.1°S). On our expedition to Punta Arenas during the December 1965 to February 1966 period NLC were observed on 9 nights, the first and last displays being seen on December 25, 1965 and January 22, 1966 respectively. These displays were found to have a general drift motion towards the west-northwest. The brightest and most extensive display observed on this expedition took place on the night night of January 3, 1966. The peak of NLC activity at 53.1°S falls around January 10, twenty days after the austral summer solstice. Comparing these results for 53°S with those obtained from stations at 53°N suggest that NLC in the southern hemisphere have the same apparent frequency of occurrence with respect to the solstice as NLC in the northern hemisphere, and that the clouds are likely to be seen at 60°S over the period December 1-February 15.

The collection and statistical analysis of all available data on NLC provides the following picture of their characteristics:

Characteristics of Northern Hemisphere
NLC

Color: bluish white

Height: (average): 82.67 km

Latitutde of Observations: 45° to 80°, best at about 60°

Season for Observations: March through October, best in June through August

Times for Observations: Nautical and part of astronomical twilight, SDA = 6° to 16°

Area: 10,000 to more than 4,000,000 km^2

Duration: Several minutes to more than 5 hours

Average Velocity: 40 m/sec towards SW; individual bands often move in directions and at speeds different from those of the display as a whole.

Thickness: 0.5 to 2 km

Vertical Wave Amplitude: 1.5 to 3 km

Average Particle Diameter: about 0.3 micron

Number Density of Particles: 10^{-2} to 1 per cm^3

Composition of Particles: Ice-coated extraterrestrial dust

Temperature in presence of NLC: about 130°K

The available evidence suggests that the dust particles in NLC are of extra-terrestrial origin and that they have a volatile coating, the nature of which is uncertain at this time. The absence of uncoated particles with diameters above the 0.20 micron from the NLC samples obtained over Sweden in 1962 indicates that there are no particles of this size in the regions above and below the cloud layer. The larger particles may be formed in the NLC layer by coagulation of smaller ones, and these particles may be retained in the NLC layer by some mechanism such as large vertical motions. Calculations of the fall speed of NLC particles indicate that the particles are likely to be of low density (below 1 g/cc) and/or non-spherical in shape. In view of the large uncertainties remaining as to the nature of NLC particles and the characteristics of the region in which they form, a satisfactory theory explaining their formation must await further experimental data.

Recommendations

Before a satisfactory understanding of NLC can be obtained, more and better data is required on the following things:

(1) the height, thickness, and vertical wave amplitude

(2) wind shears and temperature in the 75-90 km layer in the presence and absence of NLC

(3) the height variation of the particle concentration in the 75-90 km layer when NLC are present and absent

(4) the nature and thickness of the volatile coating on NLC particles and the shape and density of the dust nuclei

(5) the height of the turbopause when NLC are present and absent

(6) the water vapor concentration at the mesopause when NLC are present

(7) spectral and brightness measurements

(8) polarization measurements to determine if NLC are made visible by an increased concentration of particles at the mesopause or by the formation of coatings on the particles

(9) the effects of auroral particle bombardment on NLC displays.

REFERENCES

Aikin, A C., J. A. Kane and J. Troim, Some results of rocket experiments in the quiet D region, J. Geophys. Res., 69, 4621-4628, 1964.

Alexander, W. M., C. W. McCracken, L. Secretan, and O. E. Berg, Rocket, satellite, and space-probe measurements of interplanetary dust, Trans. Am. Geophys. Union, 43, 351-359, 1962.

Allen, C. W., The spectrum of the corona at the eclipse of 1940, Mon. Nat. Roy. Astron. Soc., 106, 137, 1946.

Arago, F., Complete works 4, 73, 1854.

Astapovich, I. S., Noctilucent Clouds, Izvest. Akad. Nuak. SSSR, Su. Geof. i. Geogr. 2, 183-204, 1939.

Astapovich, I. S., Meteoric phenomena in the earth's atmosphere, Moscow Goz. Izdat. Fiz. Mat-Lit., 1958.

Archenhold, F. S., Die Leuchtenden Nachtwolken, DasWeltall 27, Jarhgang 1928.

Backhouse, T. W., The luminous cirrus clouds of June and July, Met. Mag. 20, 133, 1885.

Belton, M. J. S., Dynamics of interplanetary dust, Science 151, 35 43, 1966.

Bessonova, T. D., The apparent frequency of noctilucent cloud phenomena according to the observation of the USSR hydrometrological service station network during 1957-1959, Research on the climatology of noctilucent clouds, Article No. 6, Academy of Sciences USSR, 1963.

Blamont, J. E. and C. deJager, Upper atmospheric turbulence near the 100 km level, Annales de Geophysique, 17, 134-144, 1961.

Brandy, J. H. and J. E. Hill, Rapid determination of auroral heights, Can. J. Phys. 42, 1813-1819, 1964.

Burov, M. I., Photogrammetric methods for determination of altitude of noctilucent clouds, Transactions of Conference on Noctilucent Clouds, Estonian Academy of Sciences, 1959.

Campbell, W. H., and M. H. Rees, A study of Auroral coruscations, J. Geophys. Res. 66, 41-45, 1961.

Chagnon, C. W. and C. E. Junge,The vertical distribution of sub-micron particles in the stratosphere, J. of Met. 18, 946-752, 1961.

Chamberlain, J. W., Physics of the aurora and airglow, Academic Press, New York, 1961

Chao, J., On the nature and shape of noctilucent cloud particles, M. S. Thesis, University of Alaska, 1965.

Chapman, S. and T. G. Cowling, The mathematical theory of non-uniform gases, Cambridge Univ. Press, 1952.

Chapman, S. and B. Fogle, Noctilucent Clouds, Geofisica International 5 (1), 15-30, 1965.

Chapman, S. and P. C. Kendall, Noctilucent clouds and thermospheric dust: their diffusion and height distribution, Quart. J. Roy. Met. Soc. 91, 115-131, 1965.

Charlson, R. J., Noctilucent clouds: A steady state model, Quart. J. Roy. Met. Soc., 91, 517-523, 1965.

Craig, R. A., The Upper Atmosphere, Academic Press, 1965.

Davies, C. N., Definitive equations for the fluid resistance of spheres, Proc. Physical Society, 57, 259-270, 1945.

Deehr, C. S., A spectrophotometric study of the aurora of 27 November 1959 at College, Alaska, Geophysical Institute Report No. UAG-R119, University of Alaska, 1961.

Deirmendjian, D. and E. H. Vestine, Some remarks on the nature and origin of noctilucent cloud particles, Planet. Space Sci., 1, 146-153, 1959.

Dole, S. H., The gravitational concentration of particles in space near the earth, Planet. Space Sci. 9, 541-543, 1962.

Dryden, H. L., F. P. Murnaghan and H. Bateman, Hydrodynamics, Dover, 1956.

Ellyett, G. D., and C. S. L. Keay, Meteors: an unexpected increase in 1963, Science 146, 1458, 1964.

Fessenkov, V. G., The mass of the atmospheric residue of the Sikhote-Alin Meteorite, Dok. Akad. Nauk., (SSR), 66, 1949.

Fogle, B., Noctilucent clouds in Alaska during 1962, Nature 199, 1080, 1962.

Fogle, B. and Y. Gotaas, Noctilucent cloud observation manual, Geophysical Institute Report No. UAG R-157, University of Alaska, 1963.

Fogle, B., Results of the study of noctilucent clouds over North America during 1963, Geophsyical Institute Report No. UAG R-159, University of Alaska, 1964a.

Fogle, B., Noctilucent cloud observation manual - southern hemisphere, Geophsyical Institute Report No. UAG R-158, University of Alaska, 1964b.

Fogle, B., Noctilucent clouds in the southern hemisphere, Nature 204, 14-18, 1964c. (See also Weather XX, 374-377.)

Fogle, B., Noctilucent clouds over Punta Arenas, Chile, Nature 207, 66, 1965a.

Fogle, B., Noctilucent clouds over North America, Nature 207, 696-698, 1965b.

Fogle, B., Noctilucent clouds, WMO Bulletin XIV, 202-208, 1965c.

Fogle, B., S. Chapman and C. Echols, Noctilucent clouds - a survey with special reference to recent observations, Geophysical Institute Report No. UAG R-162.

Fogle, B. and C. Echols, Summary of noctilucent cloud reports from 1885-1964, Geophysical Institute Report No. UAG R-163, University of Alaska, 1965.

Fiocco, G. and L. D. Smullin, Detection of scattering layers in the upper atmosphere (60-140 km) by optical radar, Nature 199, 1963.

Grishin, N. I., On the structure of noctilucent clouds, Meteorologiia i Gidrologiia Leningrad #1, 23-28, 1955.

Grishin, N. I., Research of the continuous spectrum of noctilucent clouds, All Union Ast. Geod. Soc. Bull. (USSR), 19, 3-16, 1956

Grishin, N. I., Study of wave movements of noctilucent clouds, Some problems of meteorology, Article No. 1, Academy of Sciences of the USSR, Moscow, 1960.

Gutnick, M., Mean annual mid-latitude moisture profile to 31 km, Air Force Surveys in Geophysics No. 147, Air Force Cambridge Research Labs., Bedford, Mass. 1962.

Hamilton, R. A., Observations of noctilucent clouds near midwinter, Met. Mag. 93, 201, 1964.

Handbook of Geophysics, Air Force Cambridge Research Center, Bedford, Mass., 1957.

Hanson, A., Noctilucent clouds over the arctic in November, J. Geophys. Res., 70, 4717-18, 1965.

Haurwitz, B., Frictional effects and the meridional circulation in the mesosphere, J. Geophys. Res. 66, 2391, 1961.

Haurwitz, B. Comment on wave forms in noctilucent clouds, Geophysical Institute Report No. UAG-R-160, University of Alaska, 1964.

Helmholtz, R., Met. Zs., 24, 186, 1889.

Hemenway, C. L., and R. K. Soberman, Studies of micrometeorites obtained from a recoverable sounding rocket, Astron. Jour. 67, 256-266, 1962.

Hemenway, C. L., E. F. Fullum, R. A. Skrivanek, R. K. Soberman and G. Witt, Electron-microscopic studies of noctilucent cloud particles, Te-lus 16, 96-102, 1964.

Hemenway, C. L., R. K. Soberman and G. Witt, Sampling of noctilucent cloud particles, Tellus 16, 84-88, 1964.

Hesstvedt, E., Note on the nature of noctilucent clouds, J. Geophys. Res., 66, 1885-1887, 1961.

Hesstvedt, E., On the water vapor content of the high atmosphere, Geofys. Publ. 25, 1-18, 1964.

Hesstvedt, E., On the possibility of ice cloud formation at the mesopause, Tellus 14, 290-296, 1962.

Hines, C. O., Internal gravity waves at ionospheric heights, Can. J. Phys. 38, 1441-1481, 1959.

Hoffmeister, C. Spezifische leuchtvorgänge im bereich der mittleren ionosphäre Ergebnisse der Naturewissenschaften, XXIV, 1-53, 1951.

Hoffmeister, C., Nature and origin of noctilucent clouds, Ann. Int. Geophys. 11, 13, 1961.

Houston, R. E., The effects of certain solar radiation on the lower ionosphere, J. Atmos. Terr. Phys. 12, 225, 1958.

Humphreys, W. J., Nacreous and noctilucent clouds, Monthly Weather Review 61, 228, 1933.

Hunten, D. M., The interpretation of twilight measurements of sodium emission, in The Airglow and the Aurorae, 183-192, Pergamon Press, London, 1965.

Jardetzky, W., Met. Zs. 61, 310, 1926.

Jesse, O., Untersuchungens uber die sogenannten leuchtende nachtwolken Sitzungsberichte der Kg, Preus, Akad. der Wissenschaften, 2, 1031, 1960.

Jesse, O., Die Höhe der leuchtenden nachwolken, Astr. Nachr. 140, 161, 1896.

Junge, C. E., Vertical profiles of condensation nuclei in the stratosphere, J. Meteorol. 18, 501-509, 1961.

Junge, C. E., C. W. Chagnon and J. E. Manson, Stratospheric Aerosols, J. of Meteorol. 18, 81-108, 1961.

Junge, C. E. and J. E. Manson, Stratospheric aerosol studies by aircraft, J. Geophys. Res. 66, 2163-2182, 1961.

Kaiser, T. R., Meteors and the abundance of interplanetary matter, Sp. Science Rev. 1, 554-575, 1962.

Kellogg, W. W., and G. F. Schilling, A proposed model of the circulation in the upper stratosphere, J. Met. 8, 220-230, 1951.

Kellogg, W. W. Chemical heating above the polar mesosphere in winter, J. Met. 18, 373-381, 1961.

Khvostikov, I. A., Serebristye oblaka, Priroda 5 (#5), 49-59, 1952.

Kiessling, J., Die Dammerungserscheinungen in Jahre 1883 und Ihre Physicalische Erklarung, Hamburg und Leipzig, L. Voss, 1888.

Knudsen, M. and S. Weber, Ann. Phys. Lpz. 36, 982, 1911.

Koenig, H. J. and J. H. Brandy, Parallactic height finding for rocket research, Can. J. Phys. 43, 1435-1445, 1965.

Lettau, H., Diffusion in the upper atmosphere, in Compendium of Meteorology, Am. Met. Soc., Boston, 320-333, 1951

Linscott, I., C. L. Hemenway and G. Witt, Calcium film indicator of moisture associated with noctilucent cloud particles, Tellus 16, 110-113, 1964.

London, J., Solar eruptions and the weather, Transaction of the New York Academy of Sciences 19, 138-146, 1956.

Lovell, A. C. B., Meteor Astronomy, Oxford Press, 1954.

Ludlam, F., Noctilucent clouds, Tellus 9, 341-364, 1957.

Maeda, K. and T. Watanabe, Pulsating aurorae and infrasonic waves in the polar atmosphere, J. Atmos. Sci. 21, 15-29, 1964.

Mattanch, J., Z. Phys. 32, 439, 1925.

McIntosh, B. A. and P. M. Millman, Radar meteor counts, anomalous increase during 1963, Science 146, 1457, 1964.

Meinel, A. B., B. Middlehurst and E. Whitteker, Low latitude noctilucent clouds, Science 141, 1176-1178, 1963.

Meinel, M. P. and A. B. Meinel, Late twilight glow of the ash stratum from the eruption of Agung volcano, Science 142, 582, 1963.

Millikan, R. A., Phys. Rev. 15, 545, 1920.

Millikan, R. A., Phys. Rev. 21, 217-223, 1923.

Millman, P. M. and D. W. R. McKinley, Meteors, The Moon, Meteorites and Comets, edited by B. M. Middlehurst and G. P. Kuiper, The University of Chicago Press, Chicago, 1963.

Millman, P. M. and B. A. McIntosh, A preliminary report on radar meteor counts, Air Force Cambridge Research Lab., Geophysical Research Paper Number 75, 45-52, 1962.

Minzner, R. A., K. S. W. Champion and H. L. Pond, The ARDC model atmosphere, 1959, Air Force Surveys in Geophysics No. 115, Air Force Cambridge Research Center, Bedford, Mass. 1959.

Murcray, W. B., A possible auroral enhancement of infrared radiation emitted by atmospheric ozone, Nature 180, 139-140, 1957.

Murgatroyd, R. J. and F. Singleton, Possible meridinal circulation in the stratosphere and mesosphere, Quart. J. R. Met. Soc. 87, 125-135, 1961.

Newkirk, G. and J. A. Eddy, Light scattering by particles in the atmosphere, J. Atmos. Sci. 21, 35-60, 1964.

Nordberg, W., Personal Communication, 1966.

Nordberg, W., and W. C. Stroud, Seasonal, latitudinal and diurnal variations in the upper atmosphere, NASA Technical Note D-703, April 1961.

Nordberg, W., L. Katchen, J. Theon and W. S. Smith, Rocket observations of the structure and dynamics of the mesosphere during the quiet sun period, NASA publication No. X-651-65-154, Greenbelt, Maryland, 1965.

Pant, P. S., Circulation in the upper atmosphere, J. Geophys. Res. 61, 459-474, 1956.

Parthasarathy, R. and D. B. Rai, Effective recombination coefficient in D-region, Radio Science (in publication) 1966.

Paton, J., Luminous night clouds, Met. Mag. 78, 354, 1949.

Paton, J., Aurora and luminous night clouds, Proc. Phys. Soc. London B. 63, 1039, 1950.

Paton, J., Direct evidence of vertical motion in the atmosphere at a height of about 80 km provided by photographs of noctilucent clouds, Proceedings of the Toronto Meteorological Conference 1953, 31-33, 1954.

Paton, J., Noctilucent clouds, Met. Mag., 93, 161-179, 1964.

Paton, J., Noctilucent clouds in 1964, Met. Mag. 94, 180-184, 1965a.

Paton, J., Personal Communication, 1965b.

Pavlova, T. D., Apparent frequency of the appearance of noctilucent clouds based on the observations at the stations of the hydrometeorological service for 1957 and 1958, Izd. L.G.U. Astronomicheskvia Observatorie Isslectovanica Serebristykh Oblahov 1, 3-58, 1960.

Pitwell, L. R., High altitude clouds over Addis Ababa, Bull. Geophys. Obs. Addis Ababa 3, 145, 1963.

Ratcliffe, J. A. and K. Weeks, Physics of the Upper Atmosphere, 378-413, Academic Press, New York, 1960.

Rosinski, J. and J. M. Pierrard, Condensation products of meteor vapors and their connection with noctilucent clouds and rainfall, J. Atmos. Terr. Phys. 26, 51-66, 1964.

Schilling, G. F., Latitudinal variations of mesopause height inferred from eclipse observations, Rand Rpt. No. RM-4321-PR, 1964.

Schröder, W., Simultanes Auftreten von polarlichtern und Lenchtenden Nachtwolken, Gerlands Beitrage zur Geophysik, 74, 471, 1965.

Scultetus, H. R., Altere beobach tungen von leuchtstreifen, Z. fur Met. 3, 272, 1949.

Sharanov, V. V., Photometric and colorimetric observations of noctilucent clouds during the summer of 1959, Izdat. Leningradskago Universiteta #1, 66-76, Leningrad University Press.

Skrivanek, R. A., and R. K. Soberman, Simulation of ring patterns observed with noctilucent cloud particles, Tellus 16, 114-117, 1964.

Soberman, R. K., S. A. Chrest, J. J. Manning, L. Rey, T. G. Ryan R. A. Skrivanek, and N. Wilhelm, Techniques for rocket sampling of noctilucent cloud particles, Tellus 18, 89-95, 1964.

Soberman, R. K., Noctilucent clouds, Scientific American 208 (6), 50-59, 1963.

Størmer, C., Height and velocity of luminous night clouds observed in Norway, 1932. Oslo University Publication #6, 1933.

Størmer, C., Measurements of luminous night clouds in Norway 1933 and 1934, Astrophysica Norwegica 1, 87-114, 1935.

Stroud, W. G., W. Nordberg, W. R. Bandeen, F. L. Bartman and P. Titus, Rocket grenade measurements of temperatures and winds in the mesophere over Churchill, Canada, J. Geophys. Res. 65, 2307-2322, 1960.

Van de Hulst, H. C., Ap. J. 105, 471, 1947.

Van de Hulst, H. C., Light Scattering b Small Particles, John Wiley & Sons, New York, 1957.

Vassilyev, O., Photometric contour of strips of noctilucent clouds, Trans. Conference on Noctilucent Clouds, 68-73, Tallin, 1962.

Vegard, L., Investigations of the auroral spectrum, Geofys. Pub. 10, 53, 1933.

Vestine, E. H., Noctilucent clouds, J. Roy. Astron. Soc. Can. 28, 249-272, 303-317, 1934.

Volz, F. E., Personal Communication, 1966.

Volz, F. E., and R. M. Goody, The intensity of the twilight and upper atmospheric dust, J. Atmos. Sci. 19, 385-406, 1962.

Webb, W., Morphology of noctilucent clouds, J. Geophys. Res., 70, 4463-4475, 1965.

Wegner, A., Met. Zs. 61, 103, 1926.

Whipple, F. J., The great Siberian meteor and the waves, seismic and aerial which it produced, Quart. J. Roy. Met. Soc. 56, 287, 1930.

Whipple, F. L., Photographic meteor orbits and their distribution in space, Astrophys. Journ. 59, 201, 1954.

Whipple, F. L., The dust cloud about the earth, Nature 189, 127-28, 1961.

Whipple, F. L. and G. S. Hawkins, On meteors and rainfall, J. Meteorology 13, 236-240, 1956.

Witt, G., Noctilucent cloud observations, Tellus 9, 365-371, 1957.

Witt, G., Polarization of light from noctilucent clouds, J. Geophys. Res., 65, 25-933, 1960a.

Witt, G., A note to the paper by G. Witt, Polarization of light from noctilucent clouds, J. Geophys. Res. 65, 2199-2200, 1960b.

Witt, G., Height, structure, and displacement of noctilucent clouds, Tellus 14, 1-18, 1962.

Witt, G., C. L. Hemenway, N. Lange, S. Modin, and R. K. Soberman, Composition analysis of particles from noctilucent clouds, Tellus 16, 103-109, 1964.